Targeting Cellular Retinoic Acid Binding Protein 1 to Modulate Non-Canonical Retinoic Acid Signaling

A THESIS SUBMITTED TO THE FACULTY OF THE

UNIVERSITY OF MINNESOTA

BY

Jennifer Nhieu

IN PARTIAL FULFILMENT OF THE REQUIREMENTS FOR THE DEGREEE OF

DOCTOR OF PHILOSPOHY

Advisor: Li-Na Wei

September 2023

Acknowledgements

First and foremost, I would like to thank Dr. Wei, my advisor. Dr. Wei has worked tirelessly to provide a solid and welcoming environment in the lab. Her scientific enthusiasm has been nothing but inspirational and I hope that some day I can muster even a quarter of her vigor for research. The first time I sat in her office as an undergrad and she asked what my research interest were and my response was “I don’t know.” I actually still have no clue, but because of your grace and guidance my indecisiveness is now rooted in a positive curiosity for the biological sciences. I appreciate you so much for your willingness to always be available and encouraging. I will always look back fondly on the holiday get togethers and lunch at Chili’s.

Thank you to all the current and past members of Wei Lab for the trouble-shooting, rant sessions, brunch and so much more. Thank you especially to Shawna Persaud for being a mentor in almost every sense. Thank you to Thomas Lerdall and Liming Milbauer for their support in helping with experiments. These studies would have never been published without your help.

Thank you to my committee, especially for their willingness to coordinate ZOOM during COVID. Thank you especially to Dr. Mayo and Michelle Miller for their time and expertise in NMR experiments. Thank you to Dr. Thayer for teaching me about fura-2 imaging. I really enjoyed our trouble-shooting talks.

I would like to thank the Pharmacology Graduate Program (i.e. MPaT). The community and faculty have always made me feel welcome and cared for. To all the labs in NHH, thank you so much for sharing your reagents and advice with me. Special shout

out to all the custodial staff, without them the building would be in shambles, and I would still be locked out of lab.

Thank you, my significant other Brian Cheng and his guinea pigs: Mabel, Oreo, and Mocha. Your unwavering support in the forms of spending time together on zoom during late nights in the lab, memes, food adventures, and so much more kept me going. Because of your never-ending support I was able to make it through this whole process.

Finally, thank you to my family, especially my mom and dad. They came to the U.S.A. with nothing and worked endlessly to provide and support for me and my brother. Whether it be 24-hour shifts at Fuel Plaza or late-night ingredient prep at the restaurant you taught me to always work hard and never give up. Also thank you for the night-owl tendencies, they came in super useful in the lab. I can only hope that I can someday have a fraction of your diligence and hard work.

Dedication

I dedicate this dissertation to my Grandpa and Chuck my dog. I will always cherish the times we had together and you will be dearly missed.

Abstract

All-*trans*-retinoic acid (atRA) is the principle active metabolite of vitamin A and is essential for almost all biological functions. Canonically, atRA exerts its actions through retinoic acid receptors (RARs) located in the nucleus to regulate gene transcription. atRA also possesses "non-canonical activities" that modulate cell signaling, and is defined by (1) RAR-independence, (2) a rapid time-scale and (3) cytosolic localization. The primary mediator of this non-canonical activity is the highly conserved cellular retinoic acid binding protein 1 (CRABP1). CRABP1 was previously thought to only function in the binding and sequestration of atRA to regulate cellular bio-availability. However, studies of two non-canonical pathways have established CRABP1 as a mediator of non-canonical atRA activity. The first is CRABP1-mediated regulation of the mitogen activated protein kinase (MAPK) pathway with physiological and disease relevance in stem cell proliferation, cancer, immune regulation, and obesity. The second is CRABP1-mediated regulation of calcium (Ca^{2+})-calmodulin dependent kinase II (CaMKII) activation with physiological and disease relevance in cardiac dysfunction and motor neuron degenerative diseases such as amyotrophic lateral sclerosis (ALS).

Nuclear Magnetic Resonance (NMR) spectroscopy and molecular studies determined the structural and molecular mechanism underlying CRABP1-mediated regulation of CaMKII activation. Mechanistically, CRABP1 preferentially complexes with the inactive form of CaMKII to ultimately dampen CaMKII activation. Alanine mutagenesis studies have determined that CRABP1 residues within a proposed CaMKII

interaction surface and an allosteric site maintain this preference. Mutation of these residues can shift CRABP1 preference towards the active form of CaMKII.

Two novel CRABP1 ligands (C4 and C32) were also characterized as potential therapeutic agents that may be developed to target the CRABP1-CaMKII pathway in motor neuron (MN) diseases. In a reconstituted MN culture model, C4 and C32 can dampen CaMKII activation in a CRABP1-dependent manner. In an immortalized MN cell line (MN1) C4 and C32 can protect against excitotoxic-mediated MN death induced by ionomycin treatment.

The primary sequence of CRABP1 is extremely conserved among animal species, with only one substitution observed at amino acid position 86, suggesting important functional constraints placed upon CRABP1 sequence during evolution. Data mining of reported human studies was performed to determine the relevance of CRABP1 in human health and disease. Associations of CRABP1 with various human diseases were identified, including altered human *CRABP1* gene expression and the presence of variants in cancers, ALS, and several rare diseases.

The studies within this dissertation elucidate the structural and molecular mechanism of CRABP1-mediated regulation of cell signaling, specifically in CaMKII activation. The results suggest a potential therapeutic approach in targeting the CRABP1-CaMKII pathway with CRABP1-selective ligands to manage MN diseases. These results expand our understanding of CRABP1 in mediating the non-canonical activity of atRA hormone, particularly in modulating various cell signaling pathways to maintain health.

The results also uncover complex mechanisms through which CRABP1-selective, atRA-like compounds may be further developed in therapeutic applications.

Table of Contents

List of Tables

List of Figures

List of Abbreviations

atRA	All-*trans*-Retinoic Acid
ALS	Amyotrophic Lateral Sclerosis
AMD	Age-Related Macular Degeneration
AML	Acute Myeloid Leukemia
AMPAR	α-amino-3-hydroxy-5-methyl-4-isoxazolepropionic acid Receptor
CAMBD	Calmodulin Binding Domain
CAMKII	Calcium-Calmodulin Dependent Protein Kinase II
CCI	CRABP1-CaMKII Complex Index
CKO	CRABP1 Knockout
CNS	Central Nervous System
CRABP1	Cellular Retinoic Acid Binding Protein 1
CRABP2	Cellular Retinoic Acid Binding Protein 2
CSF	Cerebral Spinal Fluid
CYP26	Cytochrome P450 Family 26
D2O	Deuterium Oxide
DCC	Dextran-Coated Charcoal
DMSO	Dimethyl sulfoxide

DSF	Differential Scanning Fluorimetry
EB	Embryoid Body
ERK1/2	Extracellular Regulated Kinase 1 and 2
ESC	Embryonic Stem Cell
EV	Empty Vector
HB9	Homeo Box HB9
HEK293T	Human Embryonic Kidney Cell 293T
HFD	High Fat Diet
HSQC	Heteronuclear Single Quantum Coherence
ISO	Isoproterenol
LRP4-MuSK	Low-density lipoprotein receptor-related protein 4- Muscle-Specific Kinase
MAPK	Mitogen Activated Protein Kinase
MEK	Mitogen-activated protein kinase kinase
MMD	Moyamoya Disease
MN	Motor Neuron
MN1	Motor Neuron 1 Cell Line
MTT	3-(4,5-dimethylthiazol-2-yl)-2,5-diphenyltetrazolium bromide
MW	Molecular Weight
NMJ	Neuromuscular Junction
NMR	Nuclear Magnetic Resonance
NOESY	Nuclear Overhauser Effect Spectroscopy

NRIP1	Nuclear receptor interacting protein 1
NSC	Neural Stem Cell
NTA	Nickel-nitrilotriacetic Acid
PEI	Polyethyleneimine
PLN	Phospholamban
RAF	Rapidly Accelerated Fibrosarcoma
RAR	Retinoic Acid Receptor
RBD	Ras Binding Domain
RXR	Retinoic X Receptor
RARE	Retinoic Acid Response Element
RFU	Relative Fluorescence Units
RIP140	Receptor-interacting protein 140
SMA	Spinal Muscular Atrophy
SNP	Single-Nucleotide Polymorphisms
TOCSY	Total Correlation Spectroscopy
WT	Wild-Type

Chapter 1: Introduction

Significant portions of this chapter have previously appeared in the following publication:

Nhieu, J.; Lin, Y.-L.; Wei, L.-N. CRABP1 in Non-Canonical Activities of Retinoic Acid in Health and Diseases. *Nutrients* **2022**, *14*, 1528.

https://doi.org/10.3390/nu14071528

Author Contributions: J.N., L.-N.W.; writing—original dRaft preparation, Y.-L.L.; writing—review and editing, L.-N.W.; supervision, project administration, and funding acquisition.

1.1 All-*trans*-Retinoic Acid (atRA) in Biology and Disease

Vitamin A (retinol) is an essential nutrient required for a myriad of physiological and biological processes[1]. These diverse actions of retinol are primarily facilitated by the principle active metabolite, all-*trans*-retinoic acid (atRA) and its isomers. Extensive, historical studies determined that atRA elicits these actions by binding to nuclear retinoic acid receptors (RARs), which then heterodimerize with retinoid X receptors (RXRs) to regulate transcriptional activity of genes containing RA response elements (RAREs). Furthermore RAR-RXR heterodimers can also work in tandem with other transcription factors to provide additional precision in controlling transcriptional programs required to maintain cellular, tissue, and system homeostasis[2,3].

Tight regulation of atRA concentrations is required in order to achieve the desired physiological or therapeutic outcomes from atRA signaling. Consequently, dysregulation of atRA concentration is often lethal or congenitally deformative, thus designating atRA as a potent teratogen[4–6]. In the clinic, atRA (also referred to as tretinoin) is readily used as a treatment for acute promyelocytic leukemia and acne vulgaris. Additionally, synthetic retinoids (isotretinoin[7], adapalene[8], tazarotene[9], trifarotene[10]) are indicated for acne vulgaris and/or psoriasis[11–13]. Currently, atRA and synthetic retinoids are also being researched for potential applications in skin disorders, immune modulation, and neurogenerative diseases[14,15].

Life-threatening and deleterious side-effects are often associated with the use of atRA and approved synthetic retinoids, which likely result from off-target canonical

activities. These side-effects include Differentiation Syndrome (also known as RA Syndrome)[16], worsening or precipitation of mood disorders[17,18], and birth defects[4]. Efforts in drug development have been made to reduce off-target effects by designing synthetic retinoids (or rexinoids) that selectively bind particular isoforms of RARs or RXRs[14]. Regardless of isoform selectivity, off-target effects still remain a critical limitation given that RAR/RXR regulate a multitude of genes (over 500) to profoundly affect various physiological and biological processes. Therefore, other avenues of development such as the non-canonical activities of RA described in the following section are of great interest to circumvent these toxic, genomic side-effects.

1.2 Canonical and Non-Canonical Retinoic Acid Activity

As mentioned, the primary mechanism of action attributed to atRA is through nuclear RARs to regulate gene transcription. Given the nature of gene transcription this activity typically occurs on the timescale of hours to days. Collectively this nuclear, RAR-dependent, pro-longed action is referred to as “canonical” activities of atRA. An extensive body of work has determined that the cellular retinoid-binding proteins (CRABPs) I and II facilitate these canonical activities of RA. Rigorous biochemical studies have characterized classical CRABP1 functions in RA binding, sequestration, and metabolism via cytochrome (CYP) P-450 enzymes[19,20] (reviewed in-depth in[21–24]), while CRABP2 is responsible for the transport of RA to the nucleus[21,22,25,26].

In 2008, a study first reported a novel activity (effect) of atRA that occurred rapidly (within minutes) to alter the protein phosphorylation status of a transcription factor TR2 in maintaining stem cell proliferation and stemness potential[27]. Subsequent

studies[28–30] further documented similar activities of atRA that shared several features: (1) RAR-independence, (2) occurring in the cytosol without altering gene expression, and (3) rapid (typically within minutes) action. These novel activities of atRA were collectively referred to as "non-canonical" and were later found to be mediated by the cellular retinoic acid binding protein 1 (CRABP1)[29]. These CRABP1-mediated non-canonical activities of atRA were ultimately validated in careful studies of Crabp1 knockout (CKO) mice and cultures, which also revealed the physiological/disease relevance of CRABP1 described later on [31–40].

Extensive molecular and cell biological studies have identified specific cytosolic signaling pathways that can be targeted by CRABP1 in a cell context-dependent manner. It is believed that CRABP1 functions as a signal integrator by forming various specific RA-regulated signaling protein complexes (signalosomes) in different cells to modulate specific cellular processes/functions.

1.3 Cellular Retinoic Acid Binding Protein 1 as a Major Mediator of Non-Canonical Retinoic Acid Activity

CRABP1 is the most highly conserved retinoid-binding protein among all the known binding proteins and nuclear receptors for retinoids[41]. CRABP1 binds, specifically, atRA with a high affinity (<1 nM)[42–45]. Given its high affinity toward atRA and cytosolic distribution, CRABP1 has been proposed and shown to sequester the poorly soluble RA from the aqueous cytosolic environment[19–24]. This led to the belief that CRABP1 functions to control RA availability in the cell, which indeed was supported by several molecular studies. These studies documented that altering the expression level of

CRABP1 caused subsequent changes in the expression of atRA-responsive genes[46,47]. As introduced earlier, CRABP1 could participate in atRA metabolism by delivering RA to CYP P-450 metabolic enzymes and microsomes via protein-protein interactions and substrate channeling[22,48]. However, the physiological role of CRABP1 in mediating the newly observed, non-canonical activity has remained largely elusive. Only recently, studies of CKO mice and cultures in various physiological/pathological conditions (see the following section) began to shed light on multiple functional roles of CRABP1 in modulating specific cellular processes, which contributed to the "non-canonical" activity. The fact that CRABP1 is important for multiple signaling pathways is consistent with the extremely high conservation of its amino acid sequence across animal species. Figure 1-1 shows the reported amino acid sequence alignment of CRABP1 among five animal species including human[49], pig[50], rat[51], mouse[52], and bovine[53]. Importantly, there is only a single residue, at position 86, that is not conserved, with alanine in human and pig sequences and proline in mouse, rat, and bovine sequences (Figure 1-1).

The extreme conservation of CRABP1 during evolution would suggest important functional constraints. The evidence for this notion was obtained in careful studies of CKO mouse phenotypes (see later). Mechanistic details were provided in biochemical and cellular studies that first revealed specific context-dependent "binding partners" of CRABP1, which were rigorously defined according to at least two criteria: (a) specific and direct binding to CRABP1, which could be validated in vitro, and (b) forming specific cytosolic protein complexes that could be validated in vivo. Functional consequences of these CRABP1-containing protein complexes were each found to be

capable of modulating certain specific cytosolic signaling pathways in a particular cell type. These CRABP1-containing protein complexes are therefore referred to as CRABP1-signalosomes. Currently, two types of CRABP1-signalosomes have been identified, which are discussed in the following sections.

1.3.1 CRABP1-MAPK (RAF-MEK-ERK) Signalosome

A specific CRABP1-signaling complex was first proposed after studying embryonal carcinoma (EC) and embryonic stem (ES) cells that were stimulated by a physiological concentration (10 nM) of atRA to modulate their proliferation/differentiation (reviewed in[54,55]). The initial study detected a very rapid (within minutes) response of these cells to atRA administration, which occurred in the cytosol and involved a mitogen-activated protein kinase (MAPK) pathway to modify target proteins for specific post-translational modifications[27–30]. This atRA-elicited signal was found to involve CRABP1, and could rapidly (within minutes) dampen the activity of the initiating kinase of the MAPK pathway, which is the rapidly accelerated fibrosarcoma (RAF) kinase and is a cell membrane-anchored kinase activated by the mitogenic signal Ras GTPase[56]. The MAPK kinase signaling cascade is comprised of Ras GTPase which activates RAF, then mitogen-activated protein kinase kinase (MEK), and then extracellular-signal-regulated kinase (ERK). Activation of this signaling pathway generally leads to cell proliferation and growth for stem/progenitor cells[56]. Through biochemical and molecular studies, it is now established that CRABP1 competes with Ras by directly interacting with RAF at its Ras-binding domain, thereby dampening MAPK signal propagation and ultimately modulating (reducing) cell proliferation of ES,

EC, and neural stem cell (NSC)[29,32,36]. The proposed mechanistic model for CRABP1-MAPK signalosome is shown in Figure 1-2.

1.3.2 CRABP1-MAPK Signalosome in Metabolism and Immunity

Lin et al. first observed that CKO mice exhibited increased high-fat diet (HFD)-induced obesity and insulin resistance (IR), suggesting a protective role for CRABP1 against the development of metabolic disorders. A molecular study of CKO mice elucidated an underlying mechanism for this metabolic phenotype that, in normal adipocytes, CRABP1 could negatively regulate ERK activity to inhibit adipogenesis and adipose hypertrophy[35]. Therefore, CKO mice are more prone to HFD-induced obesity and IR. To this end, it has been reported that pharmacological doses of RA could inhibit adipogenesis and protect against obesity, and this was attributed, primarily, to RAR-mediated activities[57–61]. These recent studies of CKO models revealed CRABP1 as an additional player in mediating physiological activities of atRA regarding metabolic homeostasis and the maintenance of healthy adipose tissue[35].

In examining the systemic inflammatory status/potential of CKO mice, it was found that HFD-fed CKO mice all had increased systemic inflammation, indicated by invading immune cells in adipose tissue[35], increased inflammatory driver Receptor Interacting Protein 140 (RIP140) (gene name Nrip1)[62] in the blood[38] , elevation in inflammatory cytokines, and significantly enhanced macrophage M1 polarization (unpublished). Previous studies also indicated that CKO mice had overall increased inflammation in the heart, indicated by increased cardiac fibrosis[33], and an altered anxiety and stress response

in their HPA axis[39]. To this end, CRABP1 was found to be involved in exosome secretion from CRABP1-expressing neurons. Specifically, the RIP140-containing exosome population was significantly expanded in the blood and cerebral spinal fluid (CSF) of CKO mice, due to, in part, increased exosome secretion from CKO neurons[38]. Importantly, these neuron-derived RIP140-containing exosomes could be engulfed by macrophages to increase their inflammatory M1 polarization, thereby increasing systemic inflammation. This study, by monitoring the intercellular transfer of the inflammatory driver, RIP140, demonstrates exosome secretion as a potent means to transfer neuronal inflammation into systemic inflammation; mechanistically, this study identifies CRABP1 as an important regulator of exosome secretion from specific CRABP1-expressing neurons, which also involves the MAPK-ERK signaling in these neurons[38].

In addition to these studies that established the physiological and disease relevance of the CRABP1-MAPK pathway, two novel CRABP1-selective compounds, C3 and C4, were found to modulate MAPK signaling pathway in CRABP1-expressing cells[31,38]. C3 and C4 also do not activate RAR. The efficacy of C3 and C4 has been demonstrated to induce apoptosis (in cancer cells)[31] and regulate exosome secretion (in neurons)[38]. These studies highlight an approach to exploit the regulation of non-canonical, CRABP1-dependent pathways while circumventing known RAR-associated, off-target effects.

1.3.3 CRABP1-CaMKII Signalosome in Cardiomyocytes and Motor Neurons

A different CRABP1-signaling complex was identified from studying deteriorated heart function of CKO mice[33,34], and their premature weakening in motor function[40]. The

expression study confirmed CRABP1 expression in cardiomyocytes[33] (relevant to the CKO heart phenotype) and motor neurons (relevant to the CKO motor function phenotype)[40]. This signaling complex is comprised of CRABP1 and calcium-calmodulin-dependent kinase 2 (CaMKII), an enzyme critical to calcium signaling/handling and highly enriched in both cardiomyocytes[63] and neurons[64,65]. It is known that CaMKII regulates contraction in cardiomyocytes[63] and long-term potentiation in neurons[64,65], respectively. Both types of cells are highly dependent upon calcium homeostasis for their functions where CaMKII is a key mediator of calcium signaling[66]. All the CaMKII isoforms have a conserved architecture comprised of the kinase, regulatory, and association/oligomerization domains, and share the same activation mechanism through the binding of calmodulin to the calmodulin-binding domain (CaMBD) within its regulatory domain. CaMKII activation occurs when intracellular (Ca^{2+}) increases and binds calmodulin. Ca^{2+}-calmodulin then binds and activates CaMKII, which is often marked by phosphorylation at threonine 286/7 (T286/7), depending on the CaMKII isoform[67,68]. In vitro data showed that CRABP1competes with calmodulin by directly interacting with CaMKII at the CaMBD[33,34]. Therefore, CRABP1 could dampen Ca^{2+}/Calmodulin activated CaMKII activity. Since over-activation of CaMKII is a major trigger of the death/damage of cardiomyocytes[69] and neurons[70], by dampening CaMKII over-activation, CRABP1 can play a protective role in maintaining the health of both the heart and neurons. These are elaborated on in the following section. The proposed mechanistic model for CRABP1-CaMKII signalosome is shown in Figure 1-3.

CKO mice naturally and gradually exhibited cardiac hypertrophy, reflected in their significantly depressed heart function in older animals[33]. Using the isoproterenol (ISO)-induced cardiomyopathy model for heart failure[71,72], studies showed that CKO mice were more sensitive/vulnerable to ISO treatment. Acute, high-dose ISO treatment activates β-adrenergic receptors to induce acute cardiomyocyte contractions, triggering a pathological condition of heart overactivation. Chronic ISO treatment induces more severe cardiac hypertrophy, and, eventually, fibrosis and necrosis occur, mimicking heart failure in human patients[71,72]. Interestingly, in the acute ISO treated model, CKO mice were more sensitive and exhibited a significantly increased CaMKII activity marked by elevated T286 phospho-status and phosphorylation of the CaMKII cardiac substrate, PLN. These were supported by molecular studies described above, that CRABP1 dampened CaMKII activation by competing with calmodulin for its binding to CaMKII[33]. In a subsequent study, it was found that pretreatment with atRA before chronic ISO administration could attenuate ISO-induced heart damage and CaMKII activity in the wild type, but not the CKO mice[34]. These studies clearly demonstrated a protective role for CRABP1, as well as the potential application of CRABP1-ligand such as RA, in certain heart damage/diseased conditions.

CRABP1 expression is tissue and cell-type specific. In the central nervous system, it is specifically and highly expressed in spinal cord MNs[40]. These neurons project to and innervate, primarily, muscles to form tightly regulated structures called neuromuscular junctions (NMJs)[73]. Neuronal activity from MNs is propagated through NMJs to elicit muscle contraction, and calcium signaling/handling (mediated by

CaMKII) is critical to the function of both presynaptic (MN)[74–76] and post-synaptic (muscle)[77,78] compartments. MNs release neurotransmitters such as acetylcholine to induce muscle contraction, and express Agrin, a proteoglycan essential for NMJ development and maintenance[73,79]. CRABP1 is specifically expressed in the presynaptic compartment, comprised of MNs, but is not expressed in the post-synaptic muscle compartment[40]. This study identified CRABP1-CaMKII signaling in MNs, which contributed to the regulation of Agrin expression and its downstream target, the muscular LRP4-MuSK signaling that maintained AChR clusters and healthy NMJ[73,80]. By comparing to wild-type mice, CKO mice were found to exhibit age-dependent more profound motor deterioration, reflected in their significantly reduced grip strength compared to the age-controlled group. Detailed histological studies revealed more severely damaged NMJs in CKO mice as compared to wild-type mice, characterized by irregular NMJ morphology, fragmentation, and reduced number. Consistently, in the CKO spinal cord tissues, CaMKII activity was significantly increased as compared to WT spinal tissues. Pathological CaMKII activation (overactivation) occurs in multiple disease states of the nervous system, frequently referred to as excitotoxicity[70]. In MN1 culture (a spinal MN cell line), inhibiting CaMKII via KN-93 (mimicking CRABP1 dampening effect) increased their Agrin expression, consistent with the reduction in Agrin detected in CKO NMJ tissues. It is concluded that CRABP1, in MNs, can target CaMKII to dampen its over-activation, which provides a protective mechanism against over-activation of CaMKII that could lead to MN degeneration. Importantly, re-expressing CRABP1 in young (before disease onset) CKO mice could partially rescue

their motor deficits and correct CaMKII activity and Agrin expression. These studies established that CRABP1 plays a physiologically relevant role in MN health. Furthermore, this CRABP1-CaMKII signalosome presents an additional pathway of interest to pharmacologically target, especially in MN disease.

The subsequent chapters in this dissertation describe studies that elucidated the structural and molecular mechanism of CRABP1-mediated regulation of CaMKII activation, and characterized a novel ligand, C32, and previously reported C4 as a pharmacological means to target this CRABP1-CaMKII pathway in MN pathology. Additionally, data mining of human studies from the literature revealed genetic associations of CRABP1 with several diseases, especially in cancer and neurodegeneration. Overall, these studies further contextualize the physiological and pharmacological relevance of CRABP1 as a mediator of non-canonical atRA signaling. In turn, these studies also provide additional insight to the mechanisms driving the profound and diverse activities and therapeutic potential of atRA.

1.4 Chapter 1 Figures

Figure 1-1 CRABP1 sequence alignment across mammals.

Reported CRABP1 protein sequences from the Uniprot database of human (ID: P29762)[49], pig (ID: B3F0B7)[50], rat (ID: P62966)[51], mouse (ID: P62965)[52], and bovine (ID: P62964)[53] were aligned using the ClustalWS alignment algorithm in Jalview. Only the residue at position 86 (indicated by bold text and arrow ↓) is not conserved and exists either as an alanine (A) in human and pig sequences or as a proline (P) in bovine, rat, and mouse sequences.

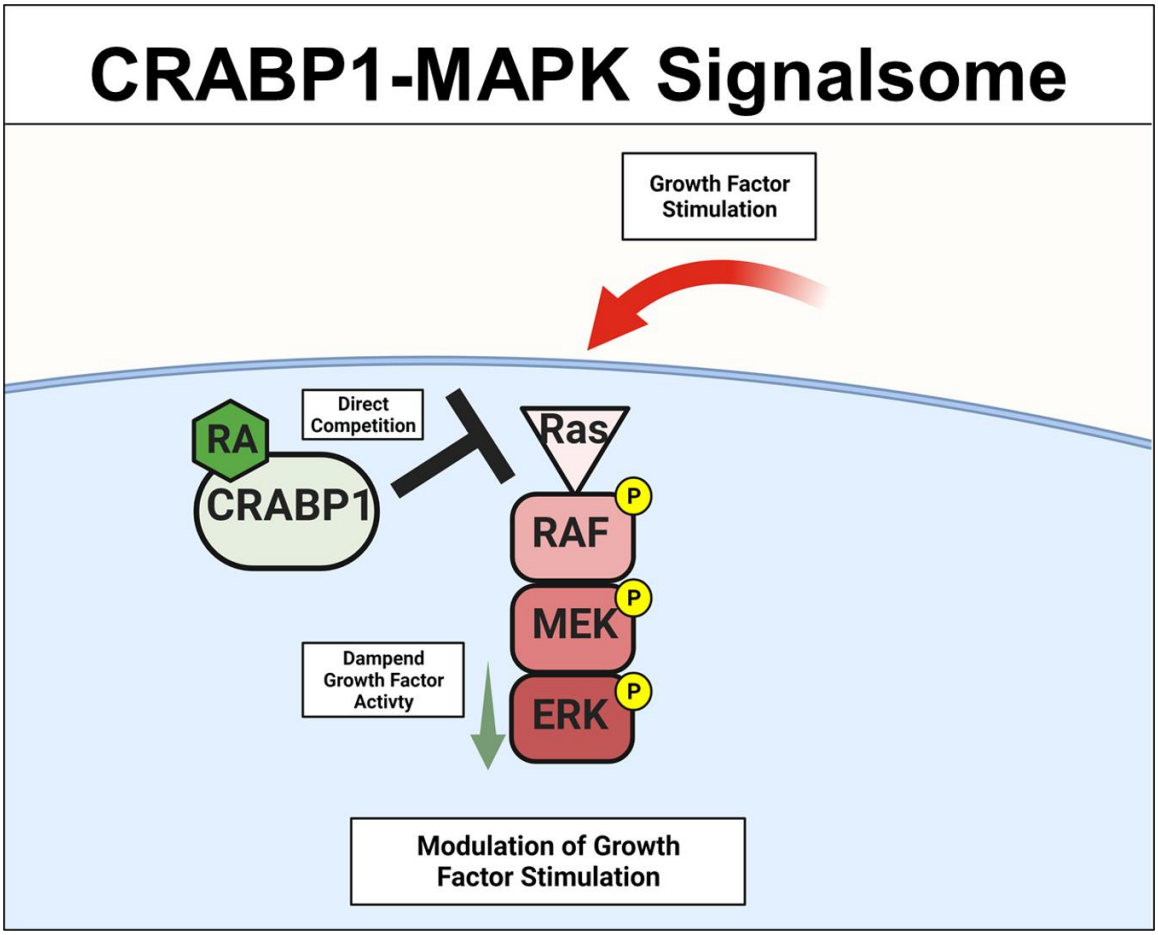

Figure 1-2 CRABP1-MAPK signalosome.

The action of CRABP1-signalosome in growth-factor stimulated MAPK activity is mediated by its direct competition with Ras, resulting in dampened MAPK activation. CRABP1: Cellular Retinoic Acid Binding Protein 1, RA: retinoic acid, RAF: rapidly Accelerated Fibrosarcoma, MEK: mitogen-activated protein kinase kinase, ERK: extracellular-signal-regulated kinase.

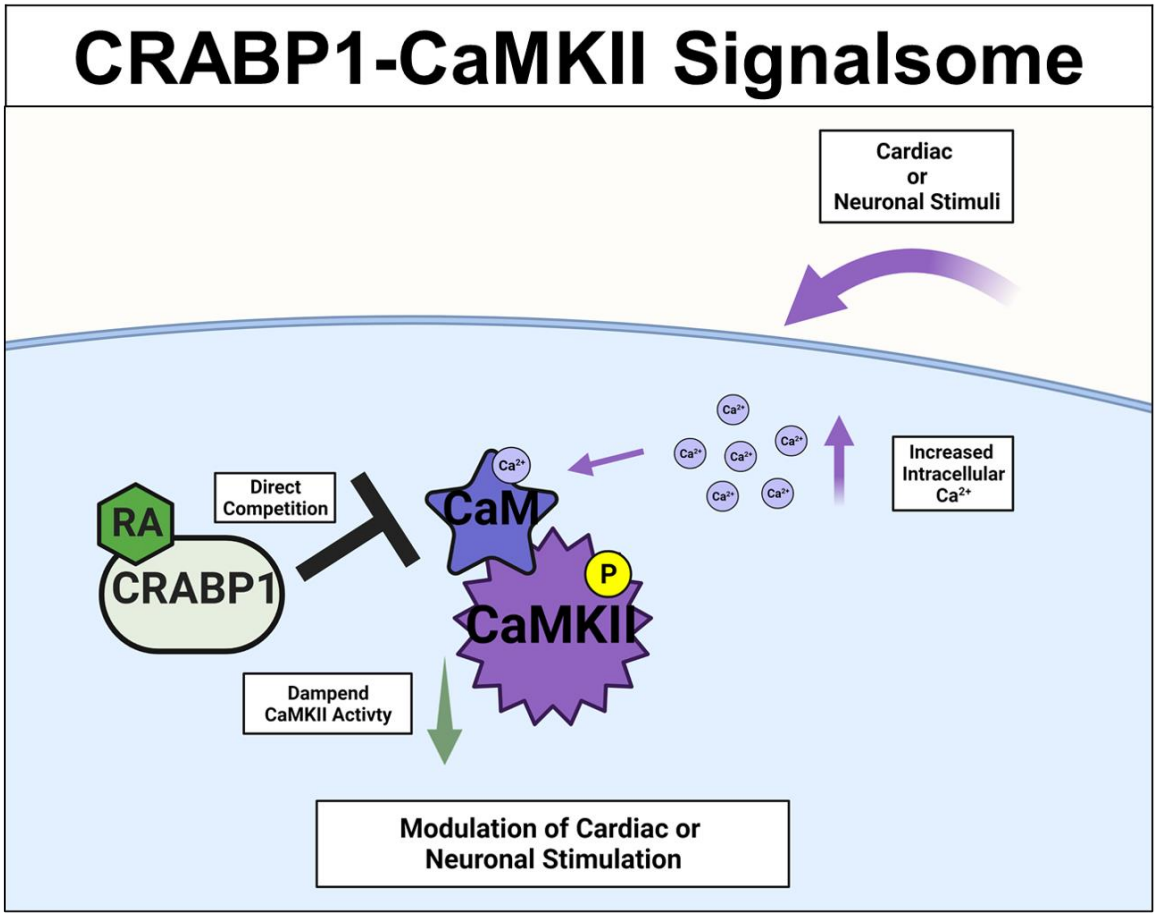

Figure 1-3 CRABP1-CaMKII signalosome.

Upon cardiac or neuronal stimulation and subsequent intracellular Ca^{2+} increase to activate CaMKII, CRABP1 directly competes with calmodulin (CaM) to dampen CaMKII enzyme activity to ultimately modulate cardiac and/or neuronal stimulation. CRABP1: Cellular Retinoic Acid Binding Protein 1, RA: retinoic acid, CaMKII: calcium-calmodulin- dependent kinase 2.

Chapter 2: Molecular Basis for Cellular Retinoic Acid Binding Protein 1 in modulating CaMKII activation

This chapter has been submitted as the following manuscript to *Frontiers in Molecular Biosciences* and is in revision:

Nhieu J, Miller MC, Lerdall T, Mayo KH, Wei LN. (2023) Molecular Basis for Cellular Retinoic Acid Binding Protein 1 in modulating CaMKII activation. *Front. Mol. Biosci.* ***(in revision)***

Author Contributions: JN- Contributed to conceptualization, methodology, validation, formal analysis, investigation, data curation, writing-original dRaft, writing- review & editing, visualization; MM contributed to formal analysis, investigation, writing-original dRaft, visualization; TL contributed to validation, Writing-review & editing; KM contributed to conceptualization, formal analysis, writing-original dRaft, writing review & editing, supervision, funding acquisition, project administration; LW contributed to conceptualization, data curation, writing-original dRaft, writing review & editing, visualization, supervision, project administration, funding acquisition.

2.1 Introduction

Cellular retinoic acid binding protein 1 (CRABP1) is a highly conserved protein that is believed to function by binding and sequestering cytosolic retinoic acid (RA), which is important in controlling cellular RA concentration [21,22]. This view centers on the well-known genomic activities of RA, mediated by nuclear RA receptors (RARs) that regulate gene expression, generally referred to as the canonical activities of RA [2,81]. Increasing studies have identified rapid cytosolic (without involving nuclear RARs) activities of RA, which could modulate cytosolic signaling pathways as demonstrated in multiple cell types including adipocytes [35,82], cardiomyocytes [33,34], stem cells [29,32] and neurons [37,40]. Recently, it has been established that CRABP1 acts as a direct mediator of these rapid cytosolic activities of RA in a cell context-dependent manner, referred to as non-canonical RA activities reviewed in [83].

In embryonic stem cells, adipocytes and neural stem cells that are extremely sensitive to growth factor-elicited signaling pathways such as the mitogen-activated protein kinase (MAPK) pathway [54,56], CRABP1 is important for stem cell proliferation [29,32], exosome secretion [38], and adipokine production [82]. The MAPK pathway is initiated by the membrane-bound Ras GTPase which serves as a molecular switch to activate the Raf-MEK-ERK kinase cascade upon growth factor stimulation [84]. In this pathway, CRABP1 competes with Ras for direct interaction with Raf kinase, ultimately resulting in dampened ERK activation in cells highly expressing CRABP1 [36,83]. Using nuclear magnetic resonance (NMR), we have revealed a Raf-interacting surface area on the β-sheet of CRABP1, providing molecular insight and a potential structural basis of

CRABP1's function in negatively regulating MAPK signaling [36]. In this context, CRABP1 is a negative regulator acting to "dampen" or "safe-guard" the activation of MAPK signaling pathway that is crucial to growth factor-sensitive cells.

We have recently uncovered that CRABP1 can also elicit specific non-canonical activity to negatively modulate Ca^{2+}-calmodulin dependent kinase 2 (CaMKII) signaling [33,40]. CaMKII is a serine/threonine kinase and a major mediator of calcium signaling for essential functions of excitable cells such as cardiomyocytes and neurons. CaMKII exists in four major isoforms: α, β, δ, and γ, with α and β predominately expressed in the CNS and δ in cardiac tissues [63,85]. In cardiomyocytes, CaMKII plays a crucial role in the coordination of excitation-contraction coupling required for the mechanical activity of cardiac tissue [63]. In neurons, CaMKII is best known for its critical role in synaptic transmission, essential for most neuronal functions including motor activity, and learning and memory [64,65]. As a major mediator of Ca^{2+} signaling in excitable cells, CaMKII is directly activated through elevated cytosolic Ca^{2+} which binds calmodulin (CaM). The Ca^{2+}-bound CaM then directly binds CaMKII, freeing the kinase from its autoinhibited, inactive state to target/phosphorylate specific downstream substrates necessary for the functions of cardiomyocytes and neurons [67,68]. Critical to disease processes, overactivation of CaMKII activity in both cardiomyocytes and neurons is a well-documented pathophysiological driver of cardiac and neurological diseases [69,70,86]. However, effective modulation or control of CaMKII activation in order to manage these diseases remains a challenge[87]. To this end, both cardiomyocytes and motor neurons highly express CRABP1, and CRABP1 can negatively regulate CaMKII activation [33,40].

In mice, upon b-adrenergic assault and subsequent CaMKII over-activation, CRABP1 protects against cardiac damage by dampening CaMKII over-activation in cardiomyocytes [33]. In mouse motor neurons (MNs), CRABP1 dampens CaMKII over-activation thereby maintaining healthy production of agrin in MNs, a proteoglycan essential for the maintenance of neuromuscular junction health [40,73]. Recently, we have further reported that RA and CRABP1-ligands, C4 and C32, can protect against excitotoxic assault in MNs grown in cultures [88]. As such, understanding how CRABP1 modulates CaMKII activation can be potentially helpful in designing therapeutic strategies for cardiac and neurological diseases.

In this study, through biochemical and molecular studies, we have uncovered a molecular/structural basis for CRABP1's action in modulating CaMKII activation. NMR data reveal a potential interaction surface on CRABP1 for interacting with the regulatory R domain of CaMKII. Molecular studies show that CRABP1 preferentially interacts with the inactive CaMKII, which provides a molecular basis for the "dampening" effect of CRABP1 with regards to the activation of CaMKII. Data of site-specific mutations of the R domain-interacting surface of CRABP1 confirm the stringent requirement for CRABP1 to maintain this R-interacting surface on the β-sheet barrel, as well as the α-helix segment outside the barrel. We also discuss the molecular and structural bases underlying the highly conserved nature of CRABP1 with regards to its signaling pathway-specificity and primary sequence conservation throughout evolution.

2.2 Results

2.2.1 Structural Regions on CRABP1 contribute to its interaction with CaMKII, and modulation of CaMKII activation

The CRABP1 protein is a member of the intracellular lipid binding proteins (iLBPs) superfamily, characterized by an anti-parallel β-barrel tertiary structure that forms the ligand binding pocket [89–91]. This CRABP1 barrel consists of ten β-strands and is linked to a helix-turn-helix motif [91]. Figure 2-1A shows the highly conserved (> 99%) sequence of the *Mus musculus* CRABP1 isoform (Uniprot ID P62965), with the relevant secondary structures superimposed over the corresponding amino acid sequence. The only non-conserved residue is proline 86, which exists as an alanine in the human and bovine orthologs (Fig. 2-1 A, asterisk) [92]. In this study we examine residues within helix 2 (blue highlight) and β-strands 7 and 8 (yellow highlight) that all contribute to its activity in interacting with, and regulating, CaMKII (Fig. 2-1A). On the crystal structure of CRABP1 (apo form, PDB: 1CBI [91], these residues are located in either the helix-turn-helix motif (blue) or the β-sheet surface of the barrel (yellow) (Fig. 2-1B). Interestingly, the only one non-conserved residue, proline 86, (Fig. 2-1B, black asterisk) is located outside of both regions (helix 2 and β-strands 7 and 8), suggesting that this non-conserved residue is probably not critical for CRABP1's function in this context.

Characterization of a CaMK-R peptide for CRABP1-CaMKII interaction studies

CaMKII is a serine/threonine kinase comprised of three major functional domains- the kinase domain, regulatory (R) segment, variable linker region, and association domain[67]

(Fig. 2-2A). Within the R segment reside three key threonine (Thr) residues: Thr286/7 (depending on isoform), 305 and 306 (Fig. 2-2A, yellow highlight) [67]. Binding of calcium-calmodulin (Ca^{2+}-CaM) to the R segment frees CaMKII from its autoinhibited basal state and exposes Thr286/7 for auto-phosphorylation, thereby activating CaMKII. Autophosphorylation of Thr305 and 306 blocks Ca^{2+}-CaM binding, preventing further activation of the kinase by Ca^{2+}-CaM[67]. Thus, phosphorylation of Thr286/7 is a key marker for activated CaMKII. In this study, activated CaMKII and CaMKII phosphorylated at Thr286/7 (pCaMKII T286/7) will be considered synonymous. It should be noted that all domains, except for the variable linker region, are highly conserved among all the CaMKII isoforms and across species, indicating the functional conservation for each of these domains regardless of CaMKII isoform or homolog [67,68].

In our previous studies, we determined that CRABP1 directly interacts with CaMKII on its three functional domains – kinase domain, R segment, and association/oligomerization domain [33,40]. Furthermore, with regards to CaMKII interaction, CRABP1 competes with calmodulin [33] which binds directly on the R segment of CaMKII and is the major positive regulator of CaMKII activation [67]. Given the "modulatory" nature of CRABP1's action in CaMKII activation, these current studies focus on characterizing CRABP1 interaction with the R-segment of CaMKII. Further, in order to understand molecular interactions of CRABP1 with the R-segment in solution, NMR spectroscopy approaches were used. We first synthesized a 29-residue peptide (Fig. 2-2A, magenta sequence) derived from residues 281-309 of the R segment of Mus musculus CaMKII (Uniprot ID P62965), referred to as "CaMK-R" in the following text.

This CaMK-R was used in lieu of the full-length protein due to mass/size limitations of using NMR [93]. For in-cell functional studies (active vs inactive CaMKII), we exploited an expression construct of the CaMKII β isoform from *Rattus norvegicus* (Addgene #21227). CaMKII itself endogenously forms protein complexes comprised of 12-14 subunits, with each subunit having a molecular weight (MW) of ~50-60 kDa. A single subunit is comprised of the three functional domains. Protein complex formation of the CaMKII multimer is facilitated by interactions between the association domains of each subunit [67,68]. Figure 2-2B shows a Pymol structure of an individual, full-length CaMKII subunit in its basal auto-inhibited form (PDB: 3SOA [94]). Residues that comprise CaMK-R are highlighted in magenta, along with Thr286/7, 305 and 306 as Van der Waals spheres in yellow.

To ensure that the CaMK-R peptide was appropriate for CRABP1-CaMKII interaction studies using NMR, we initially used the PEP-FOLD Peptide structure Prediction Server [95] to predict the secondary structure of CaMK-R. The five top-ranked models indicate that CaMK-R most probably has an α-helical structure (Supplementary Fig. S2-1). To assess whether this proposed helical structure of CaMK-R can properly form in solution, we performed NMR experiments (^{1}H TOCSY and NOESY) to make sequence-specific resonance assignments (Supplementary Fig. S2-2). For additional information on the chemical shifts of CaMK-R, we acquired a natural abundance ^{15}N-^{1}H HSQC spectrum of CaMK-R, with assigned peaks as labeled (Fig 2-2C). Calculating the difference between random coil (RC) chemical shifts and observed chemical shifts for each amino acid ($\Delta\delta = \delta RC - \delta observed$)[96] can provide information on the presence and

type of secondary structure [97]. A series of positive Δδ values (0.1 ppm above RC values) suggests the presence of α-helical structure, whereas a series of negative Δδ values suggests β-sheet structure. Positive Δδ values calculated for CaMK-R residues support the idea that N-terminal residues 4-20 (residues 284-300 in full-length CaMKII) likely have an α-helical structure (Fig. 2-2D). Given the relatively small change in Δδ between observed and RC chemical shifts, this helical "structure" in CaMK-R is actually transient, occurring within a dynamic equilibrium (fast exchange regime on the NMR chemical shift time scale) among numerous states in which only a small fraction is helical at any given instant in time. In any event, the presence of an α-helical conformation in CaMK-R peptide is consistent with this type of structure in the R segment of the parent CaMKII (Fig. 2-2B, magenta).

2.2.2 HSQC NMR reveals the CaMK-R-interacting surface on CRABP1

To first assess whether CaMK-R interacts with CRABP1 in solution, we carried out ^{15}N-^{1}H HSQC experiments with ^{15}N-labelled CRABP1 in the absence of CaMK-R (19 uM, black peaks) and in the presence of CaMK-R (19 uM CRABP1 plus 200 uM CaMK-R, red peaks) (Fig. 2-3A). As exemplified in the HSQC expansion shown in Fig 2-3B, it is apparent that some peaks are chemically shifted, indicating that CaMKII peptide indeed interacts with CRABP1. Using resonance assignments for CRABP1[36], we calculated chemical shift perturbations as plotted vs. the amino acid sequence of CRABP1 in Fig. 2-3C. This chemical shift map identifies several CRABP1 residues that are significantly shifted, ranging from > 2SD from the mean (red highlight), >1SD (pink),

equal to the mean (orange), and < 1SD (cyan). A complete list of CRABP1 residues with maximal chemical shifts is provided in Supplementary Table 2-1. These changes are highlighted on the crystal structure of CRABP1 (PDB: 1CBI) and identify a set of proximal residues within β-strands 7 and 8 as the likely CaMK-R-interacting surface (Fig. 2-3D, green circle). Furthermore, residues His94, Thr96, Tyr108, and Thr110 are solvent exposed, and therefore likely directly interact with CaMK-R. It should be noted that the residue numbering of these mutants is based on the sequence derived from the crystal structure of CRABP1 (PDB: 1CBI). Some chemically shifted resonances fall outside of this proposed interaction surface and are likely the result of allosteric effects resulting from the CRABP1-CaMK-R interaction. Taken together, these HSQC data indicate that CaMK-R interacts with CRABP1, at least at residues His94, Thr96, Tyr108, and Thr110.

As mentioned above, CaMK-R has some transient a-helical structure (Fig. 2-2, Supplementary Fig. S2-1). Interestingly, the regulatory segment of CaMKII protein itself undergoes conformational changes that depend on the CaMKII activation state. In its auto-inhibited form, the N-terminal portion of the regulatory segment indeed has a helical structure (Fig. 2-2B, magenta). However upon activation and exposure of Thr286/7 for auto-phosphorylation, the N terminal portion loses its helical structure, whereas the C-terminal portion forms helical structure [94,98]. The transient N-terminal helical structure in CaMK-R suggests that any in situ interaction would likely be in the context of the auto-inhibited, inactive, state of CaMKII.

2.2.3 Production and characterization of CRABP1 alanine mutant proteins for molecular studies

Our proposed interaction surface between CRABP1 and CaMK-R (Fig. 2-3D, green circle) was elucidated using HSQC NMR experiments. We then employed site-directed mutagenesis to produce alanine-substituted variants of proposed interacting residues His94, Thr96, Tyr108, and Thr110. In addition, we generated an Arg29 mutant to assess whether chemical shifts of this residue are indeed the result of binding-induced allosteric effects (Fig. 2-4A). Each alanine mutant was purified as His-tagged recombinant protein isolated from E. coli (Fig. 2-4B). To ensure that each mutant was folded as in the wild-type, parent protein and to avoid time-consuming production of ^{15}N-labelled proteins, we performed 1D ^{1}H NMR experiments of these mutants to compare them with the NMR spectrum of the parent protein. Because NMR spectra for wild-type CRABP1 protein (black) and each mutant are essentially the same (as indicated by the presence of several defined peaks in the 7-10 ppm amide region (Fig. 2-4C), we concluded that these mutants are folded as the wild-type, parent CRABP1 protein. Therefore, these alanine point mutants were verified as suitable for further molecular studies.

2.2.4 CRABP1 prefers interaction with inactive CaMKII

As mentioned, we have previously reported interaction of CRABP1 with CaMKII, but whether and how this interaction may be affected by CaMKII's activation status has not been determined. In order to address this issue, we employed in vitro pull-down, protein interaction assay. His-tagged CRABP1 protein was purified from E. coli as the

bait. To prepare both inactive and active forms of CaMKII (GFP-CaMKII, Addgene #21227) for pull-down reactions, we exploited mammalian (HEK293T) cells to express CaMKII and stimulated cells with ionomycin, which is known to robustly activate CaMKII [99,100]. The ionomycin-stimulated cells provide active CaMKII whereas vehicle-treated cells provide inactive CaMKII.

We used His-tagged wild-type (WT) and mutant (R29A, H94A, T96A, H94A-T96A double mutant, Y108A, and T110A) CRABP1's, as well as GFP-CaMKII (GFP-CaMKII) prepared from HEK293T cells stimulated with vehicle control or ionomycin to perform a series of pull-down assays, monitored on Western blots. We first determined and confirmed the expected position of GFP-CaMKII from control and stimulated cells using an anti-GFP antibody which detected both active and inactive CaMKII that migrated similarly (Fig. 2-5A left panel, top arrow on the upper blot). Importantly, the anti-p-CaMKII T287 (active CaMKII) antibody detected robustly activated CaMKII from cells stimulated with ionomycin (Fig. 2-5A, left panel, bottom blot). This result clearly demonstrated the success of active and inactive CaMKII preparations using this strategy. HEK293T cells transfected with empty vector expressing only the GFP protein were used as a negative control (Supplementary Fig. 2-3A).

With this strategy, experiments were carried out using the WT and mutated CRABP1 proteins as the bait to pull down inactive or active GFP-CaMKII, and results are shown in Fig. 2-5B. First, it is apparent that the WT CRABP1 was able to pull-down much more inactive CaMKII (WT, - ionomycin) than active CaMKII (WT, + ionomycin), indicating that CRABP1 prefers to interact with the inactive CaMKII, or that CRABP1

forms a more stable complex with the inactive CaMKII than its active form. The signals of inactive (- ionomycin) and active (+ ionomycin) CaMKII bands were quantified, and the ratio of inactive vs. active CaMKII signal was derived to obtain an arbitrary "CRABP1-CaMKII Complex Index" (CCI). A CCI of 1 would indicate the lack of preference for either active or inactive CaMKII, a CCI < 1 would indicate preference for the active CaMKII, whereas a CCI >1 would indicate preference for the inactive CaMKII (see experimental methods for detailed quantification and calculation). By performing multiple experiments, quantitated results are shown in Fig. 2-5B. In the case of WT CRABP1, a CCI (inactive/active CaMKII ratio) of approximately 2 was derived, i.e. CRABP1 prefers interaction with inactive CaMKII.

Interestingly, these CCI analyses show that all the mutated CRABP1s were very different from the WT CRABP1 as shown in Fig. 2-5. These CRABP1 mutants could be categorized into two groups: 1) No preference for inactive or active CaMKII (i.e. a CCI of approximately 1) such as R29A, H94A and T96A), and 2) Preferential interaction with active CaMKII (pCaMKII T287) (i.e. a CCI significantly < 1) such as H94A-T96A double mutant, Y108A, and T110A. The amount of WT or mutant CRABP1 was monitored for normalization (described in Materials and Methods section 4.9) (Fig. 2-5A, right panel, bottom blot).

All together, these data show that CRABP1 can discriminate the inactive versus the active CaMKII. Specifically, the WT CRABP1 prefers to complex with the inactive CaMKII, or it forms more stable complex with the inactive CaMKII. This would provide one mechanism underlying the observed "dampening" effect of CRABP1 in modulating

CaMKII activation. Importantly, disrupting any of the residues identified from NMR data caused a loss of this discriminating effect, probably because these residues are all important such that any alternation would compromise the unique conformation of the β-sheet surface of CRABP1 (such as H94A, T96A, and Y108A, T110A mutants) or the allosteric helix region (the R29A mutant), both are required for its ability to preferentially interact with the inactive CaMKII. Surprisingly, certain mutations, such as Y108A, T110A and H94A-T96A, completely reversed CRABP1's discriminatory property and preferred to form complex with the active CaMKII (see discussion).

2.2.5 Functional Consequences of disrupting CRABP1-CaMKII interaction

The CRABP1-mediated dampening of CaMKII activation was previously determined in an established mammalian culture system where HEK293T cells were co-transfected with CRABP1 and CaMKII, followed by monitoring the status of in-cell CaMKII activation [40]. Using this established in-cell assay, we then determined the functional consequence of expressing WT and various mutated CRABP1 proteins also examined in protein interaction studies described above in Fig. 2-5.

As expected, WT CRABP1 significantly dampened CaMKII activation, indicated by a significant decrease of relative CaMKII activation (marked by reduced phospho-Thr287, pCaMKII T287) (Fig. 2-6A and B). The mutants that lost CaMKII-discriminating ability such as R29A (allosteric, helix position), H94A, and T96A (CaMKII binding site, β-sheet face) failed to significantly affect CaMKII activation. Interestingly, H94A-T96A double mutant, Y108A, and T110A (all prefer interaction with

the active CaMKII, Fig. 2-5 above) elevated CaMKII activation (Fig. 2-6A and B). Together, the protein interaction (Fig. 2-5) and functional (Fig. 2-6) data indicate that disruption of an allosteric site (R29A) or certain residues within the CaMKII binding site (H94A and T96A) cause CRABP1 to lose its CaMKII-discriminating and dampening effects. Whereas certain mutations such as H94A-T96A, Y108A, and T110A can result in an opposing phenotype of CRABP1, i.e. they all prefer interaction with active CaMKII and elevate CaMKII activation.

These data show that the ability of CRABP1 to discriminate between inactive and active forms of CaMKII underlies its function in regulating CaMKII activation. The WT protein preferentially forms a complex with inactive CaMKII, probably stabilizing the inactive kinase thereby dampening its activation. A disruption in key CaMKII-interacting surface or the a-helix segment of CRABP1 would impact its ability to discriminate inactive from active forms of CaMKII, with corresponding changes in its functional effect with regards to CaMKII activation.

2.3 Discussion

In this study we identify an interaction surface on CRABP1 for CaMKII binding, along with an allosteric site located on the a-helix segment of CRABP1. *In vitro* interaction studies identify the ability for CRABP1 to discriminate between the inactive and active forms of CaMKII with a preference towards association the inactive CaMKII, which may underline CRABP1's dampening effect in CaMKII activation. Disruptions on residues within the CaMKII binding site on the β-sheet barrel or the allosteric region

within the a-helix cause a loss of this discriminatory ability or a shift in CRABP1 to preferentially associate with active CaMKII. Figure 2-7 depicts the proposed structural basis of CRABP1-mediated regulation of CaMKII. WT CRABP1 preferentially complexes with inactive CaMKII, resulting in dampened CaMKII activation (Box 1). Disruption of residues within the CaMKII binding surface on the β-sheet face (H94A-T96A double mutant, Y108A, T110A) result in CRABP1 preferentially complexing with the active form of CaMKII, marked by Thr287 phosphorylation. This would cause enhanced kinase activation (Box 2). Disruption of allosteric residues (R29A) causes a loss of this discriminatory function of CRABP1 in association with CaMKII (Box 3).

This finding that CRABP1 can differentiate between inactive CaMKII and active CaMKII (marked by pThr286/7) is most interesting. The inactive and active forms of CaMKII are conformationally very distinct from each other [67]; our results would indicate that CRABP1 can structurally discern the inactive and active CaMKII conformations. Further, the results suggest that CRABP1 residue side-chains are important in conferring this discriminatory ability (Fig . 2-5). It is tempting to speculate that side-chain identity is not only important in the context of CaMKII regulation, but also in a broader sense with regards to CRABP1's function in RA's non-canonical signaling pathways modulating multiple signaling pathways, such as MAPK versus CaMKII. To this end, it is interesting that the interaction surface on CRABP1 for Raf binding [36] spans strands 6 and 7; whereas, the interaction surface for CaMKII identified in this study spans stands 7 and 8. Furthermore, the allosterically affected residues are different for CaMKII binding versus Raf binding. These interesting features would support the notion that, stringent functional

constraints on CRABP1, for its role in safe-guarding multiple signaling pathways important for various physiological processes, would provide an evolutionary pressure to conserve its primary sequence across species and throughout evolution.

Finally, mutations drastically affecting side-chains within the CaMKII-interacting β-strand surface (H94A-T96A, Y108A, and T110A) revealed an especially interesting phenotype. It appears that destruction of these side-chains can apparently transform CRABP1 into an activator of CaMKII, i.e. preferentially associate with active CaMKII. This would suggest that not only do these residues aid in maintaining CRABP1's ability to differentiate amongst CaMKII conformations, but also the modulatory activity of CRABP1 could potentially be "tuned" towards a desired signaling outcome, such as by binding of various ligands. Our previous studies have reported that the binding of endogenous CRABP1 ligand, RA, dramatically increases the thermal stability of CRABP1, clearly altering the structural dynamics of CRABP1 [88,101]. Furthermore, synthetic CRABP1-binding ligands C3, C4, and C32 also increase the thermal stability, albeit with a more subtle magnitude. Nevertheless, these ligands could elicit CRABP1-dependent biological effects in cultured cell models of cancers and MN degeneration. The potentials of CRABP1 side-chains within the ligand binding pocket, i.e. the β-barrel, provide an exciting opportunity in future rationale designs of CRABP1 therapeutics

2.4 Material and Methods

DNA constructs and chemicals

GFP-CaMKII β construct was obtained from Addgene (Addgene Cat #21227). The His-tagged, wild-type (WT) CRABP1 DNA construct for bacterial expression and subsequent protein purification was generated as described in Park et al [36]. The Flag-tagged, WT CRABP1 DNA constructs for mammalian expression used in HEK293T CRABP1-CaMKII cell assays was described in Park et al [36]. Constructs of alanine point mutants of His-tagged CRABP1 and Flag-tagged CRABP1 were generated using the Q5® Site-Directed Mutagenesis Kit (New England BioLabs Inc., Cat # E0554S) according to manufacturer's instructions. To validate successful site-directed mutagenesis, the relevant regions of the CRABP1 insert from each mutant construct was validated by Sanger Sequencing, which was performed by the University of Minnesota Genomics Center Facility (Minneapolis, MN).

Chemical reagents utilized in this study are as follows: Tris-d11 solution (Sigma Cat # 486248), Sodium acetate-d3 (Sigma Cat # 176079), DTT (Dithiothreitol) (Gold Biotechnology Cat# DTT10), Tris(2-carboxyethyl) phosphine hydrochloride solution (Sigma Cat # 646547), Dimethyl sulfoxide (DMSO) (Sigma Cat # D8418), Ionomycin salt (Sigma Cat # I0634). Ionomycin for molecular and cell studies was prepared by dissolving it in DMSO.

Cell Culture

HEK293T cells (ATCC) were maintained as described in Nhieu et al [88]. Briefly, HEK293T cells were maintained in DMEM (Thermo Fisher Cat # 11965092)

supplemented with 10% FBS and 1% Penicillin-Streptomycin (Thermo Fisher Cat # 15140122) in an incubator maintained at 37 ^{o}C and 5% CO2. HEK293T cells were routinely tested for and found to be negative for mycoplasma.

Protein expression and purification of WT CRABP1, Alanine Mutants, and ^{15}N WT CRABP1

Protein expression was carried out as described in Park et al [36], with the following modification of growing the induced culture at 16 ^{o}C overnight. The bacterial pellet was isolated via centrifugation (5000 x g, 15 minutes, 4 ^{o}C) and resuspended in lysis buffer (1 x PBS, 10 mM imidazole, pH 8.0). Lysis was carried out by 3 rapid freeze-thaw cycles utilizing liquid nitrogen and a water bath warmed to 55 ^{o}C, followed by 5 rounds of sonication on ice for 90 seconds with a 2 second pulse. A 90 second resting period for cooling was conducted in between each round of sonication. The bacterial lysate was subjected to high-speed centrifugation (23,000 x g, 60 minutes, 4 ^{o}C) to clear the lysate of cell debris and/or aggregated protein. The lysate was then filtered through a 0.25 um filter (Cytvia Cat # 4652) for further clarification of debris. Additional imidazole to a final concentration of 20 mM was added to the lysate to prevent non-specific interactions with the affinity nickel column resin. The lysate was run through the nickel resin column (HisTrap FF, Cytvia Cat #17531901) twice for optimal binding to the resin. The HisTrap column was then washed with 25 column volumes (CV) of lysis buffer. His-tagged protein was eluted with 12.5 CV's of elution buffer (1 x PBS, 500 mM imidazole, pH 8.0). Dithiothreitol (DTT) was added to a final concentration of 1 mM to the eluted

protein to ensure cysteine reduction. The eluted protein was then concentrated using an Amicon spin filter with a molecular weight cut-off of 10 kDa (MilliporeSigma Cat # UFC9010) for downstream size exclusion chromatography. Size exclusion chromatography was performed using a an AKTA FPLC system with a Frac 950 fraction collector. Size exclusion chromatography was run with a Superdex 200 increase 10/300 gl column (Cytvia Cat # 28990944) in 1 X PBS, pH 8.0. Relevant fractions were collected and pooled and DTT added to a final concentration of 1mM. Protein concentration was measured using the absorbance at 280 nm (A280) on a NanoDrop machine (Thermo Fisher). For accurate quantification of protein concentration, the extinction coefficient and expected molecular weight (MW) for WT and each CRABP1 mutant was determined using the Expasy ProtoParam tool (https://web.expasy.org/protparam/). Extinction coefficients are as follows: WT CRABP1, R29A, H94A, T96A, H94A-T96A, T110- 20,970 M-1 cm-1 and Y108A 19,480 M-1 cm-1. WT CRABP1 mutants have an expected MW of approximately 17 kDa. ^{15}N-labelled WT CRABP1 used in NMR experiments was expressed and purified as described in Park et al.

Purity was assessed by running 1ug of WT CRAPB1 and mutants on a 13.8% SDS polyacrylmade (v/v) gel and stained with Coomassie Brilliant Blue R-250 Staining Solution (Biorad Cat # #1610436). Given the inherent variability across manufactures, molecular weight markers from two different manufactures (Prometheus Protein Biology Products Ca t# 83-650 and Thermo Fisher Cat # 26619) were used to assess the apparent

molecular weight WT and CRABP1 mutants. The protein gel was then de-stained by boiling with ddh20. Images were acquired using the Bio-rad Chemi Doc Imager.

CaMK-R peptide synthesis and preparation for NMR experiments

The CaMK-R peptide used in NMR experiments was synthesized by the Department of Biochemistry, Biophysics, and Molecular Biology Peptide Synthesis Services at the University of Minnesota. For NMR experiments, the CaMK-R peptide was prepared by resuspending the lyophilized peptide in NMR buffer (30 mM d11-Tris-d3-acetate, pH 6.2, 75 mM Na2SO4, 10 μM ZnCl2, 1 mM TCEP). Peptide concentration was measured using the absorbance at 205 nm with an extinction coefficient of 31 mL mg-1 cm-1 [102] on a Nanodrop machine.

NMR sample preparation, experimental parameters and data analysis

All NMR experiments were performed using samples made up as follows: 30 mM d11-Tris-d3-acetate, pH 6.2, 75 mM Na2SO4, 10 μM ZnCl2, 1 mM TCEP, made up using a 95% H2O/5% D2O mixture (v/v). All NMR experiments were carried out at 30°C on a Bruker 850 or 900 MHz Avance III NMR spectrometer equipped with an H/C/N triple-resonance probe and x/y/z triple-axis pulse field gradient unit. 1D experiments with excitation sculpting for solvent suppression were carried out on parent CRABP1 (85 uM), mutant proteins (50-210 uM) and CAMKII-R (100uM) using the following parameters: 16 ppm sweep width, 32K data points and 32 scans. A 950 uM CAMKII-R sample was used to collect a gradient sensitivity-enhanced version of the two-dimensional ^{1}H-^{15}N (natural abundance) HSQC experiment (1024 scans) with 256 (t1) x

2048 (t2) complex data points and 32 ppm and 1 ppm sweep width in the ^{15}N and ^{1}H dimensions, respectively. Phase-sensitive versions of 2D NOESY (with WATERGATE solvent suppression) and TOCSY, (with presaturation using MLEV) were collected on 100 uM CAMKII-R, using the following parameters: 256 (t1) x 2048 (t2) complex data points, 11 ppm sweep width and 32 scans. Additionally, a 2D ^{1}H-^{13}C (natural abundance) HSQC with 512 (t1) x 2048 (t2) data points and 90 ppm and 16 ppm sweep width in the ^{13}C and ^{1}H dimensions, respectively, was collected on the 100 uM CAMKII-R sample. Raw data were converted and processed using NMRPipe [103] and analysed with NMRview [104].

In vitro his-pulldown assay

For in vitro pull-down studies, purified His-CRABP1 (WT or mutants) served as the bait protein to pull-down the prey protein, GFP-CaMKII. The His-CRABP1 bait protein was prepared by binding purified His-CRABP1 (5 uM) to nickel-nitrilotriacetic acid resin (Ni-NTA, Qiagen) in a total volume of 500 ul of reaction buffer (50 mM Tris pH 8.0, 150 mM NaCl, 0.2% (v/v) NP-40, 20% glycerol, 200 mM imidazole) for 1 hour at 4 ^{o}C with agitation.

To prepare HEK293T cells as a source of GFP-CaMKII for pull-down experiments, cells first were seeded at a density of 3 x 106 cells into a10 cm dish 18-24 hours prior to transfection. On the day of transfection, cells were exchanged into incomplete DMEM medium (Thermo Fisher Cat # 11965092) and transfected with 10 ug of GFP-CaMKII DNA using polyethylenimine (PEI) max transfection reagent

(Polysciences Cat # 24765). A PEI:DNA ratio of 1:3 was used [105]. Cells were then subjected to downstream pull-down assay experiments 48 hours post-transfection. HEK293T cells transfected with the empty backbone that expresses only GFP protein was used as a negative control. In order to generate inactive CaMKII prey protein and active CaMKII prey protein, HEK293T cells were treated with DMSO (vehicle control) or ionomycin (10 uM, 10 minutes), respectively. Treated cells were immediately harvested for whole cell lysate protein extraction. Whole cell lysate protein extraction was carried out by resuspending pelleted cells in lysis buffer (50 mM Tris pH 8.0, 150 mM NaCl, 0.2% (v/v) NP-40, 20% glycerol, 1X protease-phosphatase inhibitor solution (Cell Signaling Cat # 58725)). Then cell lysate was centrifuged at high speed (16,0000 x g, 15 minutes, 4 ^{o}C) to remove debris. Then the cell lysate protein extract was quantified using Bradford Assay with Bradford reagent (Biorad Cat # 5000001) on a Biorad Smart Spec spectrometer.

250 ug of GFP-CaMKII lysate (DMSO or ionomycin treated) was pre-cleared with incubation with Ni-NTA beads alone for 1 hour at 4 ^{o}C with agitation. The pre-cleared lysate was then incubated with bait His-CRABP1 (WT or mutants) in reaction buffer (50 mM Tris pH 8.0, 150 mM NaCl, 0.2% (v/v) NP-40, 20% glycerol, 200 mM imidazole, 1X protease-phosphatase inhibitor solution) overnight with agitation at 4 ^{o}C. Then the beads from the pull-down reactions were washed for 30 seconds with agitation, five times with wash buffer (50 mM Tris pH 8.0, 150 mM NaCl, 0.2% (v/v) NP-40, 20% glycerol, 20mM imidazole). The reaction was terminated by removing the wash buffer and resuspending the reaction Ni-NTA beads in SDS lysis buffer (9 parts: 128 mM Tris

base, 10% (v/v) glycerol, 4% (w/v) SDS, 0.1% (w/v) bromophenol blue, pH to 6.8 and 1 part: β-mercaptoethanol). Then western blot was performed as a read out for pull-down assay. Anti-pCaMKII Thr286/7 was used to confirm that ionomycin stimulation indeed induced CaMKII activation. Anti-GFP was used to detect total pulled-down GFP-CaMKII and Anti-His was used to detect CRABP1 in the pull-down assay. All experiments were repeated at least three independent times (n=5).

In-Cell CRABP1-CaMKII assay

For in-cell CRABP1-CaMKII assays, HEK293T cells were seeded at a density of 2 x 105 cells into each well of a 6-well plate a day prior to transfection. PEI transfection reagent was used as described in section 4.6. A total of 2.5 ug of GFP-CaMKII and CRABP1 (WT or mutant) was co-transfected with a 1:5 ratio of DNA mass (ug) of GFP-CaMKII to CRABP1. After 48 hours post-transfection cells were then subjected to downstream in-cell CRABP1-CaMKII assays. To stimulate CaMKII activation, HEK293T cells were treated with either DMSO (vehicle control) or ionomycin (5-10 minutes, 10 uM). Preliminary studies determined that 5-10 min was the optimal window for stimulation to consistently detect WT CRABP1 dampening of CaMKII and mutant effects on CaMKII activation. Cells co-transfected with empty vector backbone and GFP-CaMKII were used as a control. Cells were then immediately harvested using SDS lysis buffer and subjected to downstream western blot procedures. Anti-pCaMKII Thr286/7 was used to detect CaMKII activation, Anti-GFP was used to detect total GFP-CaMKII, anti-β-actin was used to detect actin as a loading control, Anti-Flag was used to detect

Flag-WT or mutant CRABP1. Experiments were repeated at least three independent times (n=6).

Western Blotting

For in-cell CRABP1-CaMKII assays, cell lysates were separated on 9% (v/v) SDS polyacrylamide gels and transferred onto 0.45 μm PVDF membranes (Millipore Sigma Cat. IPVH00010). For His pull-down assays, reactions were separated on a 10% (v/v) SDS polyacrylamide gels and transferred on a 0.45 PVDF membrane. Primary antibodies and their dilutions used include, Anti-p-CaMKII (cat #: 127165, 1/1000) from Cell Signaling-Danvers, MA, USA, Anti-GFP (cat #: SC-9996, 1/1000) from Santa Cruz Biotechnology, Anti-β-Actin (cat #: SC-47778, 1/1000) from Santa Cruz Biotechnology-Dallas, TX, USA, , Anti-FLAG from Sigma (cat#: F3165, 1:1000), Anti-His (Cat # sc-8036, 1:1000) from Santa Cruz Biotechnology-Dallas, TX, USA and Secondary antibodies used include Goat Anti-Mouse-IgG-HRP (cat #: GTX26789, 1/5000) from GeneTex, Irvine, CA, USA, and Goat Anti-Rabbit-IgG (cat #: 11-035-144, 1/2000) from Jackson ImmunoResearch, Ely, UK.

Western Bright ECL substarate was used for chemiluminescent detection of western blot signals (Advansta Cat # K-12045-D50) A Bio-Rad ChemiDoc Imager, Hercules, CA, USA (cat #: 17001402) was used to collect images.

Data Analysis and Software

In order to clearly convey this discriminatory ability of CRABP1 and the functional consequences of CRABP1 mutation in pull-down assay experiments, we generated a numerical index called the "CRABP1-CaMKII Complex Index (CCI)". To calculate this CCI, we first performed densitometry analysis of western blots to normalize GFP-CaMKII to His-CRABP1 in unstimulated (-ionomycin) and stimulated (+ionomycin) conditions. This calculation determines the relative amount of CRABP1 complexed with inactive (CRABP1-inactive CaMKII) or active CaMKII (CRABP1-active CaMKII). Then the ratio of CRABP1-inactive CaMKII to CRABP1-active CaMKII (CRAPB1-inactive: CRABP1-active) was calculated. Theoretically, as this ratio approaches 1, the amount of inactive and active CaMKII bound to CRABP1 is equivalent. This would indicate a loss of the discriminatory function of CRABP1 to bind either inactive or active CaMKII. Thus, we set 1 as a threshold value to measure this discriminatory ability of CRABP1. If this ratio is greater than 1 (>1), this indicates that CRABP1 prefers inactive CaMKII. If this ratio is less than 1 (<1), this indicates that CRABP1 prefers active CaMKII. To quantify this CCI, we performed a One-sample t-test to determine if WT or CRABP1 mutants significantly differed from this theoretical threshold value of 1 [106,107]. Pulldown experiments were performed at least three independent times (n= 5).

For in-cell CRABP1-CaMKII assay experiments densitometric analysis of western blots was performed by first normalizing pCaMKII T287 signal to total GFP-CaMKII for empty vector (EV) control, WT CRABP1 and mutant conditions. Then the fold-change of empty vector (EV) (WT or mutant condition divided by EV control) was

taken to calculate relative CaMKII activation. One-way ANOVA performed followed by Dunnett's test for multiple comparisons [108] was performed to determine if WT or mutant CRABP1 differed from empty vector control. Pulldown experiments were performed at least three independent times (n= 6). Densitometric analysis was performed using Fiji ImageJ [109].

Software used in this study include: Pymol ver. 1.8.6.2 (Schrödinger, LLC; http://www.pymol.org/pymol) for rendering and creating figures for CRABP1 and CaMKII crystal structure, Bruker TopSpin ver. 3.5 or NFRAM-Sparky [110] was used to create spectra of NMR data, Origin software was used to plate chemical shifts NMR data. GraphPad Prism 6 was used for statistical analyses and graphs for pull-down and in-cell CRABP1-CaMKII assay experiments, Biorender.com was used to create the summary figure.

2.5 Chapter 2 Figures

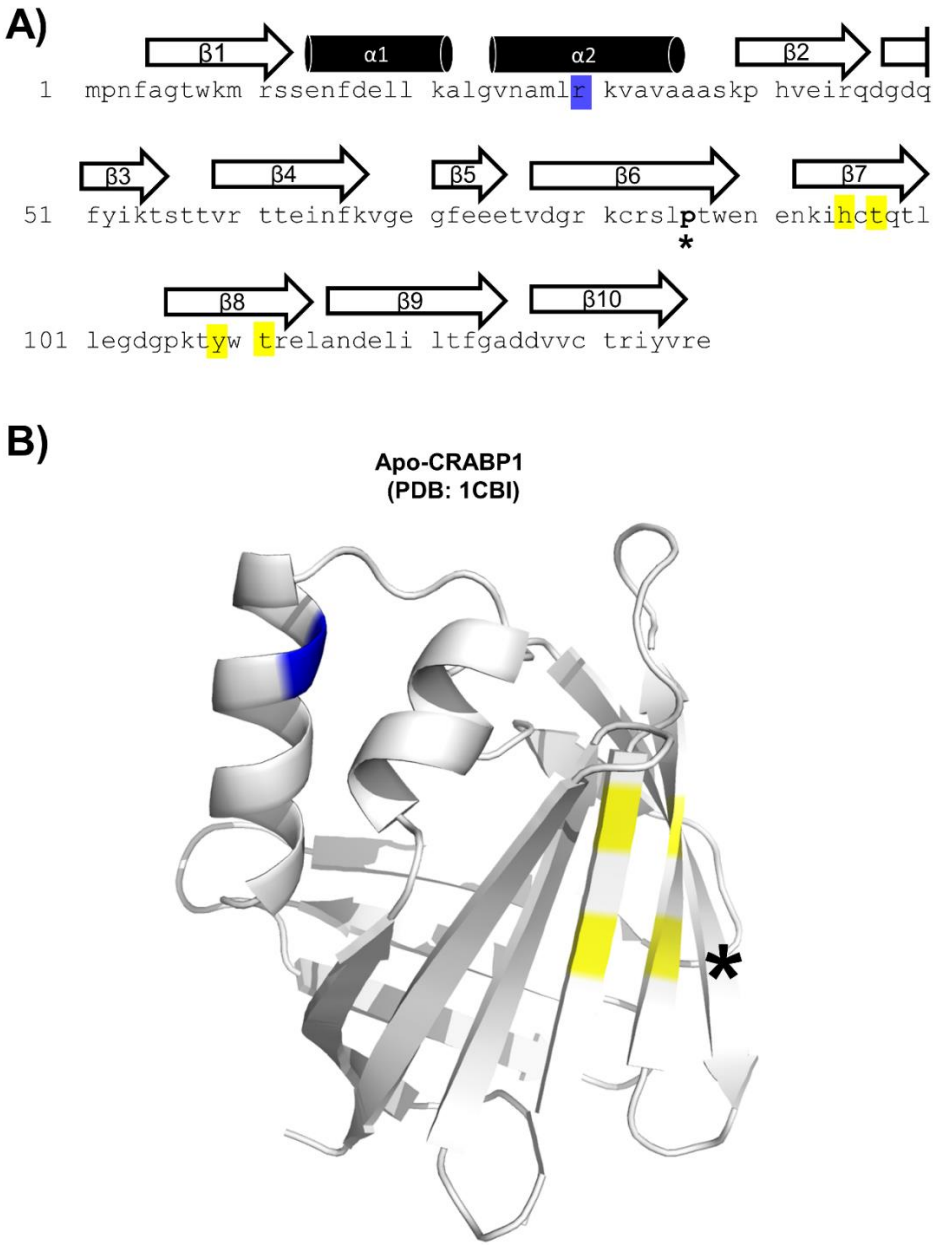

Figure 2-1 Structural details of the CRABP1 protein.

(A) The CRABP1 amino acid sequence from *Mus Musculus* (UniProt ID P62965). Secondary structures are superimposed above their relevant sequence. Yellow and blue

highlights indicate the residues identified in this study relevant to CaMKII modulation. The asterisk (*) indicates the only non-conserved residue, proline 86, across CRABP1 mammalian orthologs. (B) The crystal structure of apo-CRABP1 (ligand-free, PDB1CBI) with the residues of interest mapped to the helix-turn-helix motif (blue) and b-sheet face (yellow). The non-conserved proline 86, located outside the regions of interest, is marked by an asterisk (*). Crystal structure image was generated using Pymol software.

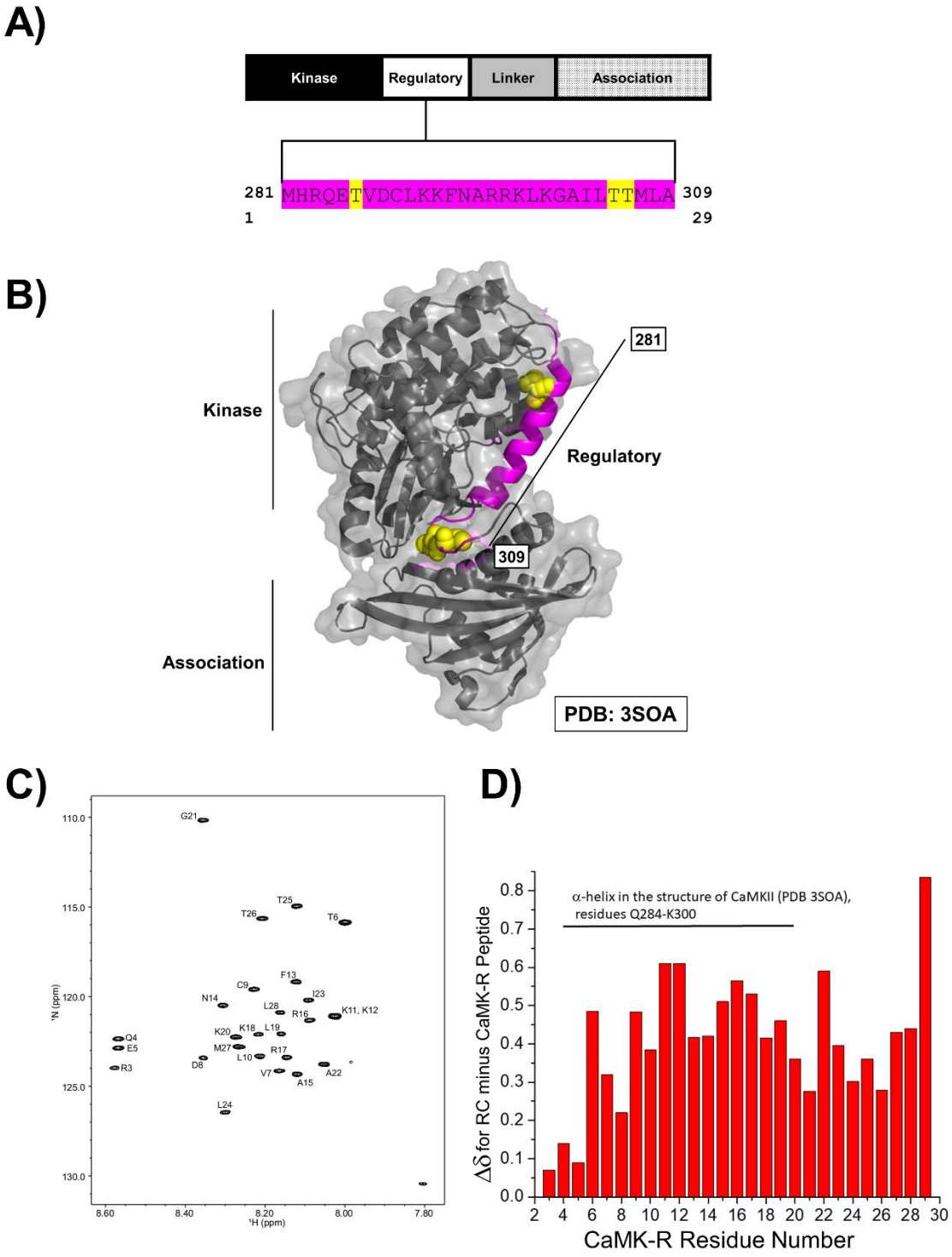

Figure 2-2 . Structural details of the CaMK-R peptide.

(A) CaMK-R peptide sequence (magenta) mapped to the full-length CaMKII and its functional domains. Major regulatory residues threonine 286/7, 305 and 306 are highlighted in yellow. (B) CaMK-R peptide sequence (magenta) mapped to the full-length crystal structure of auto-inhibited CaMKII (PDB 3SOA). Major regulatory residues threonine 286/7, 305 and 306 are displayed as yellow space-filling spheres. (C) HSQC spectra of the CaMK-R peptide. Spectra was generated using Bruker TopSpin Software. (D) Chemical shift changes ($\Delta\delta$) for the difference between random coil (RC) values and the CaMK-R peptide values plotted against CaMK-R residue number. CaMK-R residues 4-20 map to residues 284-300 of full-length mus musculus CaMKII alpha (Uniprot ID P11798). The plot was generated using Origin Software.

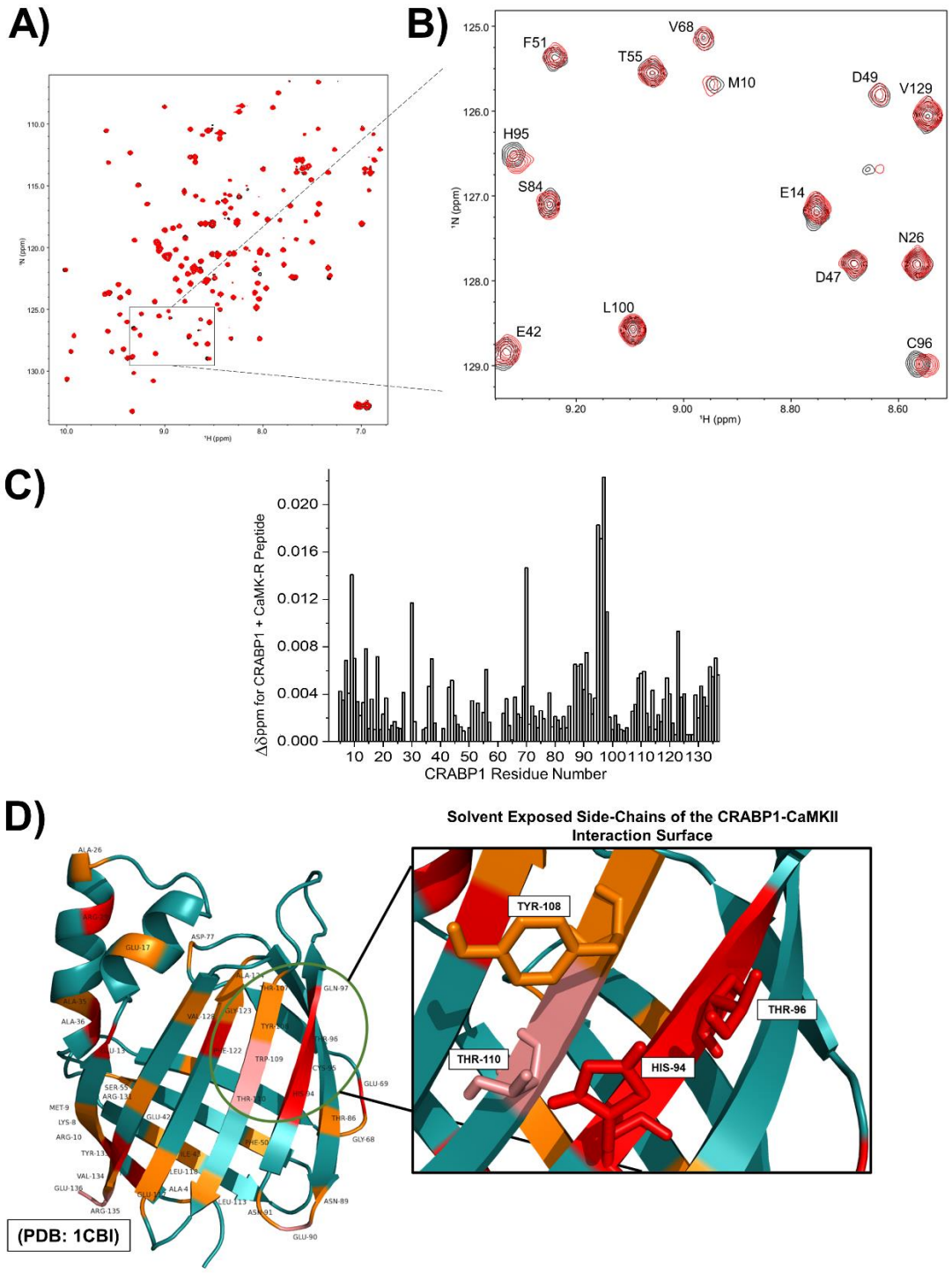
A)
B)
F51
V68
T55
M10
D49
V129
H95
S84
E14
N26
D47
L100
E42
C96
¹H (ppm)
¹N (ppm)
C)
ΔSppm for CRABP1 + CaMK-R Peptide
CRABP1 Residue Number
D)
Solvent Exposed Side-Chains of the CRABP1-CaMKII Interaction Surface
TYR-108
THR-96
THR-110
HIS-94
(PDB: 1CBI)

Figure 2-3 NMR reveals a CaMKII interaction surface on the b-sheet face of CRABP1.

(A) A full HSQC spectrum of CRABP1 alone (black, 19uM) with a spectrum of CRABP1 (19uM) + CaMK-R peptide (200uM, red) overlaid. (B) Expanded region of the HSQC showing clear chemical shifts of CRABP1 residues upon CaMK-R addition. HSQC spectra were generated using NMRFAM-Sparky. (C) Maximal chemical shift changes ($\Delta\delta$) of CRABP1 residues resulting from CaMK-R addition plotted against CRABP1 residue number. The plot was generated using Origin software. (D) CRABP1 residues with maximal chemical shift changes > 2 standard deviations above (red), > 1 standard deviation above (pink) or equal to the mean (orange) mapped to the CRABP1 crystal structure (PDB 1CBI). The green circle indicates the proposed CaMK-R binding site and the inset shows solvent exposed side-chains. Images were generated using Pymol Software.

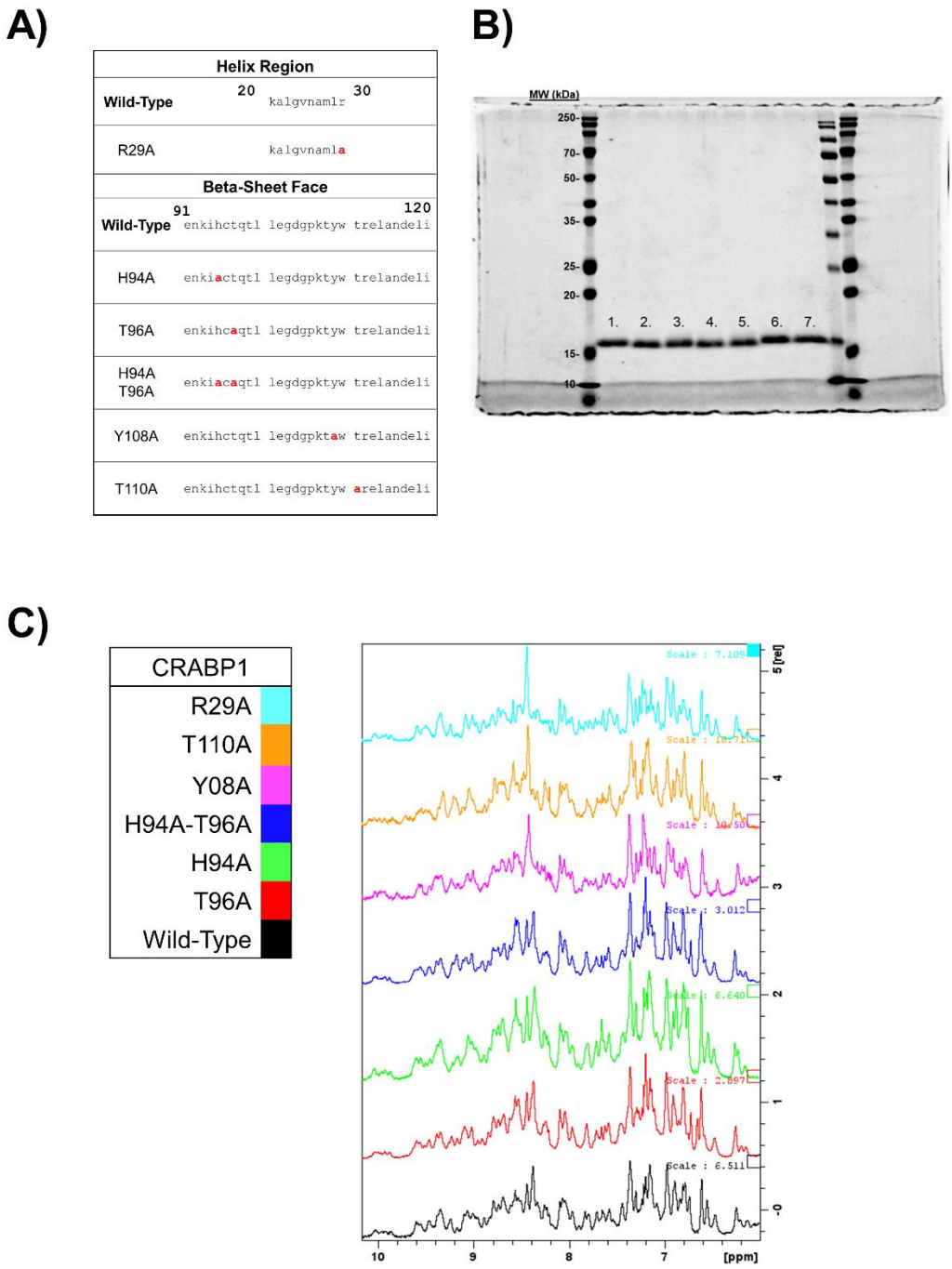

Figure 2-4 Protein fold is retained in CRABP1 mutants.

(A) Sequence positions of CRABP1 alanine point mutations (red). (B) Coomassie stained SDS-PAGE gel of purified, His-Tagged CRABP1 mutants (1ug). Lane labels are as follows: Wild-Type (WT) (1), R29A (2), H94A (3), T96A (4), H94A-T96A double mutants (5), Y108A (6), and T110 (7). The first, second to last, and last lanes contain molecular weight marker from two different manufacturers. (C) 1D NMR spectra of the amide region of WT CRABP1 and mutants. Spectra scales were adjusted accordingly to visualize signal peaks. Spectra were generated using Bruker software.

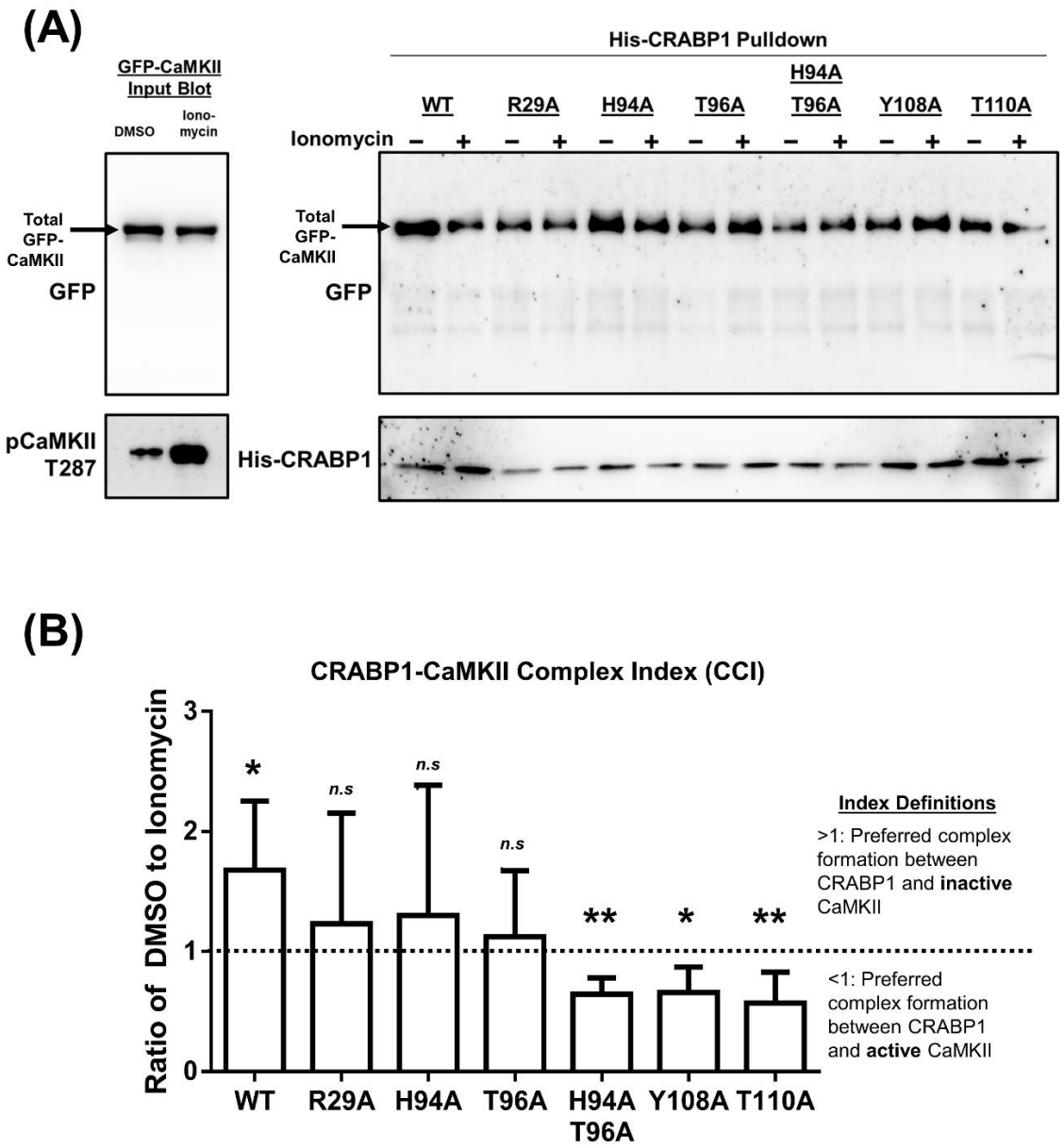

Figure 2-5 CRABP1 side-chain mutation dictates complex formation with CaMKII. (A) His-pulldown assay using purified, His-tagged wild-type (WT) CRABP1 or mutants (bait) and GFP-CaMKII (prey) lysate from HEK293T cells. Top left: Input western blot with a black arrow indicating the expected band positions for GFP-CaMKII, detected by anti-GFP antibody. Bottom left: Western blot to confirm that CaMKII is indeed activated

upon ionomycin stimulation (10 uM, 10 minutes), marked by phosphorylated threonine 287 (pCaMKII T287), and detected by an anti-pCaMKII T287 antibody. Top Right: His-pulldown assay of WT CRABP1 and mutants with unstimulated (-ionomycin) or stimulated (+ ionomycin) lysate from GFP-CaMKII lysate. The black arrow indicates the expected position of GFP-CaMKII in the pulldown assay, detected by anti-GFP antibody. Bottom right: Western blot to detect the levels of WT and mutant CRABP1 present in each pull-down reaction, detected by anti-His antibody. DMSO was used a vehicle control (unstimulated condition) for ionomycin stimulation. (B) Quantification of CRABP1-CaMKII Complex Index (CCI). The dashed line (---) marks 1 as the CCI index threshold. Values above the threshold of 1 (>1) indicate CRAPB1's preference for inactive CaMKII. Values below the threshold (<1) indicate CRAPB1's preference for active CaMKII. One-sample t-test was performed to compare if the CCI significantly differed from the threshold value of 1. * $P \leq 0.05$, ** $P \leq 0.01$. "n.s." indicates not significant. Error bars are presented as the mean ± standard deviation. (n=5).

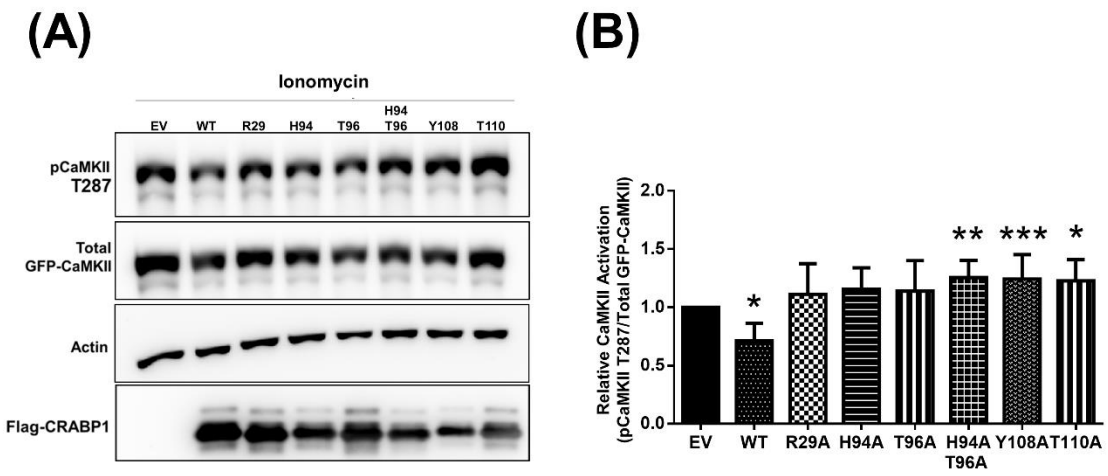

Figure 2-6 CRAPB1 side-chain mutation modulates dampening of CaMKII Activation.

(A-B) Western blot and quantification of the in-cell CRABP1-CaMKII assay under ionomycin stimulation (10 uM, 10 minutes). Flag-tagged wild-type (WT) CRABP1 or mutants were co-transfected with GFP-CaMKII β in HEK293T cells. As a control empty vector (EV) backbone was co-transfected with GFP-CaMKII β. CaMKII activation was detected by a CaMKII phospho-threonine 287 (pCaMKII T287) antibody. Anti-GFP was used to detect total GFP-CaMKII expression. β-actin was used as a loading control. Anti-Flag was used to detect WT Flag-CRABP1 and mutant expression. One-way ANOVA, followed by Dunnett's test for multiple comparisons was performed to compare WT or mutant CRABP1 against EV control. * $P \leq 0.05$, ** $P \leq 0.01$, *** $P \leq 0.001$. Error bars are presented as the mean ± standard deviation. (n=6).

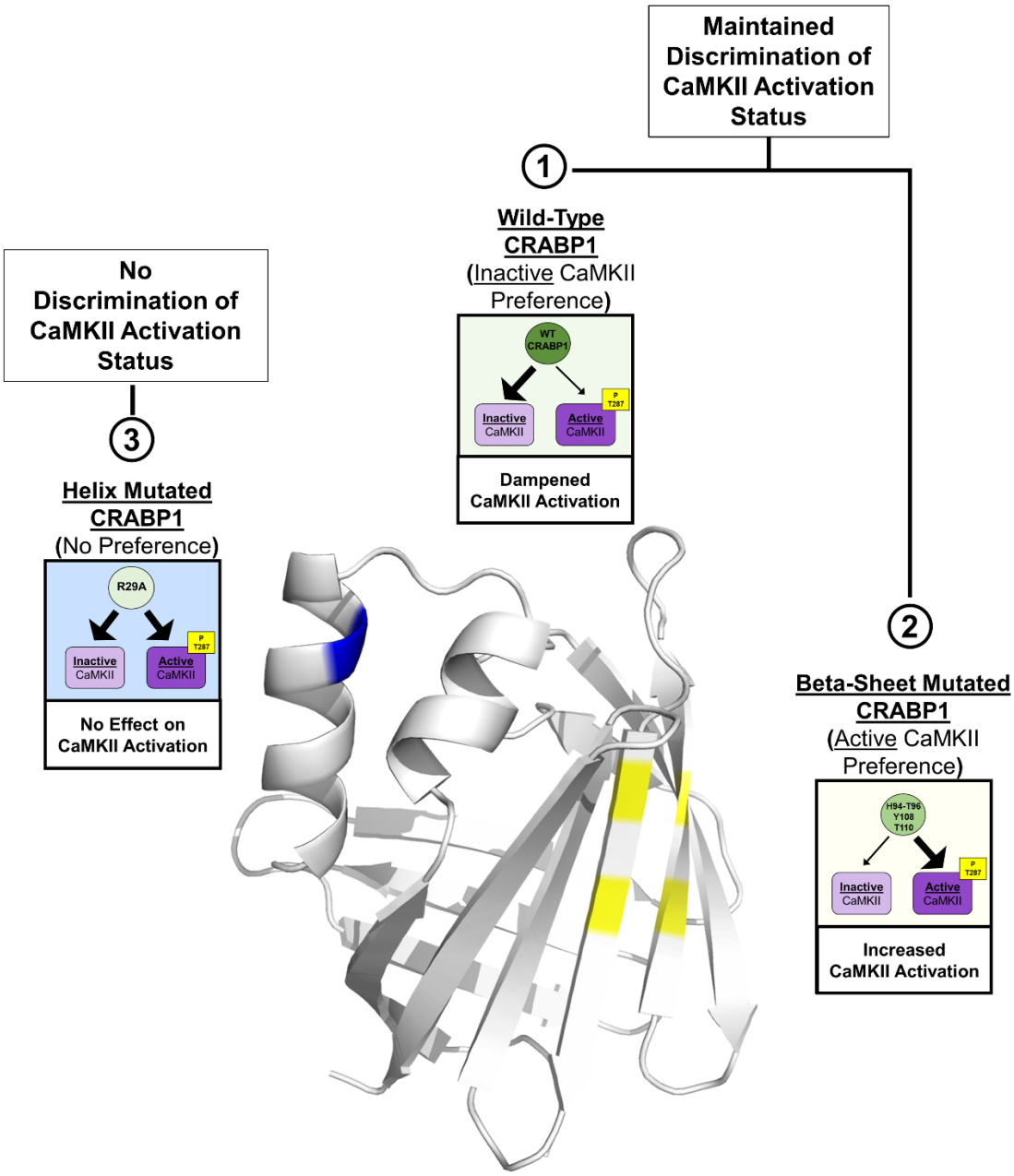

Figure 2-7 Structural model for CRABP1-mediated regulation of CaMKII.

The crystal structure for apo-CRABP1 (PDB 1CBI) with mutated sites on the helix motif (blue) and β-sheet face (yellow) indicated. Box 1 depicts the proposed dampening action of wild-type (WT) CRABP1. WT-CRABP1 has increased interaction with inactive

CaMKII (large arrow) resulting in dampened CaMKII activation. Box 2 depicts the functional consequence of disruptive mutations on the proposed interaction surface on the β-sheet face (H94A-T96A, Y108A, T110A), which result in increased interaction (large arrow) with active CaMKII and subsequent increase CaMKII activation, marked by T287 phosphorylation. Box 3 depicts mutation within the helix portion (blue) resulting in a loss of preference for either inactive or active CaMKII, resulting in no effect on CaMKII activation. Both WT CRABP1 and β-sheet surface mutations maintain the ability to discriminate between inactive and active CaMKII (Boxes 1 and 2) to modulate CaMKII activation. Whereas, mutations on the helix motif disrupt this discrimination resulting in a loss of CRABP1-mediated CaMKII modulation (Box 3). This summary image was created using BioRender.com.

2.6 Chapter 2 Supplementary Figures and Tables

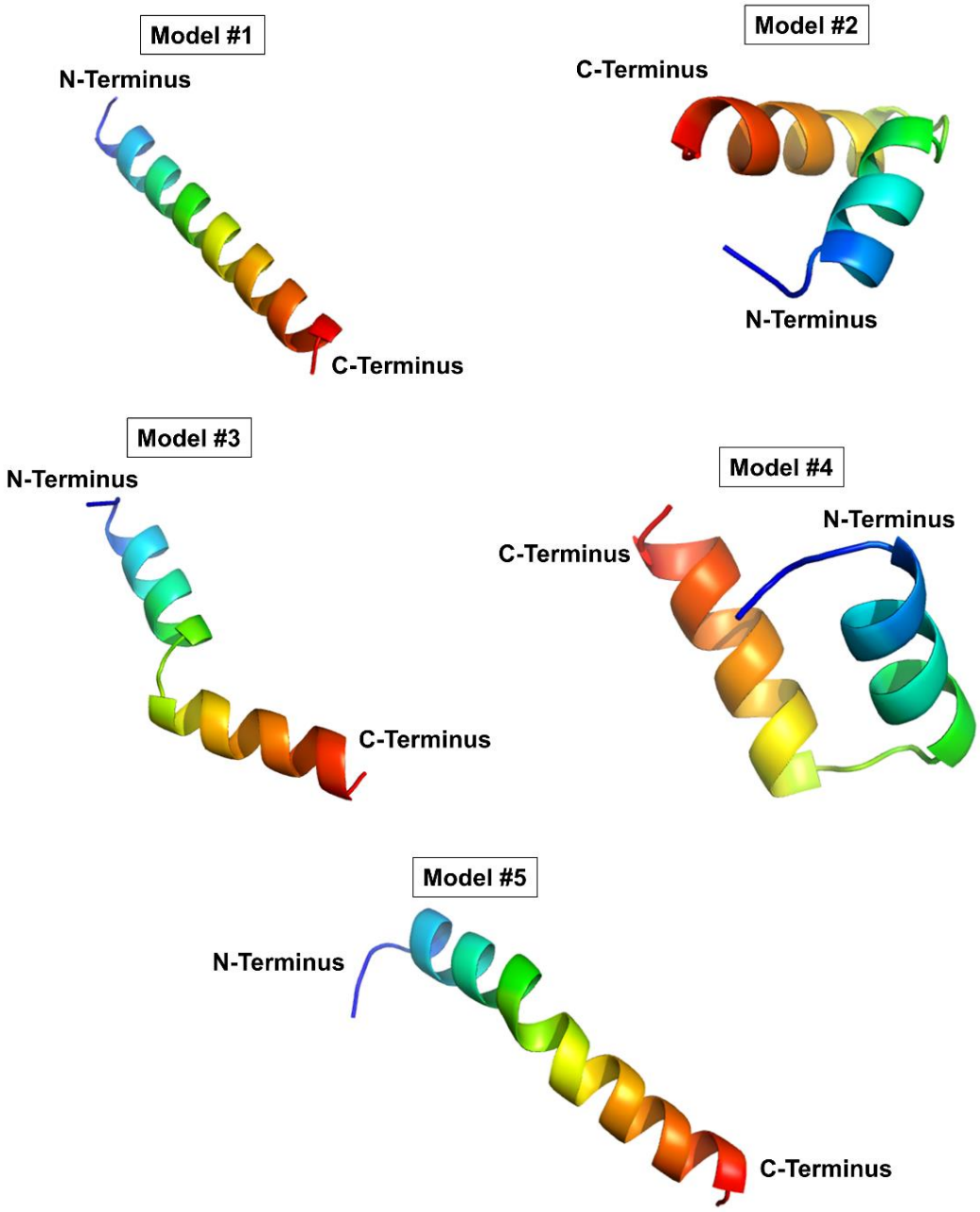

Supplementary Figure S2- 1 Predicted secondary structure models for CaMK-R peptide.

a) The top five predicted structures for the CaMK-R peptide computationally predicted using the PEP-FOLD Peptide Structure Prediction Server (https://bioserv.rpbs.univ-paris-diderot.fr/services/PEP-FOLD/)

A)

CaMK-R Peptide Sequence: MHRQETVDCLKKFNARRKLKGAILTTMLA

B)

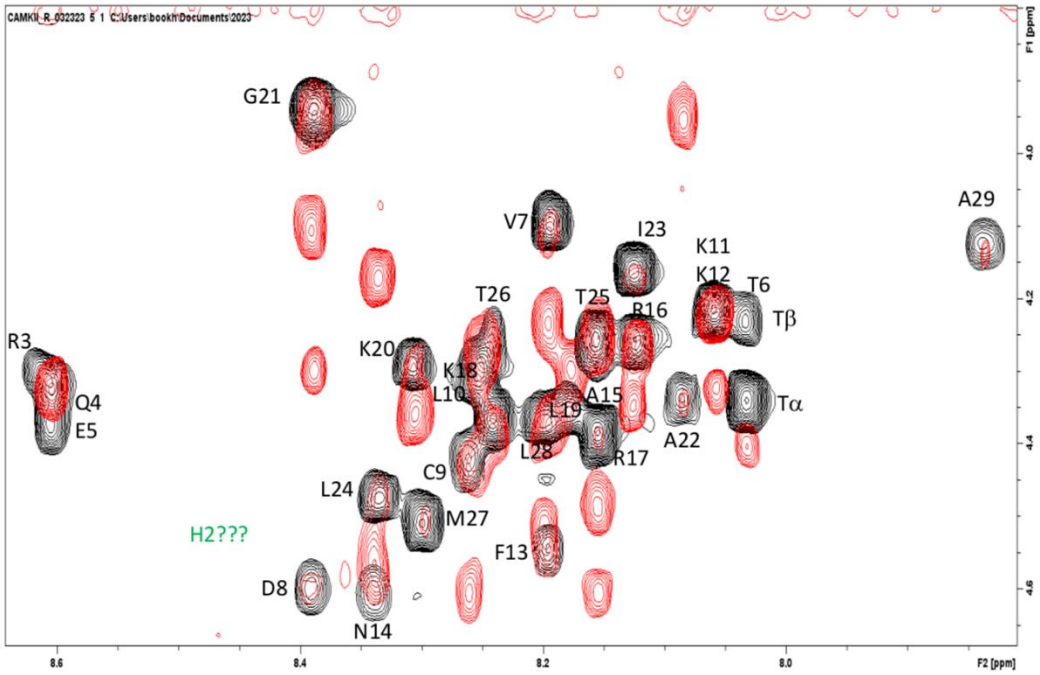

Supplementary Figure S2- 2 TOCSY-NOESY Assignments for CaMK-R Peptide.

a) The CaMK-R peptide sequence. b) Overlay of NOESY (red) spectra and TOCSY (black) spectra of the CaMK-R peptide used for CaMK-R assignment. Spectra were generated using Bruker software.

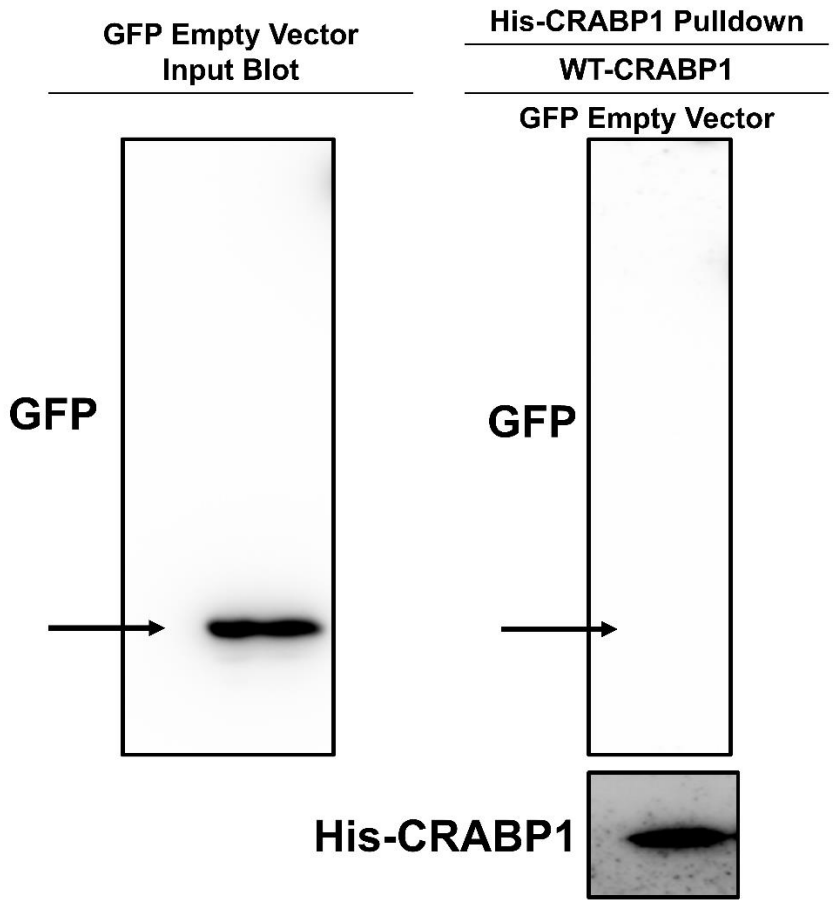

Supplementary Figure S2- 3

Negative control reaction for His pull-down assay. a) Western blot of a negative control reaction for His pull-down using WT His-CRABP1 (bait) and GFP protein cell lysate. Left: Input blot for the expected position of GFP protein indicated by a black arrow. Right: His pulldown assay using wild-type His-CRABP1 and GFP protein lysate. Anti-GFP antibody was used to detect GFP protein, anti-His antibody was used to detect His-CRABP1. (n=5)

Supplementary Table 2- 1 Maximal chemical shift changes of CRABP1 residues in the presence of CaMK-R.

CRABP1 Residue Number	
>2SD	7,9,14,30,37,70,95-98,123,134
>1SD	91,110,111,136,137
Equal to the Mean	5,10,11,18,27,36,43,44,51,56,63,69,78,87-90, 92,108,109,114,118,119,124,125,129,132,135

Chapter 3: Targeting Cellular Retinoic Acid Binding Protein 1 with Retinoic Acid-like Compounds to Mitigate Motor Neuron Degeneration

This chapter has been published as the following:

Nhieu, J.; Milbauer, L.; Lerdall, T.; Najjar, F.; Wei, C.-W.; Ishida, R.; Ma, Y.; Kagechika, H.; Wei, L.-N. Targeting Cellular Retinoic Acid Binding Protein 1 with Retinoic Acid-like Compounds to Mitigate Motor Neuron Degeneration. Int. J. Mol. Sci. 2023, 24, 4980. https://doi.org/10.3390/ijms24054980

Author Contributions:

Conceptualization, J.N. and L.-N.W.; methodology, L.M.; investigation, J.N., T.L. and L.M.; formal analysis, J.N., R.I., Y.M., H.K.; resources C.-W.W. and L.M.; writing—original dRaft, J.N., L.-N.W., L.M., T.L., F.N. and C.-W.W.; writing—review and editing, J.N., L.-N.W. and F.N.; Visualization, L.-N.W.; Supervision, L.-N.W.; Funding acquisition, L.-N.W.; Project administration, L.-N.W. All authors have read and agreed to the published version of the manuscript.

3.1 Introduction

All-*trans*-retinoic acid (atRA) is the principal active metabolite of vitamin A with well-known biological activities in development, differentiation, apoptosis, and many other biological processes[2]. These activities of atRA are known to be primarily mediated by nuclear RA receptors (RARs) that act as transcriptional factors to alter gene expression[2,81] and are referred to as atRA's canonical activities. Recently, it has been shown that atRA also elicits RAR-independent activities that can be detected rapidly (within minutes) in the cytoplasm[54,81,83], referred to as non-canonical activities[54,83]. Using a gene knockout approach, it has been established that the non-canonical activities of atRA are mediated by a specific high-affinity cytosolic atRA-binding protein named cellular retinoic acid binding protein 1 (CRABP1)[29,42].

CRABP1 is a highly conserved cytosolic protein and is expressed in multiple cell types, including embryonic stem cells (ESCs)[29], cardiomyocytes[33], adipocytes[35,82], and motor neurons (MNs)[40], etc. In ESC, CRABP1-RA modulates cell cycle progression, and deleting CRABP1 from ESC accelerates cell cycle progression[29], supporting the notion that CRABP1 can be a tumor suppressor[31,36]. In cardiomyocytes, CRABP1 protects cardiomyocytes from apoptosis triggered by adrenergic over-stimulation; therefore, *Crabp*1 knockout (CKO) mice are prone to isoproterenol-induced cardiomyopathy and heart failure[33]. In adipocytes, CRABP1 facilitates adiponectin secretion and mitochondria homeostasis; therefore, CKO mice have significantly reduced adiponectin levels and are prone to high fat diet-induced adipose inflammation[82]. In MNs, CRABP1 protects against neuronal stress/death, and CKO mice spontaneously develop

adult-onset progressive motor deterioration, mimicking amyotrophic lateral sclerosis (ALS) due to progressive MN death and neuromuscular junction defects[40]. While CRABP1-RA appears to affect various cell types and deleting CRABP1 causes different pathological outcomes in various organ systems, it is interesting that pathologies caused by CRABP1 deletion are related to two conserved signaling pathways, i.e., extracellular signal-regulated kinase (Erk) and calcium (Ca^{2+}) calmodulin-dependent kinase 2 (CaMKII).

In Erk kinase activation, CRABP1 directly interacts with rapidly accelerated fibrosarcoma 1 (Raf-1), which is the first kinase component in the mitogen-activated protein kinase (MAPK) signaling pathway, to ultimately dampen mitogen or growth factor-stimulated Erk activation. This is crucial to numerous cellular processes, especially growth[36]. CRABP1 modulation of Erk signaling plays out in the context of stem cell proliferation (in ESCs and tumors)[29,31], and for adiponectin secretion (in adipocytes)[82]. In CaMKII activation, CRABP1 directly interacts with CaMKII to dampen its enzyme activation, thereby preventing over-stimulation of CaMKII in excitable cells (such as cardiomyocytes and MNs) and protecting them from cytotoxicity and cell death[33,40]. This is supported by the finding that the physiological ligand of CRABP1, atRA, can be used to protect against isoproterenol-induced cardiomyopathy in wild-type mice but not in CKO mice, and suggests a therapeutic potential of atRA in specifically targeting CRABP1 to reduce CaMKII over-activation related pathologies[34]. However, given the well-known toxicity of atRA[16,111], via RAR activation, in long-term applications, it is

desirable to explore atRA-like compounds that can specifically target CRABP1 without activating RARs in order to avoid retinoid toxicity.

To further validate that CRABP1 can be a useful therapeutic target in managing pathological conditions caused by CaMKII over-activation, we recently carefully examined the ALS-like motor deterioration phenotype of CKO mice and the mechanism of CRABP1 action in the motor system[40]. It appears that CRABP1 is specifically expressed in spinal MNs, and elevating its expression in MNs to dampen CaMKII activation is beneficial to the neuromuscular junction (NMJ) health, partially attributable to enhanced MN agrin expression and axon extension. Specifically, CaMKII is aberrantly activated in the spinal MN population of adult CKO mice, and re-introducing CRABP1 to young CKO mice could significantly lower their CaMKII activity in spinal MNs and rescue their motor defects later. In a preliminary in vitro test using an immortalized MN cell line, MN1, we found that elevating CRABP1 levels in MN1 improved their axon extension. These experiments provided further evidence for the potential therapeutic application of targeting CRABP1, such as in dealing with diseases caused by defects in MNs[40]. Extended from these interesting findings in the CKO mouse model, this current study aims to search for CRABP1-binding (without activating RAR), atRA-like compounds that can modulate CaMKII and to establish an in vitro model for studying if and how these CRABP1-ligands may affect the process of MN differentiation and health.

While the literature has reported several MN model systems[112], there remains a need for a more reliable and reproducible in vitro system where MN differentiation can be more robustly induced for systemic studies, especially studies allowing dissection of

intermediate events in various stages of MN differentiation and maturation processes. For this current study, we, therefore, exploited P19, a widely used embryonal carcinoma cell line that is embryonic stem cell (ESC)-like and much easier to manipulate; further, P19 does not require a feeder layer in culture[113]. Using this newly developed P19-MN differentiation system, we tested the feasibility of targeting CRABP1 to modulate CaMKII activation in the process of MN differentiation and in maintaining MN health.

3.2 Results

3.2.1 Characterization of C32 as Novel atRA-like Compound That Binds CRABP1

Previously, using a rational screening approach, we have identified novel, atRA-like compounds, C3 and C4, as CRABP1 ligands that modulate Erk activation[31]. Using this approach, we define a hit CRABP1-binding compound as (1) binding to CRABP1 and (2) lacking RAR activation activity. We now report another CRAPB1 ligand, C32 (chemical name: 2-(3,5,5,8,8-Pentamethyl-5,6,7,8-tetrahydronaphthalene-2-carboxamido) thiazole-5-carboxylic acid). The chemical structures of atRA, C32, and C4 are shown in Figure 3-1A. Differential scanning fluorimetry (DSF) was utilized to determine CRABP1-binding activity. DSF is a thermal shift assay in which ligand binding to the protein of interest results in a thermal-stable, ligand-protein complex with a higher melting temperature compared to that of vehicle control[114]. The relative increase in melting temperature upon ligand binding is reported as delta Tm (ΔTm). In this assay, CRABP1 binding was defined as a ΔTm greater than or equal to 1 °C (ΔTm ≥ 1 °C). Typical high-throughput screening approaches utilize a cut-off of 3 standard deviations above the mean [115–117]. Given that CRABP1 has a highly consistent Tm (Supplementary Figure S3-1A,B), with minimal variance across biological and technical replicates, ΔTm ≥ 1 °C provides a highly

stringent cut-off for the hits. This high stringency cut-off allows the identification of robust CRABP1-binding compounds and reduces the potential for false positives

This criterium for CRABP1 binding is described in-depth in Section 4.2. In DSF, atRA (100 μM) was first used as a positive control (Figure 3-1B). When compared to the DMSO control (blue curve), RA was detected to bind CRABP1 (red curve), generating a ΔTm = 20 °C, validating this DSF assay in detecting CRABP1-binding compounds. Using this test, C32 (100 μM) appeared to bind CRABP1, generating a ΔTm = 3 °C (orange curve) compared to the DMSO control (blue curve) (Figure 3-1C). Previously identified, using a conventional ligand displacement assay[31], CRABP1 ligands C3 and C4 were also subjected to DSF (Supplementary Figure S3-1C,D). C3 and C4 at 100uM generated ΔTm = 0.26 and ΔTm = 0.09, respectively. Although these values are below the CRABP1 binding criterium of ΔTm ≥ 1 °C, the positive shift in Tm indicates a CRABP1-binding event for both C3 and C4, consistent with the previous positive result using conventional ligand displacement assay[31]. These results suggest that DSF with a stringent cut-off of ΔTm ≥ 1 °C is suitable for identifying ligands that robustly bind CRABP1.

To ensure that C32 met the second criterion, i.e., lacking RAR-activation activity, we utilized a classical luciferase-based RAR activation assay in the Cos-1 cell line. As expected, RA (0.25 μM) significantly activated RAR (298 ± 83.5-fold activation) compared to the control, whereas C32 exhibited no RAR activation (0.76 ± 0.47-fold-activation) compared to the control (Figure 3-1D). These data allowed us to identify C32 as a new atRA-like compound that binds CRABP1 without activating RAR.

3.2.2 AtRA and C32 in CRABB1-Mediated CaMKII Dampening

CaMKII activity is marked by changes in the phosphorylation status of key regulatory residue threonine 286 (or 287, depending on the isoform)[68]. The regulatory role for CRABP1 in

CaMKII activation was first examined in a reconstituted HEK293T cell model transfected with CaMKII and CRABP1 (or empty vector control). The status of pCaMKII was then assessed via western blot using an antibody specific for phosphorylated threonine 286/7. Using this system, we then determined the CaMKII-modulating activities of the three CRABP1-binding ligands, C32 and two previously reported ligands, C3 and C4 that were shown to elicit CRABP1-dependent Erk-modulating activity. The results show that atRA, C32, and C4 treatment had no significant effect on pCaMKII activity in the control vector transfected cells (Figure 3-2A, left blot; Figure 3-2B left graph). However, treatment with atRA, C32, or C4 at 0.5–5 μM for 15 min dampened CaMKII activity in CRABP1-transfected cells (Figure 3-2A, right blot; Figure 3-2B right graph), whereas C3 (that could elicit CRABP1-mediated Erk modulation) had no effect on CaMKII activation. Therefore, C32 and C4, as well as the positive control atRA, are CRABP1 ligands that can dampen CaMKII activity. This is further supported by the fact that this CRABP1-dependent CaMKII dampening activity is detected rapidly (15–60 min), confirming that this CRABP1-dependent C32 and C4 activity is non-canonical in nature.

We then sought to determine if this non-canonical activity of atRA, C32, and C4 on CaMKII modulation can be detected in a more biologically relevant context in which CRABP1 and CaMKII are endogenously present. We thus exploited the widely used P19 embryonal carcinoma cell line, which was shown to endogenously express both CRABP1[118] and CaMKII[119]. In contrast to the reconstituted HEK293T cell studies where only a single isoform CaMKII isoform (CaMKII β) was introduced, P19 cells endogenously expressed two isoforms of CaMKII, indicated by the detection of two bands with the pan-pCaMKII antibody. Four major isoforms of CaMKII -α, β, δ, and γ are known to exist and vary in expression levels depending on cell and tissue types[85], stage of development[120], and other biological and disease contexts[121,122].

Treatment with atRA, C32, or C4 at 0.5–5 μM for 15 min dampened endogenous CaMKII in P19 cells (Figure 3-2C,D), validating this CaMKII-modulatory effect of CRABP1 ligands in a physiological context. Therefore, it is concluded that C32 and C4 elicit CRABP1-dependent CaMKII-modulatory (dampening) activity.

3.2.3 A New In Vitro Stem Cell-MN Differentiation System, P19, for Studying CaMKII Activation

We have previously reported that CKO mice exhibited dramatically elevated CaMKII activation in MNs, which contributed to MN death and motor deterioration in adult mice[40]. This prompted us to carefully examine how CRABP1 signaling might affect the MN differentiation process. We thus exploited the P19 cell line, which has been extensively utilized for its differentiation potential in studying various stages of cell differentiation, including neuronal differentiation[113]. Here we developed a P19-derived motor neuron (MN) differentiation culture system to probe the effects of atRA and CRABP1 ligands in MN differentiation with regard to CaMKII activation. This P19 culture system is superior to ESC-differentiation systems which generally are very sensitive to technical complications and clonal variation[112,123].

Figure 3-3A depicts the workflow for the new P19-MN differentiation system and the data demonstrating MN differentiation efficiency. First, P19 cells in a single-cell suspension were transferred into P19 Differentiation Medium containing 0.5 μM atRA (+RA Medium, see Section 4.6 for complete media formulations) in a T75 flask. The flask was stored up-right to prevent cells from attaching to the coated surface of the flask, allowing the cells to form embryoid bodies (EB) over a two-day period (Day −4 to Day

−2). The EBs were then collected and resuspended in fresh P19 Differentiation Medium containing 0.5 μM atRA and 200 ng/mL mouse Sonic Hedgehog protein (Shh) (+RA, +Shh Medium) in a new T-75 flask for neurosphere (NS) formation over the next two-day period (Day −2 to Day 0). The flask was stored in the same manner to promote NS formation. Shh is a potent morphogen known to promote ESC differentiation into functional MNs[124]. On Day 0, the NSs were dissociated into single cells and then plated onto a Matrigel-coated 6-well plate for MN differentiation (Day 1 to Day 3). Cells were collected and analyzed at various time points for the expression of relevant markers of MNs.

Figure 3-3B shows brightfield images of undifferentiated P19 stem cells (Day −4, left) and P19-derived Day 3 MNs (right). Undifferentiated P19 cells typically grow in a clumped manner with an epithelial-like morphology. In contrast, Day 3 P19-MNs grow elongated and branched processes. In addition to MN-like morphological features, the induction of several MN-specific marker genes, HB9[125], ChAT[126], Isl1, and Isl2[127,128] (Figure 3-3C, Supplementary Figure S3-2A) and markers for other spinal neurons such as V2 interneurons, LHx3[129] (Supplementary Figure S3-2A) were also monitored. The induction of Isl2 specifically marks the presence of somatic-type spinal MNs, which innervate and maintain muscle tissue tone[130]. MN markers and spinal neuron markers appear to be readily elevated on Day 1 (Figure 3-3C, Supplementary Figure S3-2A), begin to decline after Day 3, and continue to decline on Day 5 (Supplementary Figure S3-2A). Peak expression of MN markers on Day 1–3 suggests that this could be the optimal

time window to specifically study the effect of CRABP1-ligands in the MN-differentiation process with regards to CaMKII activation.

Importantly, Crabp1 gene expression appears to be elevated from the EB stage and steadily maintained until Day 3 (Figure 3-3D, Supplementary Figure S3-2C). On Day 5 of MN differentiation, a sharp decrease in Crabp1 expression was observed (Supplementary Figure S3-2B), further supporting that Day 1–3 is the optimal time window to study the effects of CRABP1 ligands on CaMKII activation in this P19-MN differentiation system.

3.2.4 AtRA, C32, C4 Dampening CaMKII Activity in P19-MN Differentiation Process

To determine if atRA, C32, or C4 affects CRABP1-mediated CaMKII modulation, we carried out a series of experiments focusing on Day 1 and Day 3 in the P19-MN differentiation system. First, on the relevant day of interest (Day 1 or Day 3), atRA and Shh were depleted by replacing the medium with fresh differentiation medium without atRA and Shh. Additionally, dextran charcoal-treated bovine serum was used to further deplete other factors, particularly retinoids, to remove any potential contribution of genomic activities of atRA. Following this depletion step, cells were treated with atRA, C32, or C4 and then immediately harvested for western blot analyses to monitor CaMKII activation (Figure 3-3A, open circles).

On Day 1 (Figure 3-4A,B) and Day 3 P19-MN (Figure 3-4C,D), atRA, C32, and C4 significantly dampened endogenous CaMKII activity. For Day 1 MNs, RA, C32, or C4 were added at 1 μM for 15 min. For Day 3 MNs, atRA, C32, or C4 were added at 1 μM for 30 min. Together, the data show that atRA and CRABP1-binding ligands, C32

and C4, can dampen CaMKII in both Day 1 and Day 3 P19-MN differentiating/differentiated cells, suggesting their effects in multiple stages of the MN differentiation process. Note that this CaMKII-dampening activity was also detected rapidly (15–60 min), confirming that they elicited the non-canonical activity of atRA.

Interestingly, additional isoforms of CaMKII are routinely detected in P19-MNs, compared to undifferentiated P19 cells. This suggests expression of additional, neuron-specific α or β CaMKII isoforms in more differentiated cells[85]. While the intensity of isoforms differed between D1 and D3 cells, all CaMKII isoforms were dampened by these CRABP1 ligands in both D1 and D3 cells, suggesting that CRABP-modulation is effective for these various CaMKII isoforms.

3.2.5 CRABP1 in Neuroprotection against Calcium (Ca^{2+})-Induced Toxicity in MN Cells

Aberrant CaMKII activity is frequently implicated in neurodegeneration, especially in mediating the destructive downstream events of excitotoxicity, such as calcium (Ca^{2+}) overload-mediated cell death[70]. We previously reported that MN cells in CKO mice had highly elevated CaMKII activity and appeared unhealthy, which also coincided with their augmented expression of agrin protein, a proteoglycan essential for MN development and health[40,73]. This suggests that CRABP1 could be a protective player in maintaining healthy MNs.

To determine if CRABP1 indeed plays a neuroprotective role in committed MN cells, such as during excitotoxic insult, we exploited an established MN-committed cell line (MN1). We generated a stable CRABP1-overexpressing MN1 clone (CRABP1-MN1) and determined if this could provide a protective effect against ionomycin assault.

Ionomycin is a selective Ca^{2+} ionophore that causes rapid increases in intracellular Ca^{2+} concentration ($[Ca^{2+}]_i$)[99], triggering CaMKII activation[68], an event contributing to toxicity and subsequent cell death[131]. Wild-type (WT) MN1 and CRABP1-MN1 were exposed to ionomycin at 5 μM for 18 h, and cell viability was monitored immediately after the 18 h incubation period with MTT using 3-(4,5-dimethylthiazol-2-yl)-2,5-diphenyltetrazolium bromide (MTT) viability assay. MTT is metabolized by living cells to an insoluble, measurable form known as formazan[132], which directly measures live cell/viability. Indeed, the results show that CRABP1-MN1 exhibits significantly greater cell viability, as compared to WT, after ionomycin exposure (Figure 3-5A), confirming that elevating CRABP1 levels can protect MN from excitotoxicity-induced cell death.

To validate the neuroprotective, biological activity of CRABP1 ligands, atRA, C32, and C4, we determined if these ligands could protect against ionomycin assault in WT MN1 cells, a more physiologically relevant experimental system. Because this experiment is to determine the potential protective effects of the compounds, endogenous levels of CRABP1 expression provide a more biologically relevant cell context to study the effects of these compounds. First, MN1 cells were pre-treated with atRA, C32, or C4 (0.5–5 μM) for 1.5 h. Immediately after pre-treatment, ionomycin (4 μM) or DMSO (as vehicle control) was added, and cells were incubated overnight, which typically induced cell death. Compounds were present during the duration of ionomycin exposure. The next day, treated cells were subjected to an MTT assay. As expected, compared to DMSO control, ionomycin (4 μM) significantly reduced cell viability. Interestingly, atRA exhibited a trend

towards improved cell viability, while C32 and C4 significantly improved cell viability (Figure 3-5B).

To demonstrate the proposed mechanism via CRABP1-mediated CaMKII dampening, we compared Wild-type (WT) and CRABP1-MN1 (over-expressing CRABP1 to elevate CRABP1 level) treated with medium (basal), DMSO (vehicle control), or ionomycin (10 μM, 5–10 min) with regards to their CaMKII activation as reflected on threonine 286/7 phospho-status. As shown in Figure 3-5C, elevating the CRABP1 level (right panel, CRABP1 Over-Expression) clearly dampened CaMKII activity. This result supports the observations made previously using the reconstituted HEK293T system[40]. This further strengthens our hypothesis that targeting CRABP1-signaling can be developed into a protective and/or therapeutic strategy.

Taking data collected from P19-MN differentiation and MN1 systems, it is concluded CRABP1 can provide a neuroprotective effect against cell death induced by pathological Ca^{2+} overload. Furthermore, this protective effect can be exploited by using CRABP1 ligands such as C32 and C4 to enhance the protective mechanism and improve cell viability. Mechanistically this neuroprotective effect can be attributed to CRABP1-signaling that dampens CaMKII over-activation in differentiating or differentiated MNs. In summary, as depicted in the proposed model (Figure 3-5D), when MNs experience cytotoxic stimulation (step 1), it can result in pathological increases in $[Ca^{2+}]_i$ and subsequent CaMKII activation and phosphorylation of $AMPAR^{133}$ (step 2), CRABP1, as well as its ligand (such as atRA, C32, and C4), could provide an inhibitory effect to dampen this aberrant CaMKII activation (step 3), thereby preventing MN death (step 4).

3.3 Discussion

Here we report the screening of new atRA-like compounds for binding to CRABP1 without activating RAR, which allowed us to identify a new CRABP1 ligand, C32. By testing C32, as well as previously reported CRABP1-binding compounds[31] for their ability to modulate CaMKII activation, we have identified C32 and C4 (previously reported to modulate Erk activation)[31], both are CRABP1-binding ligands that can modulate CaMKII signaling in MNs. In our previous reports, C3 and C4 were identified based on their binding to CRABP1, detected using conventional ligand displacement assay, and their ability to modulate Erk signaling[31]. Together, these results show that C32 exhibits CaMKII-modulatory activity, C3 is an Erk-selective CRABP1 ligand, whereas C4 appears to be a pan-acting CRABP1 ligand. How C32 behaves in Erk signaling will require further intensive study. Nevertheless, these three compounds comprise the first series of useful CRABP1-binding ligands that may be worthy of further investigation. In order to describe the precise binding profiles of C32, C3, C4, and next-generation CRABP1-binding compounds, future studies are needed to rigorously compare their pharmacological properties. For instance, it would be of most interest to determine their binding characteristics, such as affinity and kinetics, in order to more precisely differentiate and categorize CRABP1 hit compounds. These studies will also be important for generating more rationale-designed, next-generation CRABP1 compounds that could display pathway-selective compounds. To this end, assays to confirm the various biological activities of CRABP1 ligands will be important in order to

contextualize the therapeutic potential and physiological relevance of these novel CRABP1 ligands. An important feature of these compounds is their lack of RAR-activation ability (see the following section). Preclinical models would be important for further studies to determine their potential as therapeutics by targeting CRABP1 to mitigate diseases associated with the over-activation of Erk, CaMKII, or both signaling pathways. We previously hypothesized that it is possible to design CRABP1-specific and signaling pathway-selective atRA-like compounds for safer therapeutic applications[29,31]. This current study supports such an interesting possibility.

AtRA and atRA-like compounds targeting RARs have been extensively and enthusiastically studied for therapeutic applications; however, the widely documented toxicity (RAR-mediated retinoid toxicity) has hindered the progress in this field and greatly limited their potential in clinical applications. The recently established non-canonical activities of atRA, mediated by CRABP1[92], and the demonstration of multiple human disease-mimicking phenotypes of CKO mice[33,40] prompted us to propose a new therapeutic strategy using CRABP1-binding, atRA-like compounds that lack RAR activity to modulate specific disease-related signaling pathways such as Erk and CaMKII. These compounds were designed based on, specifically, the CRABP1 binding pocket, and it is known that the binding pocket of CRABP1 has little structural or sequence relationship with the ligand binding domain of RAR[134–137]. According to the original design strategy, it is tempting to speculate that C3, C4, and C32 may not bind RAR. However, for truly "CRABP1-specific" ligands, RAR binding and potential antagonism must be ruled-out in future studies. Nevertheless, this current study provides the first

support for the possibility of designing signaling pathway-selective CRABP1-binding ligands for therapeutic intervention.

With regards to CRABP1 modulating CaMKII signaling, we have reported two spontaneously developed human disease-mimicking phenotypes of CKO mice; both are associated with aberrant CaMKII activation and cytotoxicity, i.e., cardiomyopathy/heart failure caused by cardiomyocyte apoptosis and death[33] and ALS-like motor deterioration caused by MN death/loss[40]. Importantly, in human studies, drastically reduced Crabp1 gene expression has been reported in neurodegenerative disease patients, including ALS and SMA patients[138,139]; therefore, we prioritized the studies of CRABP1-binding ligands in the context of MN degeneration. Extensive classical studies have reported aberrant CaMKII activation in neurodegeneration because over-activation of CaMKII and abruptly surged intracellular Ca^{2+} concentration is often a result of excitotoxicity, which subsequently leads to neuron death[140]. As introduced earlier, in this current study, we extended our previous findings of CKO mouse MN degenerative phenotype, aiming to develop a more reliable and feasible in vitro MN model for mechanistic studies and for screening CRABP1-specific compounds that can modulate CaMKII to improve MN health. To this end, we were able to exploit P19 and develop a P19-MN differentiation system, which allowed us to identify C32 and C4 as CRABP1 ligands that could modulate CaMKII in the context of MN differentiation. Our data also support the notion that increasing CRABP1 signaling can improve MN health, as demonstrated by the reduction of excitotoxic-induced death in an MN1 cell line with stably elevated CRABP1 expression. We also show that C32 and C4 are protective against ionomycin assault

(mimicking Ca^{2+} overload as observed in excitotoxicity). Mechanistically, this protection may be attributed to their ability to bind CRABP1 to further dampen CaMKII over-activation.

The potential role of CRABP1 in modulating MN health and motor function was first detected in CKO mice; however, it was unclear when CRABP1 and its ligands could play a role along the course of MN differentiation or maturation. Because MN1 is a committed MN cell line[141], this system is not appropriate for dissecting intermediate events during the differentiation, especially in the early differentiation stages. On the contrary, the P19-MN differentiation system spans the entire course of neural progenitor (or stem cell) progressing to MN differentiation, allowing interrogation of intermediate steps in the entire process of MN differentiation. As shown here, both C32 and C4 are effective, in terms of modulating endogenous CaMKII activation, at both early and late differentiation stages, suggesting that CRABP1 signaling can be involved in multiple steps of MN differentiation. Targeting CRABP1 may be beneficial to multiple steps in the MN differentiation process; therefore, this strategy may also be useful in preventive applications. Along with our findings that C32 and C4 pre-treatment improves cell viability after ionomycin assault in MN1 cells, it is tempting to speculate a potential clinical application as a prophylactic therapeutic to combating various neurological pathologies associated with Ca^{2+} overload/excitotoxicity. Preventative approaches may also offer an attractive strategy that can preserve a healthy neuronal population, in contrast to interventions that are typically introduced at disease onset when significant neuronal damage has already occurred[142].

Since both CaMKII and Erk signaling pathways are important for normal physiological processes in numerous organ systems and multiple cell types, pharmacological intervention to target these signaling pathways non-discriminatorily is more likely to cause toxicity. However, by selectively targeting one of these signaling pathways modulated by CRABP1 with CRABP1-specific ligands, it is possible to deliver therapeutic effects that are more specific and safer because these drug effects would be limited to certain disease-relevant cell types that are CRABP1-positive. Therefore, it would be interesting in future studies to address whether compounds like C32 and C4 can be used in therapeutic/preventive applications for diseases associated with CaMKII over-activation in CRABP1-positive cells/tissues, such as progressive motor deterioration and cardiomyopathy as revealed in the CKO mouse model. A pan-acting ligand like C4 may be useful in dealing with disease conditions where both Erk and CaMKII signaling pathways are altered, such as Alzheimer's disease (AD), amyotrophic lateral sclerosis (ALS), and Parkinson's disease (PD)[143–146].

The list of pathological conditions associated with the non-canonical activities of atRA is growing. This study provides the first insight into the potential of designing signaling pathway-selective, CRABP1-binding atRA-like ligands in mitigating diseases. In the future, CRABP1-specific compounds that can elicit the non-canonical activities of atRA may constitute an attractive and novel group of compounds that have the potential for therapeutic/preventive application for a wide spectrum of diseases with minimized retinoid toxicities.

3.4 Material and Methods

Reagents and Compound Library

All-trans retinoic acid (atRA, Sigma Cat# R2625) and ionomycin salt (Cat# I0634) were obtained from Sigma (St. Louis, MO, USA) and dissolved in DMSO. RA-like compounds C32 and C4 were synthesized by our collaborator Dr. Hiroyuki Kagechika at Tokyo Medical and Dental University. More details on the RA-like compound library can be found in[31]. For compound studies, C32 and C4 were dissolved in DMSO. All compounds were stored at −80 °C with limited freeze-thaw cycles.

Differential Scanning Fluorimetry (DSF) CRABP1 Binding Assay and Data Analysis

His-tagged CRABP1 was purified as described in[36]. 5 ug of CRABP1 (14.1 μM) was incubated with 100 μM of atRA, C32, C3, or C4 to yield a ligand to CRABP1 molar ratio of 7:1 in order to achieve saturation and preserve ligand solubility in the aqueous reaction buffer. For all experiments, DMSO was used as the vehicle control, and binding reactions were carried out in 1XPBS, pH 8.0 buffer for 1 h at room temperature on an orbital shaker. After incubation, 18 μL of the CRABP1-ligand mixture was transferred into a 96-well plate and 2 μL of 20X SYPRO Orange was added to a final concentration of 2× SYPRO Orange and a final reaction volume of 20 μL in a single well. SYPRO Orange (Invitrogen Cat. S6650, Waltham, MA, USA) was diluted from a 5000xX stock to a 20× stock in 1XPBS, pH 8.0.

Data were acquired on the QuantStudio™ 3 Real-Time PCR instrument (Applied Biosystems, Waltham, MA, USA). Data acquisition parameters were created using Design and Analysis Software (Ver 2.6.0) and are as follows: (1) starting temperature of

25 °C held for 2 min, (2) temperature was then incrementally increased from 25 to 99 °C at a ramp speed of 0.05 °C/s, (3) fluorescent readings were acquired using filter settings of 520 ± 10 nm excitation wavelength and 558 ± 11 nm emission wavelength. For each independent experiment, 6 technical replicates were included for each condition. Wells containing only ligand and SYPRO Orange were assayed as "ligand-only" controls to ensure that compounds alone did not contribute any fluorescent signal that may interfere with data analysis or generate false positives.

For data analysis, CRABP1 melt curves were generated by calculating the negative first derivative of fluorescence (RFU) over temperature (T) ($-\Delta RFU/\Delta T$) and plotting against temperature. $-\Delta RFU/\Delta T$ and temperature values were calculated in the Design and Analysis software. This melt curve data was then exported to Microsoft Excel, which was used to extract the minimum (lowest) $-\Delta RFU/\Delta T$ value of the melt curve. The corresponding temperature to the minimum $-\Delta RFU/\Delta T$ value defines the CRABP1 melting temperature (Tm)[147]. The Tm's from the 6 technical replicates were averaged and used to calculate the thermal shift values (ΔTm). ΔTm was calculated by taking the difference between DMSO control and ligand conditions (ΔTm= ligand-DMSO). A hit compound was defined as a ΔTm greater than or equal to 1 °C above the DMSO control Tm ($\Delta Tm \geq 1$ °C of DMSO). This cut-off was selected as a more stringent hit threshold to identify hit ligands that generated a robust ΔTm. Experiments were performed three independent times.

Cell Culture

Cos-1 cells were maintained as described in[31]. HEK293T cells were maintained in DMEM medium (Gibco #11965, Billings, MT, USA) containing 4.5 g/L D-glucose, 4 mM L-glutamine, 44 mM Sodium Bicarbonate, 100 U/mL penicillin, 100 mg/mL streptomycin, and 10% heat-inactivated FBS as described in [10]. HEK293T cells were co-transfected with GFP-CaMKII (Addgene #21227, Watertown, MA, USA) and either empty vector (EV) or Flag-CRABP1 (construct information described in[36]) and in a GFP-CaMKII to EV/CRABP1 to a ratio of 1:5. A total of 10 ug for a 10 cm cell culture dish was transfected using polyethylenimine (PEI, Polysciences Cat #23966, Warrington, PA, USA) in a DNA to PEI ratio of 1:5. P19 cells were purchased from ATCC, Manassas VA, USA (Cat# CRL-1825) and maintained in alpha minimum essential medium (MEM) with ribonucleosides and deoxyribonucleosides (Gibco, Cat# 12571-063) supplemented with 7.5% Bovine Calf Serum, Ion Fortified (ATCC, Cat # 30-2030), 2.5% Fetal bovine serum (R&D Systems, Cat# S11150, Minneapolis, MN, USA) and Pen Strep (Gibco, Cat #15140-122). All cells were maintained at 37 °C in a humidified 5% CO2 cell culture incubator.

For compound studies, transfected HEK293T and P19 cells were exchanged into complete medium with dextran charcoal treated (DCC) bovine serum in place of normal bovine serum to deplete exogenous RA or any other non-specific hormones for 18 h before compound treatment and downstream experiments. For P19 compound experiments, the 7.5% calf serum and 2.5% fetal bovine serum (FBS) mixture was replaced with 10% DCC fetal bovine serum.

RAR Luciferase Reporter Assay

uciferase assay for RAR activation was performed as described in[148]. Briefly, Cos-1 cells were transfected with RARE-tK-Luc and pRL renilla control plasmid using lipofectamine 3000 (Invitrogen). Following transfection, cells were washed and exchanged into fresh maintenance medium and were treated with DMSO control, RA, or compound at 0.25 μM for 24 h. Luciferase assay was performed using the Dual-Luciferase Reporter Assay kit (Promega, Madison, WI, USA). Luciferase and renilla signal was detected on an Infinite M1000 Pro Tecan (San Jose, CA, USA) plate reader. Assay was performed at least three independent times with three replicates each time. Fold activation was determined by luciferase activity and readings were normalized to renilla internal control readings.

Compound Studies and Western Blot

Preliminary studies determined that 15–60 min was the optimal window to detect compound effects on CaMKII activity for HEK293T, P19, and P19-MN experiments. For each cell line, an optimal time point within 15–60 min was identified and consistently applied across all independent experiments. DMSO, atRA, C32, or C4 were then added at 0.5–5 μM for the optimal time point determined for that particular cell line, and cells were immediately harvested for western blot analyses. All compound experiments were repeated for at least three independent times.

Western blot was performed as described in[40] with the following modification: cells were immediately lysed and harvested by adding lysis buffer (9 parts: 128 mM Tris

base, 10% (v/v) glycerol, 4% (w/v) SDS, 0.1% (w/v) bromophenol blue, pH to 6.8 and 1 part: β-mercaptoethanol) directly to the dish or plate containing treated cells. For primary antibodies, Anti-p-CaMKII (cat #: 127165, 1/1000) was obtained from Cell Signaling, Danvers, MA, USA, Anti-CRABP1 from Sigma (cat #:HPA017203), Anti-CRABP1 from Invitrogen (Cat #: MA3-813), anti-β-Actin (cat #: SC-47778, 1/2000) was obtained from Santa Cruz Biotechnology, Dallas, TX, USA. For secondary antibodies, anti-Rabbit-IgG (cat #: 11-035-144, 1/2000) was obtained from Jackson ImmunoResearch, Ely, UK, and anti-Mouse-IgG-HRP (cat #: GTX26789, 1/5000) was obtained from GeneTex, Irvine, CA, USA.

Cell lysates were separated on 9% (v/v) SDS polyacrylamide gels and transferred onto 0.45 μm PVDF membrane. The membranes were cut according to molecular weight and probed with appropriate primary and secondary antibodies. Images were acquired using the Bio-Rad ChemiDoc Imager, Hercules, CA, USA (cat #: 17001402). Image analysis was performed using BioRad Image Lab software (Ver. 6.1)of ImageJ[109].

P19-Derived Motor Neuron (MN) Differentiation, Compound Studies, and qPCR Gene Studies

P19 cells were suspended in P19 differentiation medium (50% neurobasal medium (Gibco, Cat# 21103), 25% alpha MEM and 25% P19 maintenance medium) containing 0.5 μM retinoic acid (RA) (Sigma-Aldrich, Cat# R2625) in a T75 flask to form embryo body (EB). The flask was set up-right in the culture incubator to promote EB formation. After two days, the EBs were collected and then resuspended in P19

differentiation medium with 0.5 μM RA and 200ng/mL mouse Shh (STEMCELL Technologies, Vancouver, BC, Canada, Cat# 78066) to form neurosphere (NS). After two days, the neurospheres were dissociated into single cells by using Accumax (Millipore, Burlington, MA, USA, Cat# A7089), then suspended in P19 differentiation medium with 0.5 μM RA and 200 ng/mL Shh. The cells were plated in the 6-well plate coated with 360 μg/mL Matrigel Basement Membrane (Thermal Fisher Scientific, Cat# A1413301, Waltham, MA, USA) to differentiate into motor neurons. Brightfield images were acquired on a Leica DM IRB inverted microscope with a 10× objective lens using an Infinity 1 camera and INFINITY ANALYZE software (Ver. 6.5).

For compound studies, on the relevant day (Day 1 or Day 3), media was exchanged in depletion medium (50% neurobasal medium (Gibco, Cat# 21103), 25% alpha MEM and 25% P19 culture medium). The P19 culture medium was supplemented with 10% DCC FBS instead of normal FBS to deplete RA or other non-specific hormones that can originate from FBS.

qPCR was performed as described in[40]. Briefly, TRIzol (Invitrogen, Carlsbad, CA, USA) was used to isolate total RNA. The Omniscript RT Kit (QIAGEN, Germantown, CA, USA) was used to synthesize cDNA. qPCR was performed with SYBR-Green master mix (Agilent, Santa Clara, CA, USA) and detected with Mx3005P (Agilent). Target genes for qPCR were: ChaT, Hb9, Isl1, Isl2, and Crabp1. qPCR experiments were performed two independent times. Primer sequences can be found in Supplementary Table S3-1.

Hybrid Motor Neuron (MN1) Cell Culture and Stable CRABP1 Over-Expression Clone Generation

Wild-type MN1 cells were cultured in complete DMEM medium (Gibco #11965) containing 4.5 g/L D-glucose, 4 mM L-glutamine, 44 mM Sodium Bicarbonate, 100 U/mL penicillin, 100 mg/mL streptomycin, and 10% heat-inactivated FBS. To generate the stable over-expression MN1 cell line, first, mouse Crabp1 cDNA was cloned into pCDH-EF1α-MCS-IRES-Puro plasmid (SBI, #CD532A-2) as previously described[36], resulting in 3XFlag-HA-tagged CRABP1 as a protein product. All plasmid DNA was purified using the PureLink HiPure Plasmid Filter Midiprep Kit (Invitrogen #K210014). For lentivirus production, 2 × 106 HEK-293T cells were seeded in complete DMEM medium without antibiotics dish in a 10 cm dish overnight. 9.6 µg Crabp1-pCDH target plasmid, 7.2 µg psPAX2 packaging plasmid, 2.4 µg pMD2.G envelope plasmid were co-transfected into cells with Lipofectamine 2000 transfection reagent (Invitrogen) following the manufacturer's protocol. Media was changed to 6 mL of fresh complete DMEM medium containing 1% BSA after 6 h. Infectious lentiviruses were harvested at 24 h and 48 h post-transfection and filtered through 0.45 µM pore cellulose acetate filters. For transduction, 1 × 105 MN1 cells were seeded in complete DMEM medium in 6-well plates overnight. 2 mL of lentivirus with 8 µg/mL polybrene (Millpore TR-1003-G) were added into cells, and then cells were centrifuged at 800× g, 37 °C for 60 min. Lentivirus was removed, and the medium was changed after 24 h. Puromycin selection was started at 48hrs post-transfection. Cells were selected and maintained in the same MN1 medium as described above with the addition of 3 µg/mL puromycin. After

puromycin selection, stable MN1 cells were collected and examined for Crabp1 expression by qPCR.

Ionomycin-Induced Cell Death and MTT Viability Assay

MTT reagent (Sigma Cat# M5655) was prepared by dissolving in 1XDPBS to a final concentration of 5 mg/mL and then sterile-filtered. Wild-type (WT) and the CRABP1 stable clone MN1 were then seeded into a 24-well plate at a density of 1 × 105 cells/well the night before. Puromycin selection was withdrawn from CRABP1-MN1 of these experiments. DMSO (vehicle) or ionomycin (5 μM) were treated with WT and CRABP1- MN1 for 18 h. The Final volume in each well was 1ml. Then 100 μL (10% of total well volume) of MTT reagent was added to MN1 cells and incubated at 37 °C in a humidified 5% CO2 cell culture incubator for three hours to allow for formazan crystal formation. Then cell culture and MTT reagent were gently removed via suction, and the remaining formazan crystals dissolved in 600 μL of DMSO. Formazan absorbance was measured at 570 nm, and a background reading at 690 nm was acquired using an Infinite M1000 Pro Tecan plate reader. Values were exported and analyzed in Microsoft Excel. After performing background subtraction, percent cell viability was calculated by the formula: (1−–(DMSO−–Ionomycin)) × * 100. This assay was performed 5 independent times with 4–12 replicates for each condition.

For compound experiments, WT-MN1 cells were seeded in a 24-well plate as described above. MN1 cells were pre-treated with RA, C32, and C4 at 0.5–5 μM for 1.5 h prior to ionomycin exposure. After pre-treatment, ionomycin was added to a final

concentration of 4 μM, overnight (18 h) to induce cell death. atRA, C32, and C4 were also present in the cell culture medium for the duration of ionomycin exposure. Immediately after the 18-h co-treatment, MN1 cells were subjected to an MTT viability assay as described above. This experiment was performed three independent times with 3–4 technical replicates for each condition.

Statistical Analysis

HEK293T, undifferentiated P19, and P19 MN compound experiments were analyzed using paired Student's t-test (DMSO vs. RA, C32, or C4). RAR activity luciferase assay data were analyzed using paired Student's t-test. MTT cell viability assay data were analyzed using paired Student's t-test. Significance was defined as * $p \leq 0.05$. "N.S." indicates not significant. Error bars for all data are presented as mean ± standard deviation (SD).

3.5 Chapter 3 Figures

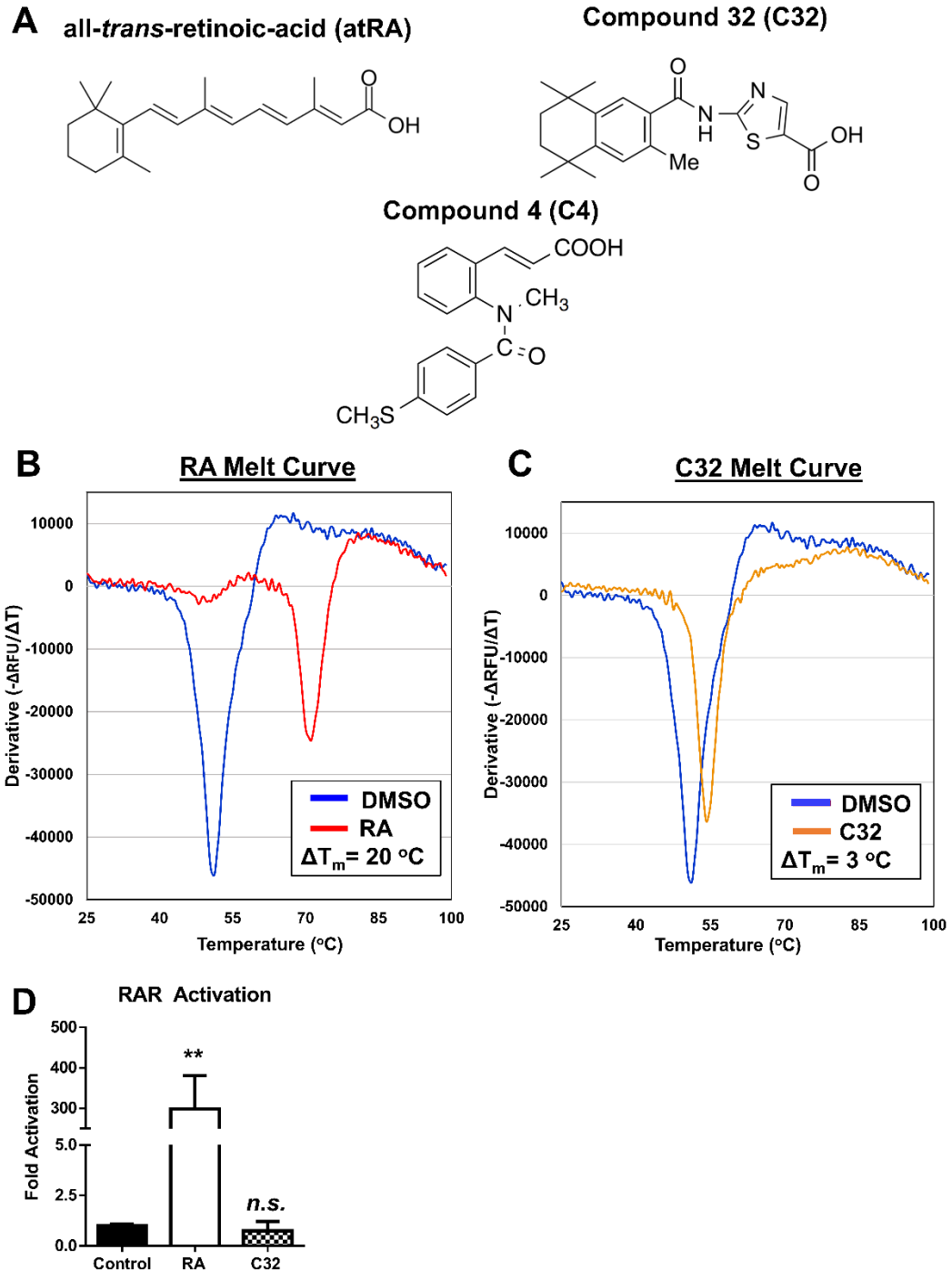

Figure 3-1 C32 is a novel CRABP1-binding compound.

(A) Chemical structures for all-*trans*-retinoic acid (atRA), C32, and C4. (B,C) Melt curves for atRA-bound (B, red, 100 μM) and C32-bound CRABP1 (C, orange, 100 μM)) overlaid with no ligand control (blue). 5 μg of CRABP1 (14.1 μM) was used for binding assays, resulting in a ligand to CRABP1 ratio of 7:1. Ligand-induced CRABP1 melting temperature shift is reported as "ΔTm". Melt curves are presented as the negative inverse derivative of fluorescence over temperature [−d(RFU)/dT]. Experiments were independently performed 3–4 times. (D) C32 does not activate RAR activity in Cos-1 cells, as determined in a luciferase reporter assay. Cos-1 cells were treated with atRA (positive control), or C32, at 0.25 μM for 24 h. A break in the y-axis shows the difference in the scale of reporter activity. $p = 0.002$ (RA) and $p = 0.45$ (C32) determined by paired Student's t-test ($n = 5$). ** $p \leq 0.01$, "n.s." not significant. Error bars are presented as mean ± SD.

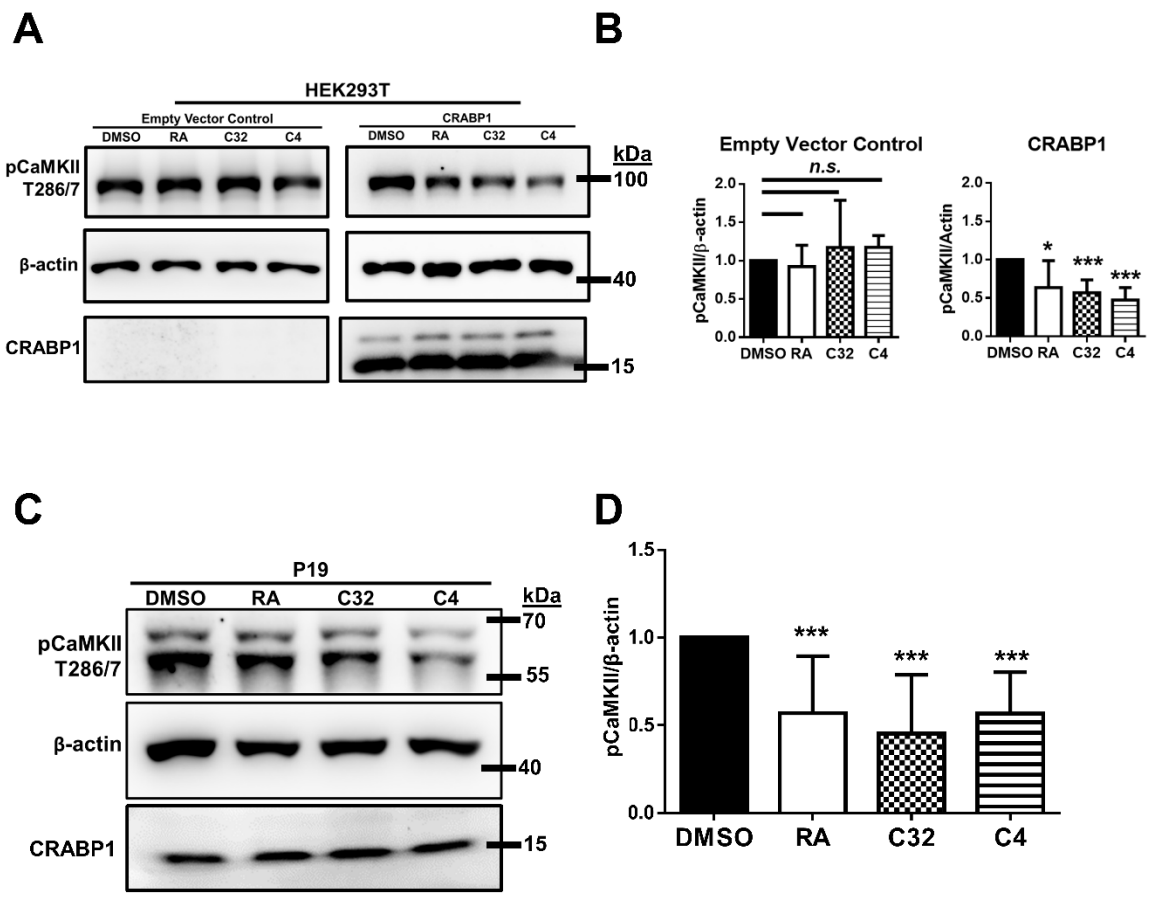

Figure 3-2 C32 and C4 dampen CaMKII activity in a CRABP1-dependent manner.

(A,B) Western blot and quantification of pCaMKII activity, marked by pThr-286/7 (pCaMKII T286/7) in HEK293T cells treated with DMSO, atRA, C32, or C4 at 0.5–5 μM for 15 min. HEK293T cells were co-transfected with GFP-CaMKII and either empty vector control or CRABP1 expressing vector. Anti-CRABP1 was used to detect CRABP1 in empty vector and CRABP1 transfected samples. p = 0.03 (RA), 0.001 (C32), 0.001 (C4), determined by paired Student's t-test (n = 4–7). (C,D) Western blot for detecting endogenous CaMKII activity, marked by pThr-286/7, in P19 cells treated with atRA, C32, or C4 at 0.5–5 μM for 15 min. Anti-CRABP1 was used to detect endogenous

CRABP1. β-actin was used as a protein loading control. $p < 0.0001$ (atRA, C32, and C4) determined by paired Student's t-test (n = 12–19). * $p \leq 0.05$, *** $p \leq 0.001$, "n.s." not significant. Error bars are presented as mean ± SD.

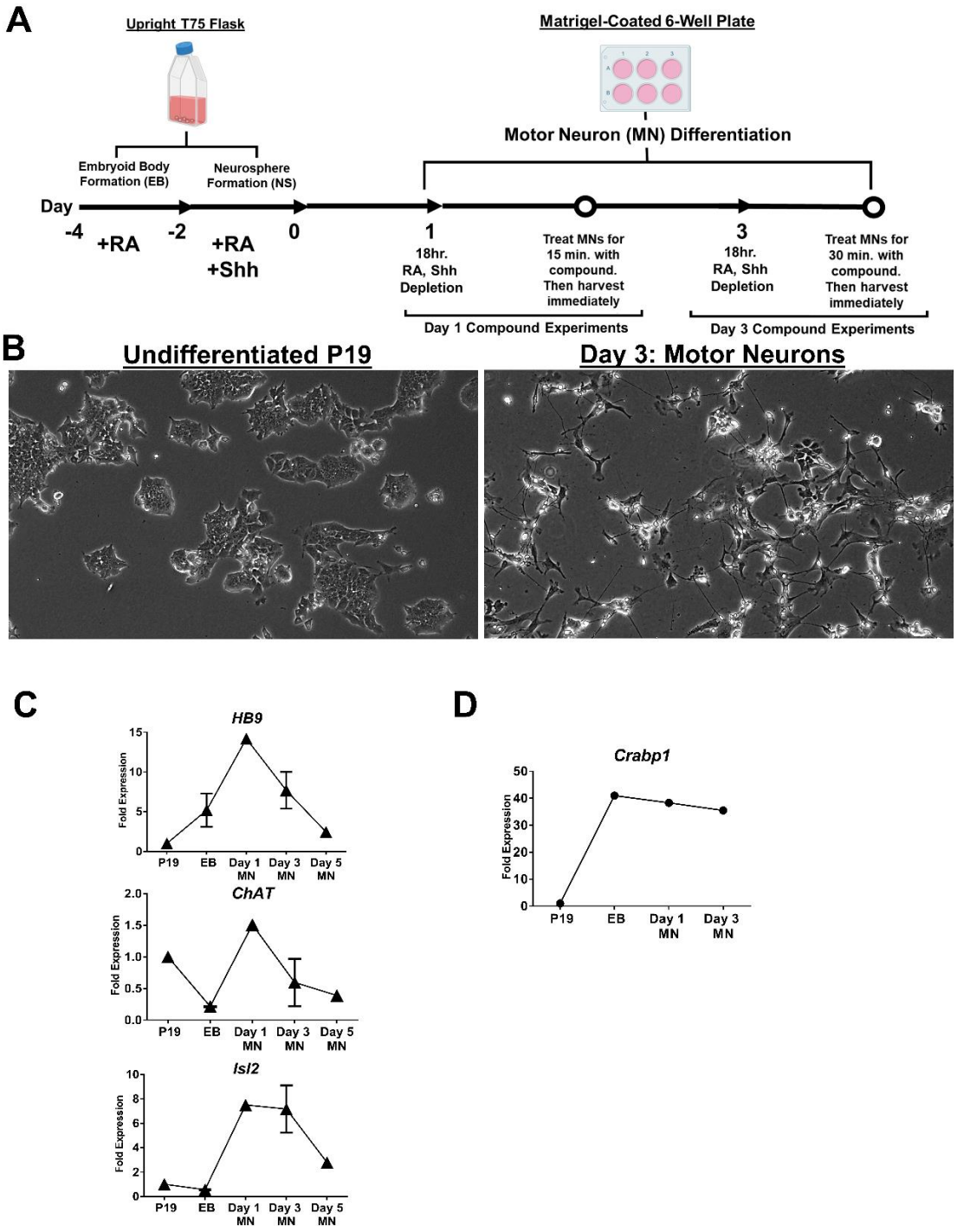

Figure 3-3 A P19-derived, in vitro MN culture system.

(A) Workflow of P19 MN differentiation. First, adherent P19 cells were suspended in +RA (0.5 μM) medium for embryoid body (EB) formation over a two-day period. EB's were then exchanged into +RA, +Shh medium for neurosphere (NS) formation. Optimal EB and NS formation was achieved through the use of an up-right T75 flask. NS were then dissociated and seeded onto a Matrigel-coated 6-well plate for MN differentiation. Compound experiments were conducted by first depleting atRA and Shh on the relevant day (Day 1 or Day 3) for 18 h. Immediately after the 18-h depletion (indicated by an open circle), MNs were treated with compound at 1 μM for 15 min for Day 1 MNs and 1 μM for 30 min for Day 3 MNs. MNs were then harvested for western blot analyses. (B) Brightfield images of undifferentiated P19 cells (left) and P19-MN differentiated cells on Day 3 (right). Scale bar (white) indicates 100 μm length. (C) qPCR detecting the expression of MN-specific markers, HB9, ChaT, and Isl2. (D) qPCR detecting the expression of Crabp1. Error bars are presented as ± SD. qPCR was conducted in two independent experiments.

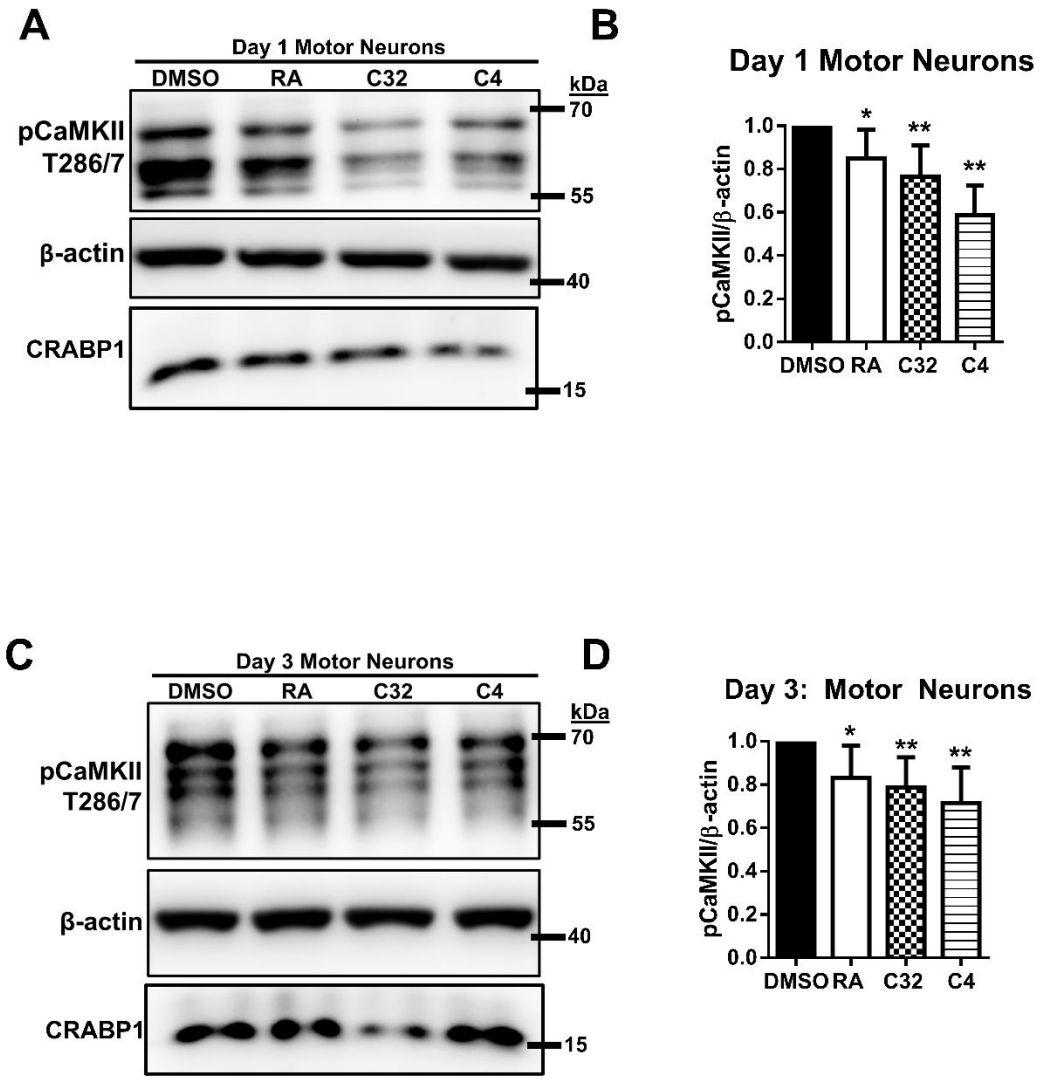

Figure 3-4 C32 and C4 dampen CaMKII activity in Day 1 and Day 3 P19-MN differentiation process.

(A,B) Western blot of RA, C32, C4 effect and quantification on endogenous CaMKII activity marked by pThr 286/7 activity in Day 1 P19-differentiated MNs. Day 1 MNs were treated with 1uM atRA, C32, or C4 for 15 min and then harvested for western blot analyses. p = 0.02 (RA), p = 0.005 (C32), and p = 0.003 (C4) determined by paired Student's t-test (n = 5–7). (C,D) Western blot and quantification of RA, C32, C4 effect

on endogenous pCaMKII T286/7 activity in Day 3, P19-MNs. Day 3 MNs were treated with 1uM atRA, C32, or C4 for 30 min and then harvested for western blot analyses. Anti-CRABP1 was used to detect endogenous CRABP1. p= 0.04 (RA), p = 0.003 (C32), and p = 0.002 (C4) determined by paired Student's t-test (n = 5–7). β-actin was used as a protein loading control. * $p \leq 0.05$, ** $p \leq 0.01$. Error bars are presented as mean ± SD.

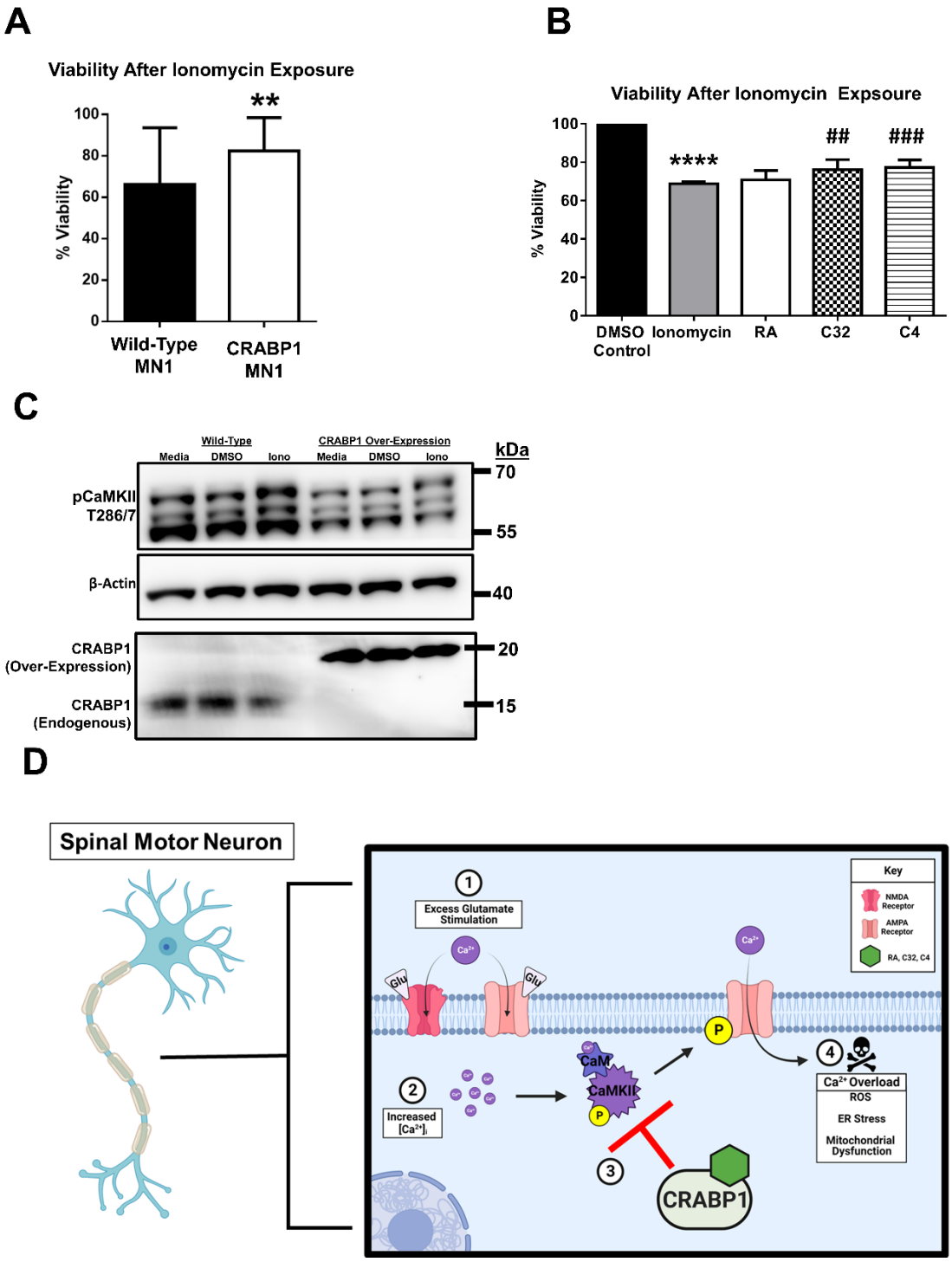

Figure 3-5 CRABP1 dampens CaMKII activity to protect against neurotoxic Ca^{2+} overload.

(A) MTT cell viability assay of WT and CRABP1-MN1 exposed to ionomycin (5 μM, 18 h). Cell viability was measured via formazan generation with an absorbance at 570 nm. p = 0.01 determined by Student's t-test. MTT assay was conducted in five independent experiments with 3–12 technical replicates per experiment. ** $p < 0.01$ determined by Student's t-test. Values are mean ± SD. (B) Cell viability assay of WT MN1 to measure the protective effects of atRA, C32, and C4. WT-MN1 cells were pretreated with atRA, C32, or C4 (0.5–5 μM) for 1.5 h. Immediately after pre-treatment, ionomycin (4 μM) or DMSO (as vehicle control) was added to induce cell death and co-incubated with atRA, C32, or C4. p = 0.34 (RA), p = 0.006 (C32), p = 0.0004 determined with Student's t-test. (C4) (**** $p < 0.0001$, DMSO vs. Ionmycin; ## $p < 0.01$ Ionomycin vs. C32; ### $p < 0.001$ Ionomycin vs. C4). Three independent experiments were performed. (C) Western blots of CaMKII activity marked by pThr 286/7 in wild-type (WT) and CRABP1 over-expressing MN1 cells treated with medium control, DMSO control, or ionomycin (10 μM, 5–10 min). β-actin was used as a loading control. Endogenous and over-expressed 3XFlag-HA-tagged CRABP1 expression was monitored with anti-CRABP1. In order to detect a much lower level of endogenous CRABP1 in WT-MN1, twice as much lysate was loaded for WT-MN1 as compared to the loaded CRABP1-MN1 (over-expression) cell lysate. (D) A model depicting the protective role of CRABP1 in MNs when they are exposed to (1) excitotoxicity which results in (2) pathological increases in $[Ca^{2+}]_i$ (purple circles), and subsequent CaMKII over-activation and phosphorylation of Ca^{2+} permeable AMPA receptors. (3) CRABP1-RA could inhibit pCaMKII over-activation, ultimately

protecting cells from AMPA-mediated Ca^{2+} overload and death (4). The model was illustrated using Biorender.com.

3.6 Chapter 3 Supplementary Figures and Table

A

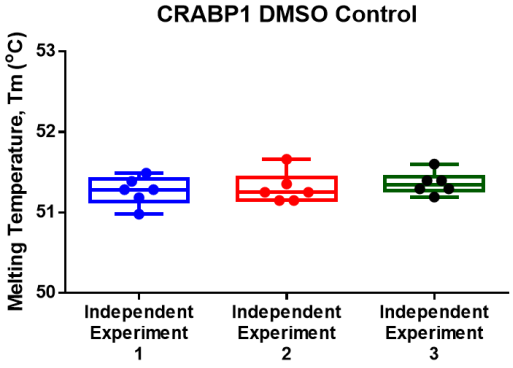

B

	DSF Exp. 1	DSF Exp. 2	DSF Exp. 3
Mean Tm (°C)	51.27	51.30	51.36
Standard Deviation	0.18	0.19	0.14

C

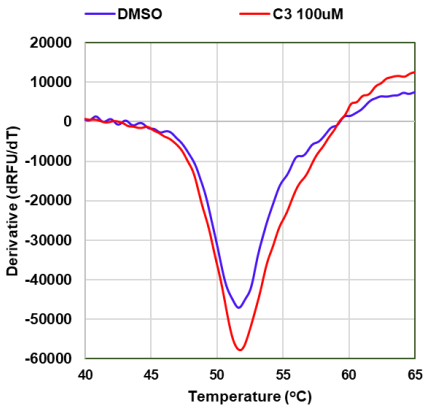

C3 Tm Shift Values		
Condition	**Tm (°C)**	**ΔTm**
DMSO	51.36	--
100uM	51.62	0.26

D

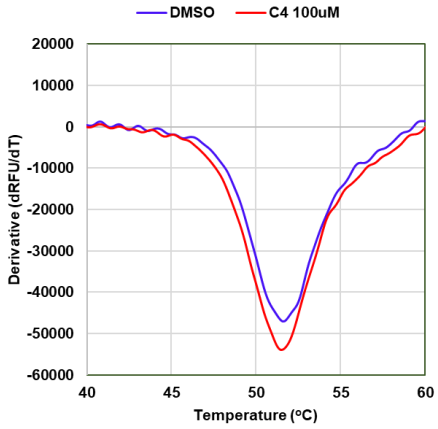

C4 Tm Shift Values		
Condition	**Tm (°C)**	**ΔTm**
DMSO	51.36	--
100uM	51.45	0.09

Supplementary Figure S3- 1 CRABP1 DMSO controls across independent and technical replicates and C3 and C4 in CRABP1 ligand binding DSF experiments.

A) Box and whisker plots of the vehicle (DMSO) controls for CRABP1 melting temperature (Tm) across 3 independent experiments. Each individual data point represents a technical replicate. B) Mean Tm and standard deviation (SD) for each independent DMSO control. Error bars are represented as ± SD. C-D) Representative melt curve profile and Tm for C3 (100uM, ΔTm= 0.26) and C4 (100uM, ΔTm= 0.09) DSF experiments.

A

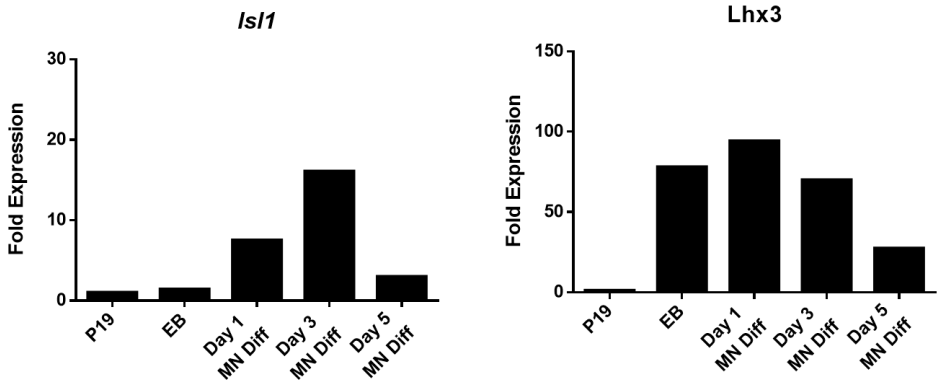

B

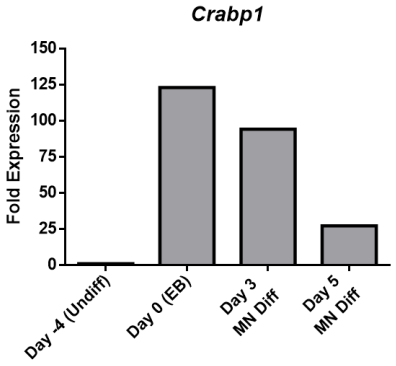

Crabp1 Gene Expression		
Stage	**Day in Vitro**	**Avg. Raw Ct**
Undifferentiated P19	-4	25.3
EB	0	17.8
Motor Neuron	3	19.1
Motor Neuron	5	20.5

C

Crabp1 Gene Expression		
Stage	**Day in Vitro**	**Avg Raw CT**
Undifferentiated P19	Day -4	24.7
EB	Day 0	18.5
Motor Neuron	Day 1	19.4
Motor Neuron	Day 3	19.5

Supplementary Figure S3- 2 Relevant gene expression patterns of MN, spinal neuron markers, and Crabp1 during the course of P19-MN differentiation.

A) qPCR data of MN specific markers, *HB9*, *ChAT*, *Isl1*, *Isl2*, and *Lhx3*, during P19-MN differentiation. B) qPCR data and raw Ct values observed for endogenous Crabp1 expression during P19-MN differentiation. C) Raw Ct values for qPCR data presented in main Figure 3D.

Supplementary Table 3- 1 Primer sequences used in qPCR analysis

Gene Name	Primer Direction	Primer Sequence
HB9	Forward	5′-TTCCAGAACCGCCGAATGAA-3′
	Reverse	5′-CCTTCTGCTTCTCCGCCTC-3′
ChAT	Forward	5′-ACTGGGTGTCTGAGTACTGG-3′
	Reverse	5′-TTGGAAGCCATTTTGACTAT-3′
Crabp1	Forward	5′-ACCTGGAAGATGCGCAGCAGCGAG-3′
	Reverse	5′-TAAACTCCTGCATTTGCGTCCGTCC-3′
Isl2	Forward	5'-GTGCTTCGTGAGAGACGGGAAA -3'
	Reverse	5'-AGCACTCGATGTGGTACACGCT-3'
Isl1	Forward	5'-GTAGAGGTGCAAAGTTACCAGCC -3'
	Reverse	5'-TTAGAGCCTGGTCCTCCTTCTG -3'
Lhx3	Forward	5'-GAAGTTCAGGGTCGGAGGGC-3'
	Reverse	5'-TGCACACATCGGGATCTCTC-3'

Chapter 4: CRABP1 in Human Diseases

Significant portions of this chapter have previously appeared in the following publication:

Nhieu, J.; Lin, Y.-L.; Wei, L.-N. CRABP1 in Non-Canonical Activities of Retinoic Acid in Health and Diseases. *Nutrients* **2022**, *14*, 1528. https://doi.org/10.3390/nu14071528

Author Contributions: J.N., L.-N.W.; writing—original dRaft preparation, Y.-L.L.; writing—review and editing, L.-N.W.; supervision, project administration, and funding acquisition.

4.1 Introduction

CRABP1 has been studied mostly in the context of nutrition, in particular vitamin A metabolism and homeostasis. The increasingly reported biological functions of CRABP1 as described above are all very different from the canonical RAR-mediated effects that typically alter genome programming and gene expression. The physiological relevance of these CRABP1-mediated effects has been illustrated in both CKO mice and tissue culture systems which model various human diseases. The multiple functions of CRABP1 would predict numerous disease conditions where CRABP1 can be involved. Indeed, CKO mice exhibited multiple phenotypes mimicking human diseases[31–39]. In tissue cultures, it is possible to examine the effects of its best-known ligand, atRA, in eliciting non-canonical activities through CRABP1, and to demonstrate holo- and apo-CRABP1's functions in specific cell types. In a genetically manipulated mouse model such as CKO, it is possible to illustrate how CRABP1 can participate in physiological processes and prevent diseased conditions/progression. However, given the technical difficulty in manipulating vitamin A and RA status in mice, the contribution of endogenous RA to the prevention of diseases, via CRABP1, remains elusive. Nevertheless, the implication of CRABP1 in human diseases can be uncovered by mining the available human data sets and literature, which has yielded some interesting information supporting a potential role for CRABP1 in human diseases. Below, we discuss several human studies/data sets that have revealed altered expression or protein sequence of CRABP1 in human patients. First, the reported genetic association of CRABP1 in various human diseases is summarized in Table 4-1, followed by a

discussion on specific implications in cancers, neurodegeneration, and other rare diseases. The relevant accession IDs of CRABP1 expression studies from the EMBL-EBI Expression Atlas Data Repository[149] are provided in Table 4-1.

4.2 CRABP1 in Cancers

Dysregulation of CRABP1 expression in cancers is a well-documented phenomenon (Table 4-1; [22,150–162]). Furthermore, cancer databases such as The Cancer Genome Atlas (TCGA) and cBioPortal[163,164] for Cancer Genomics have revealed numerous single nucleotide polymorphisms (SNPs) in patients across various cancers. These SNPs could result in various defects in CRABP1 such as synonymous mutation, splicing alternation, missense mutation, and augmented expression levels. Figure 4-1a lists SNPs present in patients from various cancer types that occurred in the −3 kb upstream regulatory region, which could affect CRABP1 expression levels; Figure 4-1b lists SNPs in the coding region that could alter the CRABP1 sequence. However, no experimental data have been provided to validate the "disease association" of these SNPs. Nevertheless, given the conservation of CRABP1 across mammals, any alterations in CRABP1 caused by these SNPs could potentially disturb CRABP1 functions and normal cellular processes especially proliferation which could impact tumor formation or progression.

4.3 CRABP1 in Neurodegeneration

CRABP1 expression has been found to be reduced in the following neurodegenerative disease conditions: amyotrophic lateral sclerosis, spinal muscular dystrophy, and age-related macular degeneration. Data mining of the ALS Variant Server

(http://als.umassmed.edu/, accessed on 31 January 2022) revealed several SNPs present in ALS patients that are located in the upstream regulatory region or in the coding region of CRABP1 (Figure 4-2a,b). These SNPs in ALS patients could potentially alter CRABP1 levels or functions, thereby contributing to disease initiation or progression. However, experiments are needed to verify the disease relevance of these SNPs. Interestingly, a study by Jiang et al. identified CRABP1 as the most significantly suppressed gene in ALS patients' motor neurons (MNs) as compared to healthy subjects, suggesting that CRABP1 may play a role in ALS etiology. This is consistent with the severe motor degeneration phenotype of CKO mice in older age groups[40]. It would be interesting to experimentally examine the potential contribution of SNPs identified from the ALS database in various neurodegenerative diseases.

The importance of CRABP1 in neurons, particularly MNs, is further supported by the finding that the mouse Crabp1 gene is tightly regulated by sonic hedgehog (Shh)[37], a potent inducer of motor neuron differentiation[124]. It appears that Shh activates glioma-associated oncogene homolog 1 (Gli1) that binds the Gli target sequence in Crabp1′s regulatory region, thereby up-regulating Crabp1 expression[37]. Therefore, for MN differentiation and function, proper expression of CRABP1 is important.

4.4 CRAPB1 in Rare Diseases

Altered CRABP1 level or function has also been observed in other diseases. In Moyamoya Disease (MMD), a vascular disease characterized by progressive occlusion of cerebral arteries[165], CRABP1 protein level was found to be increased in the CSF of MMD patients[166]. Kim et al. speculated that the increase in CRABP1 during MMD progression

might disrupt the regulatory activity of retinoids on growth factor signaling responsible for arterial occlusion[166]. A study by Hur et al. also speculated an increase in CRABP1 as a potential biomarker of diabetic neuropathy[167]. CRABP1 has also been implicated in HIV therapy associated with lipodystrophy and metabolic disorder. Carr et al. proposed that the toxic effects on adipose and metabolism associated with the use of HIV-1 protease inhibitors were, in part, due to these inhibitors' direct binding and inhibiting CRABP1 function[168]. However, no experimental data have been presented to substantiate or support a role for CRABP1 in these rare human diseases.

4.5 Discussion

A more systemic investigation into human diseases where CRABP1 could play a role is needed. Given that CKO mice have CRABP1 deleted from birth, their disease spectrum may not reflect the entire spectrum of human diseases involving CRABP1. Human genetic association studies can provide important clues into this important research direction, and may uncover more physiologically important CRABP1-signalosomes that can also deliver non-canonical activities of RA.

4.5 Chapter 4 Figures and Tables

Table 4-1 Changes in CRABP1 detected in human patients.

Cancer Type	CRABP1 Status	Reference
Breast Cancer	Over-Expression	[154]
Prostate Cancer	Over-Expression	[153]
Mesenchymal & Neuroendocrine Tumors	Over-Expression	[152]
Head and Neck Squamous Cell Carcinoma (HNSCC)	Over-Expression	[151]
Colorectal Cancer	Silenced (Promoter Hypermethylation)	[162]
Thyroid Cancer	Silenced (Promoter Hypermethylation) Reduced Expression	[161] [159]
Ovarian Cancer	Silenced (Promoter Hypermethylation) Reduced Expression	[158] [157]
Esophageal Squamous-Cell Carcinoma (ESCC)	Silenced (Promoter Hypermethylation)	[156]
Renal Cell Carcinoma	Reduced Expression	[155]
Acute myeloid leukemia (AML)	Silenced (Promoter Hypermethylation)	[150]

Neurodegenerative Diseases	CRABP1 Status	Reference
Amyotrophic Lateral Sclerosis (ALS)	Reduced Expression	[138]
Spinal Muscular Atrophy (SMA)	Reduced Expression	[139]
Late-Stage Age-Related Macular Degeneration (AMD)	Reduced Expression	[169]
Immune Disorders	**CRABP1 Status**	**Reference**
Multiple Sclerosis	Reduced Expression	[170]
Cutaneous Lupus Erythematosus (CLE)	Reduced Expression	[171] [#] E-MTAB-5542
Psoriasis	Reduced Expression	[172] [#] E-GEOD-52471
Vitiligo	Reduced Expression	[173] [#] E-GEOD-65127
Inflammatory Bowel Disease (IBD)	Silenced (Promoter Hypermethylation)	[174]
Other Diseases	**CRABP1 Status**	**Reference**
Moyamoya Disease (MMD)	Increased Protein Level	[166]
Diabetic Neuropathy	Increased Expression	[167]
HIV Therapy-Associated Lipodystrophy and Metabolic Syndrome	Inhibited Function	[168]

[#] EMBL-EBI Expression Atlas Data Repository Accession ID.

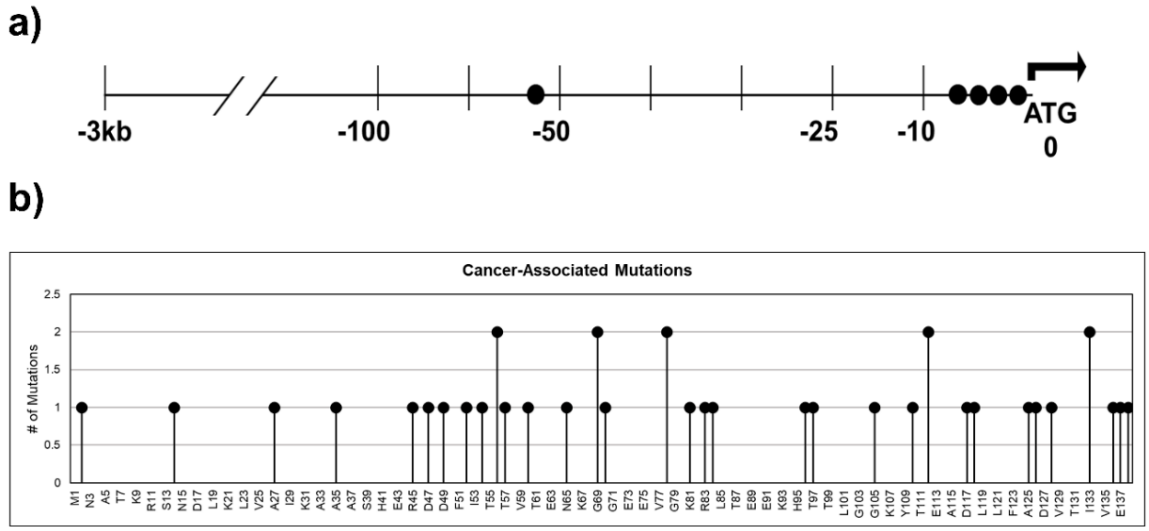

Figure 4-1 SNPs identified in cancer patients within the 3 kb upstream regulatory region and the coding sequence of CRABP1.

(a) Gene diagram of the 3 kb upstream region of CRABP1 with SNPs denoted by "●". (b) Lollipop plot indicating the location of amino acid mutations as a consequence of cancer-associated SNPs.

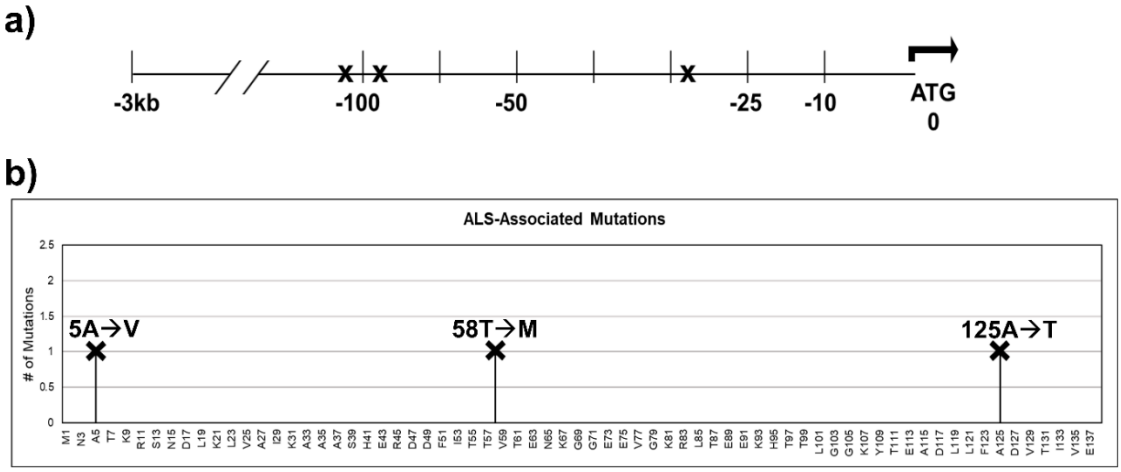

Figure 4-2 SNPs identified within the 3 kb upstream regulatory region and the coding sequence of CRABP1 in ALS patients.

(a) Gene diagram of the 3 kb upstream region of CRABP1 with SNPs denoted by "X".

(b) Lollipop plot indicating the location of amino acid mutations as a consequence of ALS-associated SNPs. Altered residues are marked above each lollipop.

Chapter 5: Conclusion and Future Directions

Significant portions of this chapter have previously appeared in the following publication:

Nhieu, J.; Lin, Y.-L.; Wei, L.-N. CRABP1 in Non-Canonical Activities of Retinoic Acid in Health and Diseases. *Nutrients* **2022**, *14*, 1528. https://doi.org/10.3390/nu14071528

Author Contributions: J.N., L.-N.W.; writing—original dRaft preparation, Y.-L.L.; writing—review and editing, L.-N.W.; supervision, project administration, and funding acquisition.

5.1 Structural and molecular Implications

The structural and molecular mechanism of CRABP1-mediated regulation of CaMKII activation reveals that CRABP1 exhibits the ability to preferentially interact with CaMKII depending on activation status. This preferential binding appears to be conferred by solvent exposed side-chains of CRABP1 residues within an interaction surface on the β-sheet face and allosteric site on the helix-turn-helix motif. Thus, this is the first study to suggest the importance of solvent exposed side-chains of CRABP1 and also provide insight as to why evolutionary selection pressures have maintained high conservation of the CRABP1 amino acid sequence.

Interestingly, the CaMKII interaction surface and Raf interaction surface are located in different regions of CRABP1, with the Raf surface on strands 6 and 7[36] and the CaMKII surface on strands 7 and 8. These findings suggest that functional modules within CRABP1, defined by particular structural features (such as specific β-sheets), may be responsible for pathway selectivity (e.g. MAPK versus CaMKII regulation). Furthermore, CRABP1 competes with both the positive regulators of Raf and CaMKII, which are Ras GTPase and calmodulin, respectively. Thus, providing an overarching thematic mechanism in driving CRABP1 functions in non-canonical signaling. For future studies, identification of other interaction partners is of most interest, especially other kinases that are regulated by their cognate binding partners.

5.2 The Future of CRABP1 Therapeutics

Initially, two novel CRABP1-selective compounds, C3 and C4, were documented to modulate the MAPK signaling pathway in CRABP1-expressing cells[31,38]. C3 and C4 can

induce apoptosis (in cancer cells)[31] and regulate exosome secretion (in neurons)[38]. These in vitro results would encourage further exploitation of this potential therapeutic strategy, such as in managing cancers and inflammation. Other groups have recently explored the use of synthetic ligands to target CRABP1. Tomlinson et al. determined the crystal structures of CRABP1 bound to fatty acids and a synthetic retinoid, DC645[175]. DC645 appeared to bind CRABP1 in a manner similar to that of RA, and the binding resulted in minimal structural changes in CRABP1. Interestingly upon ligand binding, side-chains on the β-sheet surface underwent conformational re-arrangements. Therefore, structural information obtained from these biophysical studies supports our fundamental hypothesis that CRABP1 signalosome acts, primarily, through its surface interactions that involve the β-sheet face of CRABP1. Zheng et al. determined that Maprotiline can directly bind and inhibit CRABP1, resulting in dampened ERK-mediated SREBP2 activity and ultimately reducing tumor growth in a hepatocarcinoma xenogRaft model[176].

These current studies identify and characterize a novel CRABP1 compound C32 and C4 in dampening CaMKII activation to protect against excitotoxicity in MNs. Interestingly this study also revealed that C3 does not affect CaMKII activation, suggesting ligand identity could selectively tune the function of CRABP1 towards particular target pathways. The lack of RAR activation in C3, C4 and C32 also provide a basis to design ligands that circumvent known RAR-associated toxicities. For future studies, the most important task would be to identify and develop CRABP1-selective and signaling pathway-specific ligands that do not elicit RAR-mediated toxicity. In addition to synthetic compounds, it would be of great interest to identify and study compounds derived from

naturally occurring sources, such as plants and meats. These naturally occurring ligands, if present, would be useful to the understanding and application of nutrients that may enhance the potential physiological and protective functions of CRABP1 signalosomes.

Additionally, the possibility of targeting CRABP1, such as by gene or cell therapy, is underscored by clinical data of human studies which have clearly implicated that a reduction in CRABP1 level was correlated with disease severity or its progression. To correct this deficiency, gene therapy (to deliver CRABP1-expressing vector) may be carried out to target implicated tissues. Further, a cell therapy-based strategy may also be feasible. For instance, CRABP1-expressing adipocytes may be locally delivered to adipose tissues to help correct the abnormally expanded obesity.

5.3 Summary

CRABP1 is a highly conserved mediator of non-canonical atRA activity that functions through protein-protein interactions to modulate cell signaling on a rapid time-scale in the cytosol in an RAR-independent manner. Previous studies on the CRABP1-MAPK signalosome provided the foundational mechanistic insight to lay the ground work for studies on the CRABP1-CaMKII signalosome. The results presented elucidate the structural and molecular mechanism of CRABP1-mediated regulation of CaMKII activation and characterize novel CRABP1 ligands, C4 and C32, in modulating the CRABP1-CaMKII signalosome in a motor neuron (MN) disease context. Furthermore, data mining of human studies reveals various human diseases associations with CRABP1 to further support physiological and disease relevance of CRABP1 in human health. In summary, these studies (graphically summarized in Figure 5-1) contribute the growing

repertoire of CRABP1-mediated non-canonical RA pathways. This knowledge provides insight the vast pleiotropic effects of atRA and also provides new avenues of research to discover novel functions of RA through CRABP1 and means to pharmacologically target CRABP1 in disease.

5.4 Chapter 5 Figures

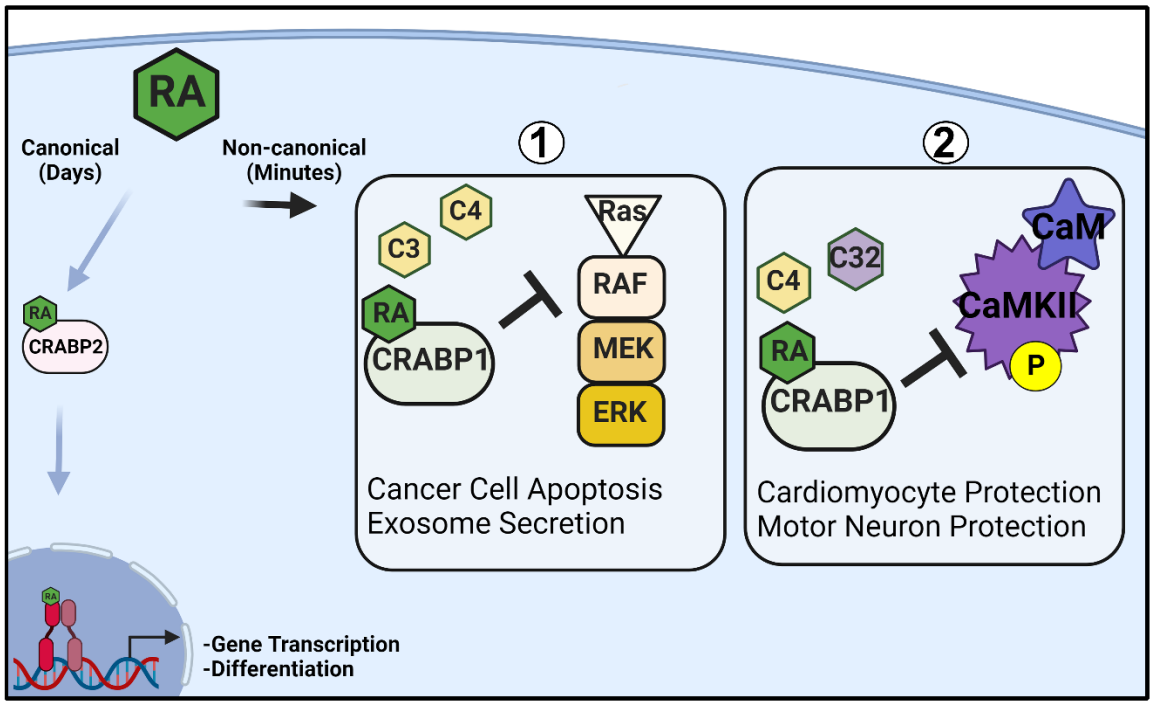

Figure 5-1 Summary of CRABP1 functions in rapid, non-canonical actions of atRA and CRABP1 ligands.

atRA canonical functions occur through RAR-RXR nuclear receptors to regulate gene transcription. Non-canonically atRA, C3, and C4 ligands bind CRABP1 to modulate MAPK activity to induce cancer cell apoptosis and exosome secretion (1). atRA, C4, and C32 bind CRABP1 to dampen CaMKII activation to protect cardiomyocytes and motor neurons from excitatory insult (2). This figure was created using Biorender.com

Bibliography

1. Tanumihardjo, S. A. *et al.* Biomarkers of nutrition for development (BOND)-vitamin A review. *J. Nutr.* **146**, 1816S-1848S (2016).

2. Cunningham, T. J. & Duester, G. Mechanisms of retinoic acid signalling and its roles in organ and limb development. *Nature Reviews Molecular Cell Biology* **16**, 110–123 (2015).

3. Duester, G. Retinoic acid synthesis and signaling during early organogenesis. *Cell* **134**, 921–931 (2008).

4. Rothman, K. J. *et al.* Teratogenicity of High Vitamin A Intake. *N. Engl. J. Med.* **333**, 1369–1373 (1995).

5. Shenefelt, R. E. Morphogenesis of malformations in hamsters caused by retinoic acid: relation to dose and stage at treatment. Teratology 5:103-18. 1972. *Birth Defects Res. A. Clin. Mol. Teratol.* **88**, 847–862 (2010).

6. Wilson, J. G., Roth, C. B. & Warkany, J. An analysis of the syndrome of malformations induced by maternal vitamin a deficiency. Effects of restoration of vitamin a at various times during gestation. *Am. J. Anat.* **92**, 189–217 (1953).

7. Ellis, C. N. & Krach, K. J. Uses and complications of isotretinoin therapy. *J. Am. Acad. Dermatol.* **45**, S150–S157 (2001).

8. Waugh, J., Noble, S. & Scott, L. J. Adapalene: a review of its use in the treatment of acne vulgaris. *Drugs* **64**, 1465–1478 (2004).

9. Chandraratna, R. A. S. Tazarotene-first of a new generation of receptor-selective retinoids. *Br. J. Dermatology, Suppl.* **135**, 18–25 (1996).

10. Cosio, T. *et al.* Trifarotene: A current review and perspectives in dermatology. *Biomedicines* **9**, 1-to (2021).

11. Orfanos, C. E., Ehlert, R. & Gollnick, H. The Retinoids: A Review of their Clinical Pharmacology and Therapeutic Use. *Drugs* **34**, 459–503 (1987).

12. Ferreira, R., Napoli, J., Enver, T., Bernardino, L. & Ferreira, L. Advances and challenges in retinoid delivery systems in regenerative and therapeutic medicine. *Nat. Commun.* **11**, 1–14 (2020).

13. Thielitz, A. & Gollnick, H. Topical retinoids in acne vulgaris: Update on efficacy and safety. *American Journal of Clinical Dermatology* **9**, 369–381 (2008).

14. Gudas, L. J. Synthetic Retinoids Beyond Cancer Therapy. *Annu. Rev. Pharmacol. Toxicol.* **62**, 155–175 (2021).

15. Clark, J. N., Whiting, A. & McCaffery, P. *Retinoic acid receptor-targeted drugs in neurodegenerative disease*. *Expert Opinion on Drug Metabolism and Toxicology* **16**, 1097–1108 (Taylor and Francis Ltd., 2020).

16. Frankel, S. R., Eardley, A., Lauwers, G., Weiss, M. & Warrell, R. P. The ‘retinoic acid syndrome’ in acute promyelocytic leukemia. *Ann. Intern. Med.* **117**, 292–296 (1992).

17. Bremner, J. D., Shearer, K. D. & McCaffery, P. J. Retinoic acid and affective

disorders: The evidence for an association. *J. Clin. Psychiatry* **73**, 37–50 (2012).

18. Bremner, J. D. & McCaffery, P. The neurobiology of retinoic acid in affective disorders. *Progress in Neuro-Psychopharmacology and Biological Psychiatry* **32**, 315–331 (2008).

19. Topletz, A. R. *et al.* Comparison of the function and expression of CYP26A1 and CYP26B1, the two retinoic acid hydroxylases. *Biochem. Pharmacol.* **83**, 149–163 (2012).

20. Topletz, A. R. *et al.* Induction of CYP26A1 by metabolites of retinoic acid: Evidence that CYP26A1 is an important enzyme in the elimination of active retinoids. *Mol. Pharmacol.* **87**, 430–441 (2015).

21. Napoli, J. L. Functions of intracellular retinoid binding-proteins. *Subcell. Biochem.* **81**, 21–76 (2016).

22. Napoli, J. L. Cellular retinoid binding-proteins, CRBP, CRABP, FABP5: Effects on retinoid metabolism, function and related diseases. *Pharmacol Ther* **173**, 19–33 (2017).

23. Stevison, F., Jing, J., Tripathy, S. & Isoherranen, N. Role of Retinoic Acid-Metabolizing Cytochrome P450s, CYP26, in Inflammation and Cancer. in *Advances in Pharmacology* **74**, 373–412 (NIH Public Access, 2015).

24. Thatcher, J. E. & Isoherranen, N. The role of CYP26 enzymes in retinoic acid clearance. *Expert Opinion on Drug Metabolism and Toxicology* **5**, 875–886

(2009).

25. Dong, D., Ruuska, S. E., Levinthal, D. J. & Noy, N. Distinct roles for cellular retinoic acid-binding proteins I and II in regulating signaling by retinoic acid. *J Biol Chem* **274**, 23695–23698 (1999).

26. Majumdar, A., Petrescu, A. D., Xiong, Y. & Noys, N. Nuclear translocation of cellular retinoic acid-binding protein II is regulated by retinoic acid-controlled SUMOylation. *J. Biol. Chem.* **286**, 42749–42757 (2011).

27. Gupta, P. *et al.* Retinoic acid-stimulated sequential phosphorylation, PML recruitment, and SUMOylation of nuclear receptor TR2 to suppress Oct4 expression. *Proc. Natl. Acad. Sci. U. S. A.* **105**, 11424–9 (2008).

28. Chuang, Y.-S. S. *et al.* Promyelocytic leukemia protein in retinoic acid-induced chromatin remodeling of Oct4 gene promoter. *Stem Cells* **29**, 660–669 (2011).

29. Persaud, S. D., Lin, Y.-W., Wu, C.-Y., Kagechika, H. & Wei, L.-N. Cellular retinoic acid binding protein I mediates rapid non-canonical activation of ERK1/2 by all-trans retinoic acid. *Cell. Signal.* **25**, 19–25 (2013).

30. Wu, C. Y., Persaud, S. D. & Wei, L. N. Retinoic Acid Induces Ubiquitination-Resistant RIP140/LSD1 Complex to Fine-Tune Pax6 Gene in Neuronal Differentiation. *Stem Cells* **34**, 114–123 (2016).

31. Persaud, S. D. *et al.* All trans-retinoic acid analogs promote cancer cell apoptosis through non-genomic Crabp1 mediating ERK1/2 phosphorylation. *Sci Rep* **6**,

22396 (2016).

32. Lin, Y. L., Persaud, S. D., Nhieu, J. & Wei, L. N. Cellular Retinoic Acid-Binding Protein 1 Modulates Stem Cell Proliferation to Affect Learning and Memory in Male Mice. *Endocrinology* **158**, 3004–3014 (2017).

33. Park, S. W. *et al.* CRABP1 protects the heart from isoproterenol-induced acute and chronic remodeling. *J. Endocrinol.* **236**, 151–165 (2018).

34. Park, S. W., Nhieu, J., Lin, Y. W. & Wei, L. N. All-trans retinoic acid attenuates isoproterenol-induced cardiac dysfunction through Crabp1 to dampen CaMKII activation. *Eur. J. Pharmacol.* **858**, 172485 (2019).

35. Lin, Y. W., Park, S. W., Lin, Y. L., Burton, F. H. & Wei, L. N. Cellular retinoic acid binding protein 1 protects mice from high-fat diet-induced obesity by decreasing adipocyte hypertrophy. *Int. J. Obes.* **44**, 466–474 (2020).

36. Wook Park, S. *et al.* A new regulatory mechanism for Raf kinase activation, retinoic acid-bound Crabp1. *Sci. Rep.* **9**, 10929 (2019).

37. Lin, Y. L., Lin, Y. W., Nhieu, J., Zhang, X. & Wei, L. N. Sonic hedgehog-gli1 signaling and cellular retinoic acid binding protein 1 gene regulation in motor neuron differentiation and diseases. *Int. J. Mol. Sci.* **21**, (2020).

38. Lin, Y. W. *et al.* Regulation of exosome secretion by cellular retinoic acid binding protein 1 contributes to systemic anti-inflammation. *Cell Commun. Signal.* **19**, 1–11 (2021).

39. Lin, Y. L., Wei, C. W., Lerdall, T. A., Nhieu, J. & Wei, L. N. Crabp1 modulates hpa axis homeostasis and anxiety-like behaviors by altering fkbp5 expression. *Int. J. Mol. Sci.* **22**, 12240 (2021).

40. Lin, Y.-L. Y.-W. *et al.* CRABP1-CaMKII-Agrn regulates the maintenance of neuromuscular junction in spinal motor neuron. *Cell Death Differ.* 1–13 (2022). doi:https://doi.org/10.1038/s41418-022-00959-4

41. Schaap, F. G., van der Vusse, G. J. & Glatz, J. F. C. Evolution of the family of intracellular lipid binding proteins in vertebrates. in *Cellular Lipid Binding Proteins* 69–77 (Springer US, 2002). doi:10.1007/978-1-4419-9270-3_9

42. Ong, D. E. & Chytil, F. Cellular retinoic acid-binding protein from rat testis. Purification and characterization. *J. Biol. Chem.* **253**, 4551–4 (1978).

43. Fiorella, P. D., Giguère, V. & Napoli, J. L. Expression of cellular retinoic acid-binding protein (type II) in Escherichia coli: Characterization and comparison to cellular retinoic acid-binding protein (type I). *J. Biol. Chem.* **268**, 21545–21552 (1993).

44. Norris, A. W., Cheng, L., Giguère, V., Rosenberger, M. & Li, E. Measurement of subnanomolar retinoic acid binding affinities for cellular retinoic acid binding proteins by fluorometric titration. *Biochim. Biophys. Acta* **1209**, 10–8 (1994).

45. Wang, L., Li, Y. & Yan, H. Structure-function relationships of cellular retinoic acid-binding proteins: Quantitative analysis of the ligand binding properties of the

wild- type proteins and site-directed mutants. *J. Biol. Chem.* **272**, 1541–1547 (1997).

46. Wei, L. N., Chang, L. & Lee, C. H. Studies of over-expressing cellular retinoic acid binding protein-I in cultured cells and transgenic mice. *Transgenics* **2**, 201–209 (1997).

47. Wei, L. N., Chang, L. & HU, X. Studies of the type I cellular retinoic acid-binding protein mutants and their biological activities. *Mol. Cell. Biochem.* **200**, 69–76 (1999).

48. Nelson, C. H. *et al.* Direct protein–protein interactions and substrate channeling between cellular retinoic acid binding proteins and CYP26B1. *FEBS Lett.* **590**, 2527–2535 (2016).

49. Eller, M. S., Oleksiak, M. F., McQuaid, T. J., McAfee, S. G. & Gilchrest, B. A. The molecular cloning and expression of two CRABP cDNAs from human skin. *Exp. Cell Res.* **198**, 328–336 (1992).

50. Tang, Z. *et al.* LongSAGE analysis of skeletal muscle at three prenatal stages in Tongcheng and Landrace pigs. *Genome Biol.* **8**, (2007).

51. Chapman, J. M. & Curley, R. W. Affinity purification of retinoic acid-binding proteins using immobilized 4-(2-Hydroxyethoxy)retinoic acid. *Protein Expr. Purif.* **1**, 63–69 (1990).

52. Stoner, C. M. & Gudas, L. J. Mouse Cellular Retinoic Acid Binding Protein:

Cloning, Complementary DNA Sequence, and Messenger RNA Expression during the Retinoic Acid-induced Differentiation of F9 Wild Type and RA-3-10 Mutant Teratocarcinoma Cells. *Cancer Res.* **49**, 1497–1504 (1989).

53. NILSSON, M. H. L. *et al.* Isolation and characterization of a cDNA clone corresponding to bovine cellular retinoic-acid-binding protein and chromosomal localization of the corresponding human gene. *Eur. J. Biochem.* **173**, 45–51 (1988).

54. Wei, L.-N. Non-canonical activity of retinoic acid in epigenetic control of embryonic stem cell. *Transcription* **4**, 158–161 (2013).

55. Wei, L. N. Cellular retinoic acid binding proteins: Genomic and non-genomic functions and their regulation. *Subcell. Biochem.* **81**, 163–178 (2016).

56. Zhang, W., Liu, H. T. & Liu, Tu, H. MAPK signal pathways in the regulation of cell proliferation in mammalian cells. *Cell Res.* **12**, 9–18 (2002).

57. Berry, D. C., DeSantis, D., Soltanian, H., Croniger, C. M. & Noy, N. Retinoic acid upregulates preadipocyte genes to block adipogenesis and suppress diet-induced obesity. *Diabetes* **61**, 1112–1121 (2012).

58. Berry, D. C. & Noy, N. All- trans -Retinoic Acid Represses Obesity and Insulin Resistance by Activating both Peroxisome Proliferation-Activated Receptor β/δ and Retinoic Acid Receptor. *Mol. Cell. Biol.* **29**, 3286–3296 (2009).

59. Jeyakumar, S. M., Vajreswari, A., Sesikeran, B. & Giridharan, N. V. Vitamin A

supplementation induces adipose tissue loss through apoptosis in lean but not in obese rats of the WNIN/Ob strain. *J. Mol. Endocrinol.* **35**, 391–398 (2005).

60. Kamei, Y., Kawada, T., Mizukami, J. & Sugimoto, E. The prevention of adipose differentiation of 3T3-L1 cells caused by retinoic acid is elicited through retinoic acid receptor alpha. *Life Sci.* **55**, (1994).

61. Murray, T. & Russell, T. R. Inhibition of adipose conversion in 3T3-L2 cells by retinoic acid. *J. Supramol. Cell. Biochem.* **14**, 255–266 (1980).

62. Lee, B., Ho, P.-C. & Wei, L.-N. Nuclear Receptor-Interacting Protein 1 (NRIP1). in *Encyclopedia of Signaling Molecules* 3606–3616 (Springer, Cham, 2018). doi:10.1007/978-3-319-67199-4_280

63. Erickson, J. R. Mechanisms of CaMKII activation in the heart. *Frontiers in Pharmacology* **5 APR**, 59 (2014).

64. Lisman, J., Schulman, H. & Cline, H. The molecular basis of CaMKII function in synaptic and behavioural memory. *Nat. Rev. Neurosci.* **3**, 175–190 (2002).

65. Lisman, J., Yasuda, R. & Raghavachari, S. Mechanisms of CaMKII action in long-term potentiation. *Nature Reviews Neuroscience* **13**, 169–182 (2012).

66. Berridge, M. J., Lipp, P. & Bootman, M. D. The versatility and universality of calcium signalling. *Nat. Rev. Mol. Cell Biol.* **1**, 11–21 (2000).

67. Bhattacharyya, M., Karandur, D. & Kuriyan, J. Structural insights into the regulation of Ca^{2+} /calmodulin-dependent protein kinase II (Camkii). *Cold Spring*

Harb. Perspect. Biol. **12**, 1–20 (2020).

68. Stratton, M. M., Chao, L. H., Schulman, H. & Kuriyan, J. *Structural studies on the regulation of Ca^{2+}/calmodulin dependent protein kinase II*. *Current Opinion in Structural Biology* **23**, 292–301 (Curr Opin Struct Biol, 2013).

69. Zhang, P. CaMKII: The molecular villain that aggravates cardiovascular disease. *Exp. Ther. Med.* **13**, 815–820 (2017).

70. Ashpole, N. M. & Hudmon, A. Excitotoxic neuroprotection and vulnerability with CaMKII inhibition. *Mol. Cell. Neurosci.* **46**, 720–730 (2011).

71. Garg, M. & Khanna, D. Exploration of pharmacological interventions to prevent isoproterenol-induced myocardial infarction in experimental models. *Ther. Adv. Cardiovasc. Dis.* **8**, 155–169 (2014).

72. Nichtova, Z., Novotova, M., Kralova, E. & Stankovicova, T. Morphological and functional characteristics of models of experimental myocardial injury induced by isoproterenol. *Gen. Physiol. Biophys.* **31**, 141–151 (2012).

73. Li, L., Xiong, W. C. & Mei, L. Neuromuscular Junction Formation, Aging, and Disorders. *Annual Review of Physiology* **80**, 159–188 (2018).

74. Martinez-Pena Y Valenzuela, I., Mouslim, C. & Akaaboune, M. Calcium/calmodulin kinase II-dependent acetylcholine receptor cycling at the mammalian neuromuscular junction in vivo. *J. Neurosci.* **30**, 12455–12465 (2010).

75. Koh, Y. H., Popova, E., Thomas, U., Griffith, L. C. & Budnik, V. Regulation of

DLG localization at synapses by CaMKII-dependent phosphorylation. *Cell* **98**, 353–363 (1999).

76. Gillespie, J. M. & Hodge, J. J. L. CASK regulates CaMKII autophosphorylation in neuronal growth, calcium signaling, and learning. *Front. Mol. Neurosci.* **6**, 27 (2013).

77. Chin, E. R. Role of Ca^{2+} /calmodulin-dependent kinases in skeletal muscle plasticity. *J. Appl. Physiol.* **99**, 414–423 (2005).

78. Rose, A. J., Kiens, B. & Richter, E. A. Ca^{2+}-calmodulin-dependent protein kinase expression and signalling in skeletal muscle during exercise. *J. Physiol.* **574**, 889–903 (2006).

79. Taetzsch, T. & Valdez, G. NMJ maintenance and repair in aging. *Current Opinion in Physiology* **4**, 57–64 (2018).

80. Glass, D. J. *et al.* Agrin acts via a MuSK receptor complex. *Cell* **85**, 513–523 (1996).

81. Wei, L.-N. Retinoid Receptors and Their Coregulators. *Annu. Rev. Pharmacol. Toxicol.* **43**, 47–72 (2003).

82. Wei, C. W., Nhieu, J., Lin, Y. L. & Wei, L. N. Modulation of adipose inflammation by cellular retinoic acid-binding protein 1. *Int. J. Obes.* **46**, 1759–1769 (2022).

83. Nagpal, I. & Wei, L. N. All-trans retinoic acid as a versatile cytosolic signal

modulator mediated by CRABP1. *International Journal of Molecular Sciences* **20**, 3610 (2019).

84. Cargnello, M. & Roux, P. P. Activation and Function of the MAPKs and Their Substrates, the MAPK-Activated Protein Kinases. *Microbiol. Mol. Biol. Rev.* **75**, 50–83 (2011).

85. Zalcman, G., Federman, N. & Romano, A. *CaMKII isoforms in learning and memory: Localization and function*. *Frontiers in Molecular Neuroscience* **11**, 445 (Frontiers Media S.A., 2018).

86. Robison, A. J. Emerging role of CaMKII in neuropsychiatric disease. *Trends Neurosci.* **37**, 653–662 (2014).

87. Pellicena, P. & Schulman, H. CaMKII inhibitors: From research tools to therapeutic agents. *Frontiers in Pharmacology* **5 FEB**, 21 (2014).

88. Nhieu, J. *et al.* Targeting Cellular Retinoic Acid Binding Protein 1 with Retinoic Acid-like Compounds to Mitigate Motor Neuron Degeneration. *Int. J. Mol. Sci.* **24**, 4980 (2023).

89. Schaap, F. G., Vusse, G. J. van der, Glatz, J. F. C. C., Van der Vusse, G. J. & Glatz, J. F. C. C. Evolution of the family of intracellular lipid binding proteins in vertebrates. *Mol. Cell. Biochem.* **239**, 69–77 (2002).

90. Banaszak, L. *et al.* Lipid-binding proteins: a family of fatty acid and retinoid transport proteins. *Adv Protein Chem* **45**, 89–151 (1994).

91. Thompson, J. R., Bratt, J. M. & Banaszak, L. J. Crystal Structure of Cellular Retinoic Acid Binding Protein I Shows Increased Access to the Binding Cavity due to Formation of an Intermolecular B-Sheet. *J. Mol. Biol.* **252**, 433–446 (1995).

92. Nhieu, J., Lin, Y. L. & Wei, L. N. CRABP1 in Non-Canonical Activities of Retinoic Acid in Health and Diseases. *Nutrients* **14**, (2022).

93. Puthenveetil, R. & Vinogradova, O. Solution NMR: A powerful tool for structural and functional studies of membrane proteins in reconstituted environments. *J. Biol. Chem.* **294**, 15914 (2019).

94. Chao, L. H. *et al.* A Mechanism for Tunable Autoinhibition in the Structure of a Human Ca^{2+}/Calmodulin- Dependent Kinase II Holoenzyme. *Cell* **146**, 732–745 (2011).

95. Lamiable, A. *et al.* PEP-FOLD3: faster denovo structure prediction for linear peptides in solution and in complex. *Nucleic Acids Res.* **44**, W449–W454 (2016).

96. Wüthrich, K. *NMR of proteins and nucleic acids*. (Wiley, 1986).

97. Wishart, D. S., Sykes, B. D. & Richards, F. M. Relationship between nuclear magnetic resonance chemical shift and protein secondary structure. *J. Mol. Biol.* **222**, 311–333 (1991).

98. Rellos, P. *et al.* Structure of the CaMKIIδ/calmodulin complex reveals the molecular mechanism of CamKII kinase activation. *PLoS Biol.* **8**, e1000426 (2010).

99. Liu, C. M. & Hermann, T. E. Characterization of ionomycin as a calcium ionophore. *J. Biol. Chem.* **253**, 5892–4 (1978).

100. Hudmon, A. *et al.* A mechanism for Ca^{2+}/calmodulin-dependent protein kinase II clustering at synaptic and nonsynaptic sites based on self-association. *J. Neurosci.* **25**, 6971–6983 (2005).

101. Celej, M. S., Montich, G. G. & Fidelio, G. D. Protein stability induced by ligand binding correlates with changes in protein flexibility. *Protein Sci.* **12**, 1496–1506 (2003).

102. Anthis, N. J. & Clore, G. M. Sequence-specific determination of protein and peptide concentrations by absorbance at 205 nm. *Protein Sci.* **22**, 851–858 (2013).

103. Delaglio, F. *et al.* NMRPipe: a multidimensional spectral processing system based on UNIX pipes. *J Biomol NMR* **6**, 277–293 (1995).

104. Johnson, B. A. & Blevins, R. A. NMR View: A computer program for the visualization and analysis of NMR data. *J Biomol NMR* **4**, 603–614 (1994).

105. Boussif, O. *et al.* A versatile vector for gene and oligonucleotide transfer into cells in culture and in vivo: Polyethylenimine. *Proc. Natl. Acad. Sci. U. S. A.* **92**, 7297–7301 (1995).

106. Canavos, G. C. The sensitivity of the one-sample and two-sample student t statistics. *Comput. Stat. Data Anal.* **6**, 39–46 (1988).

107. Student, B. The probable error of a mean. *Biometrika* **6**, 1–25 (1908).

108. Dunnett, C. W. A Multiple Comparison Procedure for Comparing Several Treatments with a Control. *J. Am. Stat. Assoc.* **50**, 1096 (1955).

109. Schindelin, J. *et al.* Fiji: An open-source platform for biological-image analysis. *Nature Methods* **9**, 676–682 (2012).

110. Lee, W., Tonelli, M. & Markley, J. L. NMRFAM-SPARKY: enhanced software for biomolecular NMR spectroscopy. *Bioinformatics* **31**, 1325–1327 (2015).

111. Nau, H. Embryotoxicity and teratogenicity of topical retinoic acid. *Ski. Pharmacol.* **6**, 35–44 (1993).

112. Bucchia, M., Merwin, S. J., Re, D. B. & Kariya, S. Limitations and challenges in modeling diseases involving spinal motor neuron degeneration in vitro. *Front. Cell. Neurosci.* **12**, 61 (2018).

113. Bain, G., Ray, W. J., Yao, M. & Gottlieb, D. I. From embryonal carcinoma cells to neurons: The P19 pathway. *BioEssays* **16**, 343–348 (1994).

114. Gao, K., Oerlemans, R. & Groves, M. R. Theory and applications of differential scanning fluorimetry in early-stage drug discovery. *Biophys. Rev.* **12**, 85–104 (2020).

115. Malo, N., Hanley, J. A., Cerquozzi, S., Pelletier, J. & Nadon, R. Statistical practice in high-throughput screening data analysis. *Nat. Biotechnol.* **24**, 167–175 (2006).

116. Luan, C. H., Light, S. H., Dunne, S. F. & Anderson, W. F. Ligand screening using fluorescence thermal shift analysis (FTS). *Methods Mol. Biol.* **1140**, 263–289

(2014).

117. Samuel, E. L. G., Holmes, S. L. & Young, D. W. Processing binding data using an open-source workflow. *J. Cheminform.* **13**, 1–11 (2021).

118. Wei, L. -N & Lee, C. -H. Demethylation in the 5′-flanking region of mouse cellular retinoic acid binding protein-I gene is associated with its high level of expression in mouse embryos and facilitates its induction by retinoic acid in P19 embryonal carcinoma cells. *Dev. Dyn.* **201**, 1–10 (1994).

119. Omar Faison, M., Perozzi, E. F., Caran, N., Stewart, J. K. & Tombes, R. M. Axonal localization of delta Ca^{2+}/calmodulin-dependent protein kinase II in developing P19 neurons. *Int. J. Dev. Neurosci.* **20**, 585–592 (2002).

120. Bayer, K. U., Löhler, J., Schulman, H. & Harbers, K. Developmental expression of the CaM kinase II isoforms: Ubiquitous γ- and δ-CaM kinase II are the early isoforms and most abundant in the developing nervous system. *Mol. Brain Res.* **70**, 147–154 (1999).

121. Bangaru, M. L. Y. *et al.* Differential expression of CaMKII isoforms and overall kinase activity in rat dorsal root ganglia after injury. *Neuroscience* **300**, 116–127 (2015).

122. Hoch, B., Meyer, R., Hetzer, R., Krause, E. G. & Karczewski, P. Identification and expression of δ-isoforms of the multifunctional Ca^{2+}/calmodulin-dependent protein kinase in failing and nonfailing human myocardium. *Circ. Res.* **84**, 713–721

(1999).

123. Elliott, J. L. Experimental models of amyotrophic lateral sclerosis. *Neurobiology of Disease* **6**, 310–320 (1999).

124. Soundararajan, P., Lindsey, B. W., Leopold, C. & Rafuse, V. F. Easy and Rapid Differentiation of Embryonic Stem Cells into Functional Motoneurons Using Sonic Hedgehog-Producing Cells. *Stem Cells* **25**, 1697–1706 (2007).

125. Arber, S. *et al.* Requirement for the homeobox gene Hb9 in the consolidation of motor neuron identity. *Neuron* **23**, 659–674 (1999).

126. Barber, R. P. *et al.* The morphology and distribution of neurons containing choline acetyltransferase in the adult rat spinal cord: An immunocytochemical study. *J. Comp. Neurol.* **229**, 329–346 (1984).

127. Tsuchida, T. *et al.* Topographic organization of embryonic motor neurons defined by expression of LIM homeobox genes. *Cell* **79**, 957–970 (1994).

128. Varela-Echavarría, A., Pfaff, S. L. & Guthrie, S. Differential expression of LIM homeobox genes among motor neuron subpopulations in the developing chick brain stem. *Mol. Cell. Neurosci.* **8**, 242–257 (1996).

129. Sharma, K. *et al.* LIM homeodomain factors Lhx3 and Lhx4 assign subtype identities for motor neurons. *Cell* **95**, 817–828 (1998).

130. Thaler, J. P. *et al.* A Postmitotic Role for Isl-Class LIM Homeodomain Proteins in the Assignment of Visceral Spinal Motor Neuron Identity. *Neuron* **41**, 337–350

(2004).

131. Gwag, B. J. *et al.* Calcium ionophores can induce either apoptosis or necrosis in cultured cortical neurons. *Neuroscience* **90**, 1339–1348 (1999).

132. Gerlier, D. & Thomasset, N. Use of MTT colorimetric assay to measure cell activation. *J. Immunol. Methods* **94**, 57–63 (1986).

133. Kristensen, A. S. *et al.* Mechanism of Ca^{2+}/calmodulin-dependent kinase II regulation of AMPA receptor gating. *Nat. Neurosci.* **14**, 727–735 (2011).

134. Huang, P., Chandra, V. & Rastinejad, F. Retinoic acid actions through mammalian nuclear receptors. *Chem. Rev.* **114**, 233–254 (2014).

135. Newcomer, M. E. Structure of the epididymal retinoic acid binding protein at 2.1 Å resolution. *Structure* **1**, 7–18 (1993).

136. Newcomer, M. E., Pappas, R. S. & Ong, D. E. X-ray crystallographic identification of a protein-binding site for both all-trans- and 9-cis-retinoic acid. *Proc. Natl. Acad. Sci. U. S. A.* **90**, 9223–9227 (1993).

137. Kleywegt, G. J. *et al.* Crystal structures of cellular retinoic acid binding proteins I and II in complex with all-trans-retinoic acid and a synthetic retinoid. *Structure* **2**, 1241–1258 (1994).

138. Jiang, Y. M. *et al.* Gene expression profile of spinal motor neurons in sporadic amyotrophic lateral sclerosis. *Ann. Neurol.* **57**, 236–251 (2005).

139. Rizzo, F. *et al.* Key role of SMN/SYNCRIP and RNA-Motif 7 in spinal muscular atrophy: RNA-Seq and motif analysis of human motor neurons. *Brain* **142**, 276–294 (2019).

140. Arundine, M. & Tymianski, M. Molecular mechanisms of calcium-dependent neurodegeneration in excitotoxicity. *Cell Calcium* **34**, 325–337 (2003).

141. Salazar-Grueso, E. F., Kim, S. & Kim, H. Embryonic mouse spinal cord motor neuron hybrid cells. *Neuroreport* **2**, 505–8 (1991).

142. Golde, T. E. The therapeutic importance of understanding mechanisms of neuronal cell death in neurodegenerative disease. *Mol. Neurodegener.* **4**, 1–7 (2009).

143. Kim, E. K. & Choi, E. J. Pathological roles of MAPK signaling pathways in human diseases. *Biochimica et Biophysica Acta - Molecular Basis of Disease* **1802**, 396–405 (2010).

144. Ghosh, A. & Giese, K. P. Calcium/calmodulin-dependent kinase II and Alzheimer's disease. *Molecular Brain* **8**, 1–7 (2015).

145. Convertini, P. *et al.* Genome wide array analysis indicates that an amyotrophic lateral sclerosis mutation of FUS causes an early increase of CAMK2N2 in vitro. *Biochim. Biophys. Acta - Mol. Basis Dis.* **1832**, 1129–1135 (2013).

146. Picconi, B. *et al.* Abnormal Ca^{2+}-calmodulin-dependent protein kinase II function mediates synaptic and motor deficits in experimental parkinsonism. *J. Neurosci.* **24**, 5283–5291 (2004).

147. Bai, N., Roder, H., Dickson, A. & Karanicolas, J. Isothermal Analysis of ThermoFluor Data can readily provide Quantitative Binding Affinities. *Sci. Rep.* **9**, 1–15 (2019).

148. Lee, C. H., Chang, L. & Wei, L. N. Molecular cloning and characterization of a mouse nuclear orphan receptor expressed in embryos and testes. *Mol. Reprod. Dev.* **44**, 305–314 (1996).

149. Papatheodorou, I. *et al.* Expression Atlas update: From tissues to single cells. *Nucleic Acids Res.* **48**, D77–D83 (2020).

150. Guidez, F. *et al.* RARalpha-PLZF overcomes PLZF-mediated repression of CRABPI, contributing to retinoid resistance in t(11;17) acute promyelocytic leukemia. *Proc. Natl. Acad. Sci. U. S. A.* **104**, 18694–18699 (2007).

151. Won, J. Y. *et al.* The effect of cellular retinoic acid binding protein-I expression on the CYP26-mediated catabolism of all-trans retinoic acid and cell proliferation in head and neck squamous cell carcinoma. *Metabolism.* **53**, 1007–1012 (2004).

152. Kainov, Y. *et al.* CRABP1 provides high malignancy of transformed mesenchymal cells and contributes to the pathogenesis of mesenchymal and neuroendocrine tumors. *Cell Cycle* **13**, 1530–1539 (2014).

153. Choi, N. *et al.* miR-93/miR-106b/miR-375-CIC-CRABP1: A novel regulatory axis in prostate cancer progression. *Oncotarget* **6**, 23533–23547 (2015).

154. Liu, R. Z. *et al.* CRABP1 is associated with a poor prognosis in breast cancer:

Adding to the complexity of breast cancer cell response to retinoic acid. *Mol. Cancer* **14**, 1–16 (2015).

155. Pfoertner, S. *et al.* Cellular retinoic acid binding protein I: expression and functional influence in renal cell carcinoma. *Tumour Biol.* **26**, 313–323 (2005).

156. Tanaka, K. *et al.* Frequent methylation-associated silencing of a candidate tumor-suppressor, CRABP1, in esophageal squamous-cell carcinoma. *Oncogene* **26**, 6456–6468 (2007).

157. Miyake, T. *et al.* CRABP1-reduced expression is associated with poorer prognosis in serous and clear cell ovarian adenocarcinoma. *J. Cancer Res. Clin. Oncol.* **137**, 715–22 (2011).

158. Wu, Q. *et al.* DNA methylation profiling of ovarian carcinomas and their in vitro models identifies HOXA9, HOXB5, SCGB3A1, and CRABP1 as novel targets. *Mol. Cancer* **6**, 1–11 (2007).

159. Hawthorn, L. *et al.* TIMP1 and SERPIN-A overexpression and TFF3 and CRABP1 underexpression as biomarkers for papillary thyroid carcinoma. *Head Neck* **26**, 1069–1083 (2004).

160. Celestino, R. *et al.* CRABP1, C1QL1 and LCN2 are biomarkers of differentiated thyroid carcinoma, and predict extrathyroidal extension. *BMC Cancer* **18**, 1–16 (2018).

161. Huang, Y., de la Chapelle, A. & Pellegata, N. S. Hypermethylation, but not LOH,

is associated with the low expression of MT1G and CRABP1 in papillary thyroid carcinoma. *Int. J. Cancer* **104**, 735–744 (2003).

162. Lind, G. E. *et al.* ADAMTS1, CRABP1, and NR3C1 identified as epigenetically deregulated genes in colorectal tumorigenesis. *Cell. Oncol.* **28**, 259–272 (2006).

163. Cerami, E. *et al.* The cBio Cancer Genomics Portal: An open platform for exploring multidimensional cancer genomics data. *Cancer Discov.* **2**, 401–404 (2012).

164. Gao, J. *et al.* Integrative analysis of complex cancer genomics and clinical profiles using the cBioPortal. *Sci. Signal.* **6**, (2013).

165. Scott, R. M. & Smith, E. R. Moyamoya Disease and Moyamoya Syndrome. *N. Engl. J. Med.* **360**, 1226–1237 (2009).

166. Kim, S. K. *et al.* Elevation of CRABP-I in the Cerebrospinal Fluid of Patients with Moyamoya Disease. *Stroke* **34**, 2835–2841 (2003).

167. Hur, J. *et al.* The identification of gene expression profiles associated with progression of human diabetic neuropathy. *Brain* **134**, 3222–3235 (2011).

168. Carr, A., Samaras, K., Chisholm, D. J. & Cooper, D. A. Pathogenesis of HIV-1-protease inhibitor-associated peripheral lipodystrophy, hyperlipidaemia, and insulin resistance. *Lancet* **351**, 1881–1883 (1998).

169. Nordgaard, C. L. *et al.* Proteomics of the retinal pigment epithelium reveals altered protein expression at progressive stages of age-related macular degeneration.

Investig. Ophthalmol. Vis. Sci. **47**, 815–822 (2006).

170. Satoh, J. I. & Kino, Y. Expression profiles of RNA-Seq-based grey matter-specific genes versus white matter-specific genes in grey matter lesions of multiple sclerosis. *Clin. Exp. Neuroimmunol.* **6**, 289–298 (2015).

171. Scholtissek, B. *et al.* Immunostimulatory Endogenous Nucleic Acids Drive the Lesional Inflammation in Cutaneous Lupus Erythematosus. *J. Invest. Dermatol.* **137**, 1484–1492 (2017).

172. Jabbari, A. *et al.* Dominant Th1 and minimal Th17 skewing in discoid lupus revealed by transcriptomic comparison with psoriasis. *J. Invest. Dermatol.* **134**, 87–95 (2014).

173. Regazzetti, C. *et al.* Transcriptional analysis of vitiligo skin reveals the alteration of WNT pathway: A promising target for repigmenting vitiligo patients. *J. Invest. Dermatol.* **135**, 3105–3114 (2015).

174. Rosa, I. *et al.* Methylation patterns in dysplasia in inflammatory bowel disease patients. *Scand. J. Gastroenterol.* **55**, 646–655 (2020).

175. Tomlinson, C. W. E., Cornish, K. A. S., Whiting, A. & Pohl, E. Structure-functional relationship of cellular retinoic acid-binding proteins i and II interacting with natural and synthetic ligands. *Acta Crystallogr. Sect. D Struct. Biol.* **77**, 164–175 (2021).

176. Zheng, C., Zhu, Y., Liu, Q., Luo, T. & Xu, W. Maprotiline Suppresses Cholesterol

Biosynthesis and Hepatocellular Carcinoma Progression Through Direct Targeting of CRABP1. *Front. Pharmacol.* **12**, 1243 (2021).